UNIVERSITEIT VAN PRETORIA
UNIVERSITY OF PRETORIA
YUNIBESITHI YA PRETORIA

BIOREMEDIATION OF METALLIC FISSION PRODUCTS IN NUCLEAR WASTE: BIOSORPTION AND BIORECOVERY

NONHLANHLA NGWENYA

A thesis submitted in fulfilment of requirements for the degree of

PHILOSOPHIAE DOCTOR (CHEMICAL TECHNOLOGY)

in the

FACULTY OF ENGINEERING, BUILT ENVIRONMENT AND INFORMATION TECHNOLOGY

UNIVERSITY OF PRETORIA

2011

ABSTRACT

BIOREMEDIATION OF METALLIC FISSION PRODUCTS IN NUCLEAR WASTE: BIOSORPTION AND BIORECOVERY

By

Nonhlanhla Ngwenya

Supervisor: Professor EMN Chirwa

Department: Chemical Engineering

Degree: Philosophiae Doctor (Chemical Technology)

The performance of a growing sulphate reducing bacteria consortium for Sr^{2+}, Co^{2+} and Cs^{+} removal from solution in a batch sulphidogenic bioreactor was investigated. Metal removal by the growing bacterial consortium, and microbial culture growth and metabolic activities (biological sulphate removal) were continuously monitored in the bioreactors over the duration of the treatment period. On the other hand, diversity changes within the bacterial consortium before and after bioreactor operation (28 days) were performed using the partial 16S rRNA fingerprinting method.

In the original bacterial consortium, *Enterococcus* and *Staphylococcus* sp. were the dominant bacterial species. However, the presence of Sr^{2+}, Co^{2+} and Cs^{+} in the growth media, resulted in the emergence of new bacterial species belonging to the *Citrobacter*, *Paenibacillus,* and *Enterococcus* and *Stenotrophomonas* genera, respectively. The *Citrobacter* and *Paenibacillus* sp. demonstrated high tolerance towards the presence of the divalent cations, Sr^{2+} and Co^{2+}, respectively, while the *Enterococcus* and *Stenotrophomonas* sp., demonstrated Cs^{+} high tolerance. The bacterial growth and sulphate removal rate were significantly decreased at initial metal ion concentrations ≥100 mg/L. The toxicity and inhibitory effects of the metals on the present SRB consortium was observed in the order Sr>Co>Cs.

The metal uptake capacity (q_t) of the bacterial consortium decreased with increasing initial metal concentration, and complete Sr^{2+}, Co^{2+} and Cs^{+} removal was observed at initial metal concentrations ≤75 mg/L. Overall, the present SRB consortium demonstrated a superior $Sr2^{+}$ removal capacity (q_{max}= 405 mg/g), and the least for Cs^{+}, where q_{max} = 192 mg/g. The presnt SRB culture exhibited a superior Sr^{2+} and Cs^{+} binding capacity, compared to other studies in literature. Results from Sr^{2+}, Co^{2+} and Cs^{+} biosorption kinetics indicate that initial concentration and solution pH played a vital role in determining the rate of metal removal kinetics. The experimental data was successfully analysed by the pseudo-second-order rate model, demonstrating that chemisorption is the main rate limiting step for the removal of Sr^{2+}, Co^{2+} and Cs^{+} from solution. In this study, the adsorption behaviour of protons and of Sr^{2+}, Co^{2+} and Cs^{+} onto the bacterial consortium cell surfaces was evaluated under anaerobic conditions as a function of pH (4-10), ionic strength (0.01, 0.05, 0.1M) and temperature (25, 50 and 75°C). Acid-base titrations of the bacterial suspension indicated that the titration data could be adequately described by a four site nonelectrostatic model, with pK_a values of 4.41, 6.69, 8.10 and 10.

The Sr^{2+}, Co^{2+} and Cs^{+} adsorption data could be fitted with a two site nonelectrostatic model, involving the type 1 and 2 sites (carboxylic and phosphoryl sites). Increasing the ionic strength had a negative effect on the adsorption of metal ions from solution. There was no observed temperature dependence on the adsorption of Co^{2+} and Cs^{+} from solution. In summary, results obtained in this study have shown that the processes involved in microbial Sr^{2+}, Co^{2+} and Cs^{+} removal from contaminated sources is a direct function of the microbial characteristics and efficiency, mass transfer and surface complexation effects under varying environmental conditions. One important goal to be achieved in future studies will be the determination of the intrinsic stability constants and the structure of the formed metal-complexes species. These constants can be used directly in risk assessment programs.

DECLARATION

I Nonhlanhla Ngwenya, declare that the thesis which I hereby submit for a Doctor of Philosophy in Chemical Technology degree at the University of Pretoria is my own work and has not been previously submitted by me for any degree at this or other institutions.

_____ _____

Nonhlanhla Ngwenya Date

ACKNOWLEDGEMENTS

A major research project like this is never the work of anyone alone. First and above all, I thank God for the wisdom and perseverance that he bestowed upon me and for granting me the capability to succeed.

I would also like to extend my sincere gratitude to:

- The study leader, Prof. Evans Chirwa, for accepting me into his research group, and for his generous time and support throughout the duration of this study.
- Dr Chris Daughney for his generosity by sharing with me the program FITMOD and also his time and assistance with surface complexation modeling studies.
- The South African Nuclear Human Asset Research Programme (SANHARP) team and the National Research Foundation (NRF) of South Africa, for financial assistance to whom I am indebted to.
- Colleagues and friends from the Water Utilisation Research Group for their support and friendship

I would like to pass my heartfelt gratitude to my family for their unconditional support. To my Father, who bid this life an early farewell, I wish you would have lived longer to see me graduate, rest in peace Mabuya. To George, my true friend and partner, thank you for encouraging me to enter the doctoral program, and for giving up your PhD degree so I can have mine; for having more faith in me than I had in myself; you have always built my confidence and sustained faith in my abilities, thank you. During my time as a student I had the opportunity to be a mother to an energetic little boy, who also contributed immensely in shaping me as a person.

'I Owe You All More Than Words Can Tell'

TABLE OF CONTENTS

LIST OF FIGURES

PAGE

LIST OF TABLES

PAGE

NOMENCLATURE

A	External sorption area (m^2/g)
a_{RP}	Redlich–Peterson adsorption constant ($(l\ mg^{-1})^{\beta}$)
β	Redlich–Peterson adsorption constant
b	Langmuir adsorption constant ($l\ mg^{-1}$)
C	Metal concentration at time t (mg/L).
C_{eq}	Residual metal ion concentration at equilibrium ($mg\ l^{-1}$)
C_{ini}	Initial concentration of metal in solution (mg/L),
C_t	Metal concentration at time t (mg/L)
C_0	Initial metal ion concentration ($mg\ l^{-1}$)
k_1	First-order adsorption rate constant (min^{-1})
k_2	Second-order adsorption rate constant ($g\ mg^{-1}\ min^{-1}$)
k_C	Second-order rate coefficient (L/mg/h)
k_f	External diffusion coefficient (cm/s).
k_i	Intraparticle diffusion rate ($mg.g.min^{0.5}$).
k	Freundlich adsorption constant
K_s	Half saturation constant (mg/L)
n	Freundlich adsorption constant
n_p	Number of data points
n_{II}	Number of chemical components for which both total and free concentration are known
n_u	Number of adjustable parameters.
q	Adsorbed metal ion quantity per gram of biomass at any time ($mg\ g^{-1}$)
q_{eq}	Adsorbed metal ion quantity per gram of alga at equilibrium ($mg\ g^{-1}$)

Q^0	Langmuir adsorption constant (mg g^{-1})
q_{max}	Maximum sorption capacity (mg.g^{-1})
R	Gas constant (=8.314 J mol^{-1} K^{-1})
R^2	Correlation coefficient
S	Sulphate concentration (mg/L)
$S_{,mod}$	Calculated (model) concentration at time t (mg/L),
$S_{,exp}$	Experimental concentration at time t (mg/L)
S_Y	Default experimental error calculated by FITMOD
t	Time (minutes)
T	Solution temperature (°C, K)
μ	Specific growth rate (1/h)
μ_{max}	Maximum specific growth rate (1/h)
Y	*E*rror in the mass balance calculations
X	Bacterial concentration (mg l^{-1})
$Y_{x/s}$	Bacterial yield coefficient (mg of biomass produced per mg substrate utilized)

CHAPTER 1

INTRODUCTION

1.1 INTRODUCTION

In the early days of the nuclear technology, nuclear waste management was thought to be an easy task that is modest and readily amenable to solutions. The underground deposition of nuclear and uranium waste materials in sealed steel canisters was identified as one of the key strategies that can ensure the protection of people and the environment, now and in the future. However, sixty years into the nuclear age, radioactive waste disposal in subsurface nuclear repositories has become an increasingly intractable problem (Crowley, 1997). Currently, designing efficient nuclear waste isolation canisters is not the only problem faced by the nuclear industry; there are still unresolved problems of possible groundwater pollution due to the leakage of radionuclides from sites of their disposal. In particular, the presence of radioisotope fission products, even at low concentrations, in the environment is of more concern (Francis, 1998). This is due to their high radiological decay rates, their decay-heat production, and their potential biological hazards to lower and higher living organisms. Among these, cesium (Cs) and strontium (Sr), which are produced by the fission of uranium or plutonium in relatively high yields, are among the most hazardous radiotoxic contaminants for the environment (Watson et al., 1989). Sr-90 is among the radionuclides of concern because of its long half-life (28 years), and most importantly high retention in the body due to its chemical similarity with calcium. The radioisotopes of Cs (Cs-137 and Cs-135) also pose a serious radiation hazard due to their long half-life (2×10^6 and 30 years, respectively), and high solubilities, mobilities and bioavailability in aqueous systems (Chicote et al., 2004).

In the past, contaminated groundwater sources have been treated using the pump and treat method. However, this method is neither cost effective nor reliable as it can not guarantee complete remediation of the contaminated site. On the other hand, the use of conventional adsorbents, such as zeolites and synthetic organic ion exchangers, for radionuclide clean-up is their unsuitability at high pH, high sodium concentrations, and in irradiated environments (Chaalal and Islam, 2001). Therefore, these findings advocate an urgent ideological shift from the current conventional nuclear waste management practices to new or existing paradigms to ensure sustainability of the nuclear technology. The basic concepts of these paradigm shifts include**;** the use of environmentally friendly waste management methods, the

development of cost-effective methods for *in situ* containment and stabilization of contaminants, and maintaining retrievability of the disposed waste (National Research Council, 1996; North, 1999). The present study is a detailed investigation on the potential role and applicability of biological remediation (bioremediation) methods as an alternative for the selective uptake of metallic fission products from contaminated water sources. This study is an effort towards elucidation of the crucial microbial mechanisms during metal bioremediation as an initial step towards the successful development and proper design of biological containment barrier technologies at radionuclide-contaminated aquifers.

1.2 AIM AND OBJECTIVES

The main aim of this study is to investigate the potential role of natural microbial processes, as means for controlling radionuclide dispersion in the environment through biological containment. The specific objectives for this study are:

- To investigate the kinetics of bacterial growth and inhibition, as well as culture diversity changes during Sr^{2+}, Co^{2+} and Cs^{+} bioremediation in a batch anaerobic bioreactor
- To evaluate the biosorption kinetics and identify mechanisms of Sr^{2+}, Cs^{+} and Co^{2+} biosorption in a batch SRB bioreactor under bacterial growth and non-growth conditions.
- To identify the key bacterial surface reactive sites that effect metal adsorption, and determine the stability of the metal complexes formed during microbial metal immobilization.
- To evaluate the effect of ionic strength and temperature on the bacterial adsorptive properties, as well as the stability of Sr, Co and Cs complexes on the bacterial cell surface.

1.3 SCOPE OF THE STUDY

The present study investigates the potential application of microbial technology (or bioremediation) for controlling radionuclide dispersion as a strategy of safeguarding against long term environmental pollution. In essence, this study addresses three sets of questions; (1) can these microorganisms survive and perform satisfactorily under conditions of variable (low to high) metal concentrations?, (2) What are the main mechanism(s) for metal immobilization in the bioreactor under bacterial growth and non-growth conditions, (3) What

are the effect(s) of varying pH, ionic strength and temperature on the biosorptive properties of the bacteria, and stability of the immobile metal complexes formed? Currently, several studies focusing on the application of *in situ* bioprecipitation (ISBP) in the presence of sulphate reducing bacteria (SRB), as an effective method of metal removal from contaminated groundwater have been undertaken. However, there are limited studies on the immobilization of metal pollutants, mainly through biosorption, in the presence of SRB. Thus, this thesis establishes the applicability and performance of different bioremediation techniques for metal removal in an artificial contaminated aqueous system under anaerobic conditions. This study also enhances the scope of metal/radionuclide chemistry, speciation and the stability of the metal complexes in contaminated aqueous systems, under variable environmental conditions. It also considers the basic requirements for microorganism survival and performance in these conditions. This thesis can be also considered among the few to investigate the SRB cell-metal interactions with prospects of controlling subsurface radionuclide decontamination under high metal, ionic strength and anaerobic conditions.

1.4 METHODOLOGY

This study includes four basic parts; (1) an introduction to the present study, and a review of the relevant literature necessary for tackling the subject at hand, (2) an overview of the approach used to conduct the research, and (3) a thorough discussion of the results obtained and implications for addressing the problem, and lastly (4) conclusions based on the results obtained, as well recommendations. Experiments are conducted under conditions that closely represent radionuclide contaminated aqueous system, which is anoxic and of variable pH, temperature and ionic strength. Prior to metal removal experiments, SRB growth was stimulated by a series of enrichment procedures. Functional bench-scale batch anaerobic bioreactors (2L) were used for evaluating the bacterial population and diversity changes, sulphate consumption, pH changes and metal removal over the treatment period. By monitoring the SRB community responses, the potential use of metal-specific SRB cultures as the reactive component in PRBs for metal immobilization, were revealed. Further batch equilibrium metal adsorption experiments were conducted in rubber-sealed anaerobic serum bottles (100 mL) under non-growth conditions, to investigate the complexation of metal ions onto bacterial cell surfaces. Results from these experiments, were able to provide vital information on the stability of the metal complexes, and the effect of pH, ionic strength and temperature on the passive adsorption of the metals by the bacterial culture.

1.5 SIGNIFICANCE OF THE STUDY

The value of the present study is that it presents a different perspective on a topic that has raised concern but has not been systematically addressed due to lack of information. This study presents a conceptual framework for the applicability of bioremediation as means of controlling radionuclide mobility in the subsurface environment. The biological and chemical reaction mechanisms that facilitate metal uptake, stability of the metal ion-bacteria complexes formed and other considerations regarding microbial metal immobilization processes are presented. The well researched scientific ideas, analytical information and findings contained in this thesis can help to improve the scientific basis for the performance assessment of microbial technologies for radionuclide immobilization. At the same time, it also prepares other researchers for the challenges and conditions to be met for undertaking such study. Taken in combination with other research findings, this study should considerably progress the development of a rational strategy to the vexing challenge of radionuclide mobility and migration in underground nuclear waste repositories, and a useful contribution towards implementation of national policy towards radioactive waste management.

CHAPTER 2

LITERATURE REVIEW

2.1 BACKGROUND

Due to the impact of the rapidly growing demand for energy, as well as the concerns about global warming, there has been a resurgence of interest in nuclear energy. Nuclear energy is one of the few economically viable base-load electricity generation technologies, which could help reduce the current output of CO_2 emissions in to the atmosphere by approximately 8% (Mourogov et al., 2002). The world's nuclear generating capacity currently stands at about 372 GWe, with the United States of America and France as the major producers, 27 and 17 percent, respectively (Figure 2.1). Electricity consumption in South Africa has been steadily increasing since the 1980s and it is predicted that by the year 2025 electricity demand will exceed supply (Musango et al., 2009). Therefore, in order to be able to meet future domestic and industrial electricity demands, there has been a renewed interest in the production of nuclear power. While there has been an improved public perception of the nuclear technology, some of the leading problems associated with this technology still remain. Up to date, no suitable alternative route of radioactive waste treatment has yet been formulated; while in the interim huge amounts of spent fuel are discharged globally (Lior, 2008).

The primary waste form resulting from nuclear energy production is spent nuclear fuel (SNF). The presence and toxicity of long-lived actinides and their fission products in spent fuel is of primary concern because of their potential for migration from the waste repositories and contaminated sites to the environment (Francis, 1998). Currently, two spent fuel management paths are being pursued; reprocessing and direct disposal. In some countries, reprocessing has been thought to be a better option; while in some there is broad scientific agreement that deep geologic disposal using a system of engineered and natural barriers to isolate the waste is the best. However, about 40 years after geological disposal has been recommended, neither the United States of America nor any other country has succeeded in developing a safe repository for their high level waste (HLW) (North, 1998).

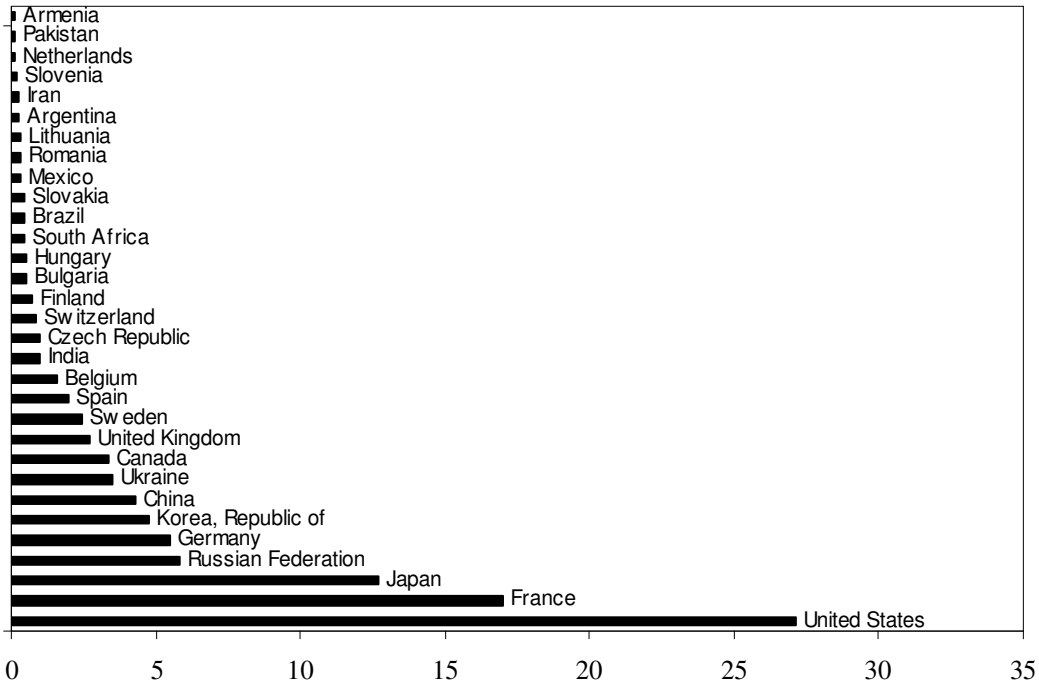

Figure 2.1: Global nuclear power generating capacity (%) per country (IAEA, 2009).

2.2 SPENT NUCLEAR FUEL MANAGEMENT

2.2.1 Structure and Composition of Spent Nuclear Fuel

The most predominant type of fuel used in most nuclear reactors is UO_2, and in some cases metallic U or a combination of UO_2 and PuO_2 (Kleykamp, 1985). The UO_2 fule contains radionuclides, which can be separated into a number of distinct categories; (1) fission products which migrate to grain boundaries in the fuel and occur as finely dispersed fission gas bubbles, such as Xe and Kr; (2) metallic fission products, such as Mo, Tc, Ru, Rh, and Pd, which occur in the grain boundaries as immiscible, micron to nanometre sized metallic precipitates (ε-particles); (3) fission products that occur as oxide precipitates of Rb, Cs, Ba, and Zr, and (4) fission products that form solid solutions with the UO_2 fuel matrix, such as Sr, Zr, Nb, and the rare earth elements (Figure 2.2) (Kleykamp, 1985; Shoesmith et al., 2000; Buck et al., 2004; Bruno and Ewing, 2006).

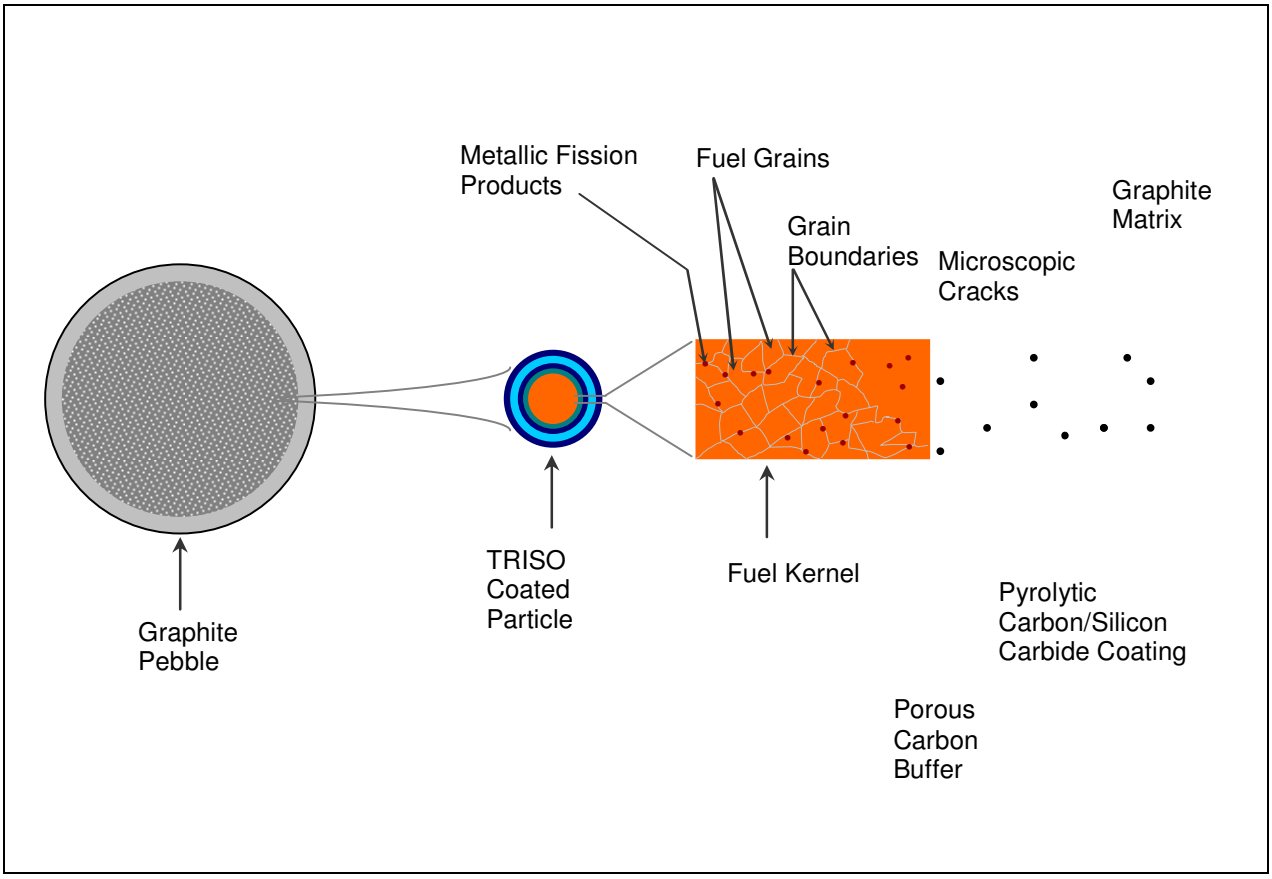

Figure 2.2: Schematic representation of spent nuclear fuel structure and propagation of fission products and impurities (Adapted from Chirwa, 2010).

2.2.2 Spent Nuclear Fuel Reprocessing

Currently, spent fuel reprocessing is the most widely used method, and different countries employ different reprocessing techniques, depending on the type of waste, level of activity and their state (gas, liquid or solid) (Figure 2.3). Commercial reprocessing methods that have been developed for use include variants of the PUREX (plutonium/uranium extraction) process, and UREX+ reprocessing with transmutation (Lagus, 2005). During the PUREX process plutonium and uranium are each separated from the other spent fuel products which are then vitrified and stored in a geological repository. The UREX+ technology with accelerated transmutation of waste (ATW) improves on the conventional PUREX technology by mixing the plutonium with minor actinides, making the process more proliferation-resistant (Lagus, 2005). Apart from the

high costs involved, reprocessing results in the generation of huge amounts of radioactive solid and liquid wastes. Solid radioactive waste such as fuel element cladding hulls, hardware, and other insoluble residues are generated during fuel dissolution. They may contain activation products, as well as some undissolved fission products, uranium and plutonium (Buck et al., 2004). Therefore, proliferation risks are and will be the major detriments to reprocessing. Although new technologies, such as transmutation, have been demonstrated to help curb proliferation risks, much research is still needed to formalize their industrial application (Bunn et al., 2003).

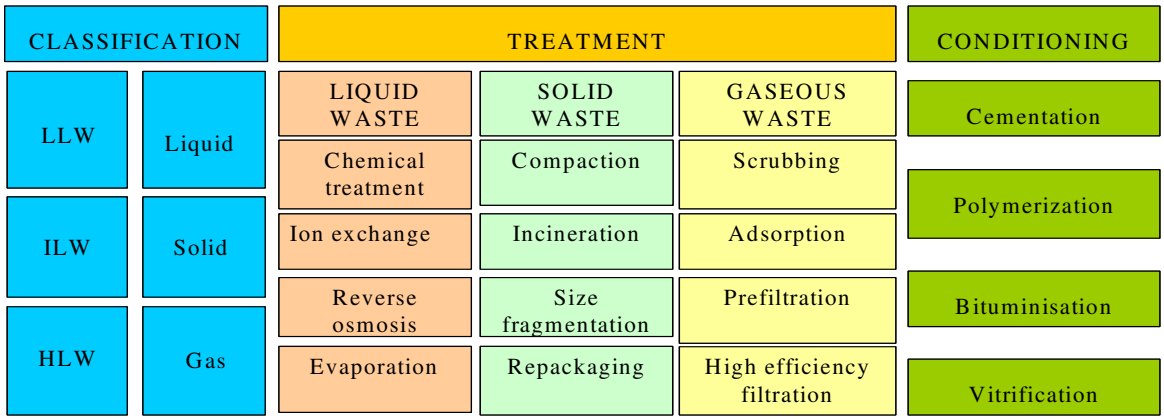

Figure 2.3: Common nuclear waste management practices. LLW= low level waste, ILW=intermediate level waste and HLW=high level waste (Adapted from Raj et al., 2006).

2.2.3 Spent Nuclear Fuel Disposal

The predominant form of high level nuclear waste available for disposal is the spent fuel bundle discharged from reactor. The radioactivity, chemistry and thermal output are the main factors that are considered for proper spent nuclear fuel disposal (Long and Ewing, 2004). The fundamental concept of nuclear waste disposal sites is the isolation of the high level waste in deep geologic settings; and that the geologic medium itself coupled to the waste form and other engineered barriers should isolate the waste from the biosphere without active monitoring or control by future societies. Geologic disposal relies on the concept of a series of multiple barriers, each designed to limit radionuclide release, and these include the natural barriers (the

groundwater flow system and the rocks/clays that constitute the geologic setting) and the engineered barriers (such as the waste form, canisters, and backfill). For high-level waste (HLW) including spent nuclear fuel, massive engineered barriers have been designed which, where in an appropriate geological setting, should provide the required assurance of safety. However, numerous recent studies have shown that waste repositories are sites of enhanced ecological danger mainly due to canister corrosion problems resulting in the release of the waste contents into the environment (Kosareva et al., 2006; Bazansak et al., 1999). The main factors that have been found to exacerbate canister corrosion problems include; presence of water and oxygen, high temperatures, and most importantly the presence of microorganisms, causing the so called 'microbially-induced corrosion' (Bennett and Gens, 2008; Johnson and King, 2008; Bruhn et al., 2009). In several cases, spent fuel repositories have been compromised, leading to contamination of huge volumes of soil and groundwater. For example, at the Hanford site through leakage from surface disposal sites and tank leakage at the near-surface transuranic storage facilities at the Savannah River site. Buried nuclear wastes consist of concentrated forms of various radioactive chemical compounds, which if exposed to the general population, may cause serious life-threatening disorders (Bazansak et al., 1999).

2.3 ENVIRONMENTAL FISSION PRODUCT CONTAMINATION

2.3.1 Speciation and Chemistry of Fission Products

Migration of radionuclide contaminants depends on, among others, the radio element itself, speciation and the nature of the exchanging medium. Particularly, it has been suggested that aqueous speciation of some radionuclides (e.g., Co-60, Cs-137, Am-241, Pu-239, and Cm-244) plays an important role in sorption, hence retardation of contaminants in aquifers (Caron and Mankarios, 2004). The redox chemistry of fission products differs from other radionuclides because of the limited oxidation states. For example, both Cs and Sr exist in only one oxidation state, (Cs^+ and Sr^{2+}, respectively) and their environmental behaviour is therefore not dependent on any redox chemistry. Their oxidation states account for their high bioavailability and mobility in the environment (Siminoff et al., 2007). Cs^+ is a very soft, ductile, alkali metal that is liquid at 28.4°C. It is the most electropositive and reactive of the alkali metals and forms compounds with a variety of anions and alloys with the other alkali metals and with gold. The predominant aqueous species in groundwater is the uncomplexed Cs^+ ion (Lujaniene et al., 2006). Sr^{2+}, like

other alkaline earth metals, forms complexes and insoluble precipitates. Technetium (Tc) is known to exist in all oxidation states from +7 to -1. However, there are only two environmentally stable oxidation states, Tc(VII), as the anion TcO_4^- and Tc(IV). The dominant species in natural aqueous solutions in equilibrium with the atmosphere is the pertechnetate (TcO_4^-), which has a high geochemical mobility and bioavailability (Lloyd et al., 2002; Lloyd and Renshaw, 2005). One other specific radionuclide of concern is Co-60 due to its strong potential for offsite migration. In the presence of organic chelating agents, such as EDTA, Co-60 forms stable complexes, thus increasing its aqueous solubility and potential for transport offsite (Means et al., 1978). Cobalt isotopes are also important contaminants, and they are activation products in metallic structures of nuclear power plants. Co only exists in two oxidation states; Co(III) and Co(II), with the latter/former, being the most predominant in aqueous ecosystems (Simonoff et al., 2007).

2.3.2 Mechanisms of Release into the Environment

One of the key processes here is the dissolution of the spent nuclear fuel matrix in groundwater, liberating radioactive fission products and actinides (Smellie and Karlsson, 1999). In subsurface granitic groundwaters (500-700 m deep), the conditions are reducing and UO_2 has very low solubility. However, the ionizing radiation emitted from the spent nuclear fuel induces radiolysis of the groundwater resulting in the production of both oxidants ($OH^\bullet$, H_2O_2, $HO_2^\bullet$, and O_2) and reductants (e^-_{aq}, $H^\bullet$ and H_2) at the fuel interface. The oxidants produced can result in the oxidation of the insoluble U(IV) in the fuel matrix to the significantly more soluble U(VI), and thereby enhance matrix dissolution. Microbial gas production has also been reported to result in a local increase in pressure in the repository, allowing the development of fissures, and consequently the discharge of radionuclides into the adjacent environment (West and McKinley, 2001; Jonsson et al., 2007). Bioleaching of the waste form due to microbially produced ligands is another most likely mechanism by which radionuclides could be mobilized and distributed to the biosphere (Brainard et al., 1992). Microbially-induced corrosion (MIC) has also been reported to facilitate the release of radionuclides to the biosphere (Little et al., 1991; King and Stroes-Gascoyne, 1995; Parmar et al., 2000; Johnson and King, 2008; Bruhn et al., 2009).

2.3.3 Biological Hazards of Fission Products

The presence of fission products in the environment is of particular concern because of their high radiological decay rates, their decay-heat production, and their potential biological hazards. Fission products such as cesium (Cs-137) and strontium (Sr-90), which are produced by the fission of uranium or plutonium in relatively high yield, are the most hazardous radiotoxic contaminants for the environment. These products pose a serious radiation hazard to the health of man and the environment. Due to its chemical similarity with calcium, Sr-90 is easily incorporated into bone and continues to irradiate localized tissues with the eventual development of bone sarcoma and leukemia (Kossman and Weiss, 2000; Noshchenko et al., 2001; Dewiere et al., 2004; Greve et al., 2007). The radioisotopes of Cs (Cs-137 and Cs-135) are also hazardous due to their long half-lives (2×10^6 and 30 years, respectively), and high solubilities, mobilities and bioavailability (Lujaniene et al., 2006). Cs is analogous to K^+, and enters cells via pathways for K^+, and the specific mechanisms by which Cs^+ is transported into the cell have been reviewed by Lloyd and Macaskie (2000). The activation product, Co, is another radionuclide of concern, particularly in radiation protection as it is a key γ-ray source. The conventional approach for radiation protection is based on the International Commission of Radiological Protection (ICRP) model, the linear no threshold (LNT) model of radiation carcinogenesis, which implies that ionizing radiation is always harmful, no matter how small the dose (Chen et al., 2007).

2.3.4 Fission Product Treatment Options

Common methods used for the removal of Sr-90, Cs-137 and Co-60 from storage pool water are *ex situ* removal technologies, which include; adsorption on zeolites and synthetic organic ion exchangers (Ebner et al., 2001; Paterson-Beedle et al., 2006; Smiciklas et al., 2006). However, the main disadvantages with the above methods is their unsuitability at high pH, high sodium concentrations, and in irradiated environments (Chaalal and Islam, 2001). The efficient removal and recovery of other fission products, particularly radioiodine, technetium, using physical and chemical methods are somewhat more difficult, and are still under development. In Japan, the use of inorganic sorbents for fission product removal is under investigation, while the use of extractants such as crown ethers, cobalt dicarbollides and calix-crown ethers have also been studied with some success in the United States of America, Czech Republic and France, respectively.

Apart from the high costs involved, physical and chemical methods are well known to be aggressive and invasive treatment strategies that can have negative impacts on biodiversity and can even result in increased dispersion of radioactive materials (Bazansak et al., 1999; Lloyd and Renshaw, 2005). Given the technical limitations of physico-chemical approaches, there has been an unprecedented attention on the application of innovative techniques for fission products waste treatment. Among the most successful and widely used innovative technologies for cleanup of sites contaminated with hazardous chemicals is bioremediation (the use of microorganisms or microbial processes to treat environmental metal/radionuclide contamination) (Kumar et al., 2007). Bioremediation exploits the metabolic reactions of microorganisms to destroy contaminants or to transform them into species whose mobility is controlled (Banazsak et al 1999). Bioremediation is relatively cost effective, as target compounds are stabilized and/or detoxified by the biomass, eliminating the need for expensive chemical additions to achieve the desired treatment goals (Mulligan et al., 2001). Given the potential environmental and financial benefits of bioremediation, the microbial immobilization of long-lived fission products under geologic repository settings, surprisingly, has received less attention.

The main treatment goals for nuclear wastes by biological approaches include, for example, the selective accumulation of radionuclides for possible recovery or ultimate disposal, the immobilization of radionuclides in a subsurface aquifer to prevent migration into water supplies, or the selective leaching of radionuclides from contaminated soil (Lloyd and Lovley, 2001). Ideally subsurface bioremediation strategies should require less or no maintenance; and for this reason there has been a widespread investigation of passive biological remediation techniques (Hedin et al., 1994; Younger et al., 2002). On the other hand, active *in situ* bioremediation treatment depends on the viability and activity of the microorganisms, which might not always be the case under high metal and radioactive stress conditions. Active bioremediation treatment requires regular monitoring of the inhabiting microbial communities. Nonetheless, both techniques rely on microbial processes that effect the retardation of fission products mobility in subsurface environments, through bioprecipitation, bioaccumulation, biosorption, and biotransformation (Lloyd and Macaskie 2000; Lloyd et al., 2002; Lloyd and Renshaw, 2005).

2.4 METAL IONS UPTAKE BY BACTERIA

2.4.1 Microbial Mechanisms of Metal Uptake

Microorganisms possess mechanisms by which metal ions can be taken up and accumulated from their environment. An understanding of these mechanisms is vital for the optimization of the bioremediation process. In addition, this understanding is essential in order to fully utilize the selectivity and efficiency of the process and to overcome ionic competition and interference effects by other ionic species which exist along with the targeted element in the ionic matrix of the contact solution (Tsezos and Volesky, 1982; Lovley and Phillips, 1992; Avery and Tobin, 1992; Beveridge and Murray, 1980). Based on cell metabolism, the uptake of metals can be classified into two classes; metabolism dependent and non-metabolism dependent metal uptake. The process of metabolism dependent metal uptake is strictly dependent on cell metabolism and involves active translocation of metals into the cell, which results in the accumulation of the metal inside the cell (Gadd, 1989). On the other hand, during non-metabolism dependent, physico-chemical interactions, such as; physical adsorption, ion exchange and chemical sorption; between the metal and microbial cell surface facilitate metal uptake (Kuyucak and Volesky, 1988). The four well known microbial processes that effect metal uptake; bioprecipitation, bioaccumulation, biotransformation and biosorption, are briefly presented below, and are used as illustration of the wide variety of physical-chemical phenomena which are involved during metal uptake.

Bioprecipitation

Bioprecipitation of metals by microorganisms may be either metabolism dependent or independent. During metabolism-dependent precipitation or dissimilatory reduction, the transformation of the metal is unrelated to its intake by the microbial catalyst. Consequently, the reduced metal is precipitated in the extracellular medium, as a defense system (Valls and de Lorenzo, 2002). For example, Cd removal from solution by *Arthrobacter* and *Pseudomonas* (Scott and Palmer, 1990) and the enzymatic precipitation of various heavy metals including; U(VI), Cr(VI), Tc(VI) and As(V) by SRB (Lloyd, 2003). In the case where precipitation is independent of cellular metabolism, it is normally a result of the chemical interaction between the metal and a biogenic ligand (Veglio and Beolchini, 1997). Biogenic ligands are generated during cell metabolism and they inclide; phosphates, carbonates and sulphides, which can result

in the precipitation of metals and radionuclides (stable or radioactive) ions, and hence their immobilization. Examples include; the formation of less soluble metal sulphides in the presence of SRB (White et al., 1997), the precipitation of strontium carbonate, by carbonates produced by *Ralstonia eutropha* and *Pseudomonas fluorescens* (Anderson and Appanna, 1994), and precipitation of soluble U(VI) compounds to insoluble U(IV) hydroxide or carbonate at neutral pH (Phillips et al., 1995). In other microorganisms metal precipitation is mediated by the liberation of inorganic compounds, such as; oxalates, phosphates or hydroxides from organic donor molecules (Tucker et al., 1998). A well documented example involves the precipitation of metals as by *Citrobacter sp.* This bacterium was found to be tolerant to high concentrations of U, Ni, and Zr through the formation of highly insoluble metal phosphates (Macaskie et al., 2000).

Bioaccumulation

Bioaccumulation is an energy dependent process of metal uptake against a concentration gradient. During bioaccumulation metals are transported from the outside of the microbial cell, across the cellular membrane, and into the cell cytoplasm, where the metal is sequestered and therefore immobilized. Examples include the intracellular accumulation of Hg, Pb, Ag and Cd by *Escherichia coli* using an energy dependent transport system (Gadd, 1988). In the case of radionuclides, they may enter microbial cells through a classical transport system, as would an ion normally involved in the physiology of the cell, for example; Cs^{+} instead of K^{+} or Sr^{2+} and Ra^{2+} instead of Ca^{2+} (Simonoff et al., 2007; Greve et al., 2007). Once in the cell, radionuclide is sequestrated by cystein-rich metallothioneins (Turner and Robinson, 1995).

Biotransformation

Radionuclides, including U(VI), Pu(VI), Tc(VII), Co(III), have been subjected to enzymatic biotransformation by microorganisms from soluble mobile forms to reduced and less soluble forms (Francis, 1998; Gorby et al., 1998; Istok et al., 2004). Bioreduction can result in the precipitation of solid radionuclides through enzymatic reduction, or biomethylation (production of volatile derivatives). The extracellular enzymatic transformation of radionuclides by microbial isolates, such as, *Desulfovibrio desulfuricans*, *Geobacter sulfurreducens, Geothrix fermentans*, *Deltaproteobacteria*, and *Clostridium*, is well documented (Lloyd et al., 2003; Suzuki et al., 2003; Brodie et al., 2006). Biomethylation can produce volatile methyl derivates, as for Se, Tc,

Hg, I, and so decrease the concentration of soluble contaminants in water or soil. Biodegradation of associated organic compounds has been observed with citrate, which forms highly soluble radionuclide citrate complexes. These complexes can then be degraded by microorganisms resulting in the precipitation of the radionuclides as observed with *Pseudomonas aeruginosa* and *P. putida* (Thomas et al., 2000).

Biosorption

Biosorption, the passive sequestration of metals by interactions with live or dead biological materials, is a practical and rather widely used approach for the bioremediation metal and radionuclide contamination (Barkay and Schaefer, 2001). Mechanisms responsible for biosorption, may be one or a combination of ion exchange, complexation, coordination, adsorption, electrostatic interaction, chelation and microprecipitation (Veglio and Beolchini, 1997; Vijayaraghavan and Yun, 2008; Wang and Chen, 2006). The surface of cells carries a net negative charge due to the presence of carboxyl, hydroxyl, phosphate and sulphydryl groups, and so during biosorption the metal cations are strongly bound (Beveridge, 1989). In the laboratory, the process of metal biosorption can be performed using several approaches; in batch and continuous modes of operation. Most industrial applications prefer a continuous mode of operation, however, batch bioreactor experiments have been found to be useful in evaluating required fundamental information, such as biosorbent efficiency, optimum experimental conditions, biosorption rate and possibility of biomass regeneration (Veglio and Beolchini, 1997; Gadd, 2009). Over the years, metal adsorption onto bacteria has acquired great importance in existing efforts towards environmental bioremediation, and there is still ongoing research on the adsorption of metal ions under varying conditions (Avery and Tobin, 1992; Lloyd and Macaskie, 2000; Parmar et al., 2000; Borrok and Fein, 2005).

2.4.2 Genetic Diversity of Bacterial Biosorbents

In the last decade or so, a significant amount of research has been conducted on the genetic diversity of microorganisms capable of accumulating metal ions from solution (Volesky and Holan, 1995; Gadd, 2000; Valls and de Lorenzo, 2002; Zouboulis et al., 2004). Among these, bacteria have received increasing attention for heavy metal removal and recovery due to their good performance, low cost and abundance (Wang and Chen, 2009). In addition, bacteria are

capable of growing under controlled conditions and are resilient to a wide range of environmental situations, including radionuclide polluted sites (Urrutia, 1997). Since then, a wide array of bacterial species has been discovered as excellent biosorbents for the removal of different metal and radionuclide ions (Table 2.1). One of the most successful and well documented bacterial bioremediation strategies involves sulphate reducing bacteria (SRB). Maximum SRB growth occurs around slightly acidic to slightly alkaline pH (between pH 6-8), with a few exceptional strains that are acid-tolerant and can grow in the pH range 3-4 (White et al., 1997). Most SRB are mesophilic, attaining optimum growth at a temperature range of 25°C-30°C. Some, however, are able to grow at temperatures below 5°C while spore forming thermophilic species grow at temperatures ranging from 65°C to 85°C. SRB are important members of microbial communities with economic, environmental and biotechnological interest. They have been investigated for the removal of a wide variety of metals and radionuclides, such as As, Cr, Fe, Hg, Pd, Pt, Mn, Mo, Rh, Se, Te, Tc, U and Zn (Lovley and Phillips, 1992; Lloyd et al., 1998; Tebo and Obraztsova, 1998; Tucker et al., 1998; Smith and Gadd, 2000; Lloyd et al., 2001; Rashamuse, 2003; Ngwenya and Whitely, 2006; Jin et al., 2007).

Table 2.1 Genetic diversity of bacterial biosorbents

SPECIES	METAL ION	REFERENCES
Bacillus sp.	Al, Cd, Cr, Co, Cu, Fe, Ni, Pb, Sr	Fein et al., 1997; Zouboulis et al., 2004; Philip and Venkobachar , 2001; Srinath et al., 2003
Citrobacter sp.	Ag, Pb, Cd, Th, U, Zn	Macaskie et al., 1987; Jeong et al., 1997; Yong and Macaskie, 1997; Puranik and Paknikar, 1999; Xie et al., 2008
Sulphate reducing bacteria *sp.*	Au, Cr, Cu, Mo, Pd, Se, Tc, U, Zn	Chen et al., 2000; Creamer et al., 2006; Lovley and Phillips, 1992; Lloyd et al., 1999; Tucker et al., 1998
Escherichia coli	Ag, Au, Cd, Cr, Cu, Fe, Hg, Ni	Churchill et al.,1995; Weon et al., 2003; Ansaria and Malik, 2007; Deplanche and Macaskie, 2008; Quintelas et al., 2009
Pseudomonas sp	Cd, Cr, Co, Cu, Mn, Ni, U, Zn	Pardo et al., 2003; Vullo et al., 2008; Choi et al., 2009; Ziagova et al., 2007
Thiobacillus sp	Cu, Zn	Liu et al., 2004
Geobacillus sp	Cd, Cu, Mn, Ni and Zn	Ozdemir et al., 2009
Enterobacter sp	Cu, Cd, Pb	Lu et al., 2006
Streptomyces sp	Cd, Fe, Ni	Puranik et al., 1995, Selatnia et al., 2004

They are obligate anaerobes that decompose simple organic compounds using sulphate as the terminal electron acceptor. The result is the production of sulphide that may be given off as H_2S gas or react with metals to form less soluble metal sulphides (White and Gadd, 1996; White et al., 1995). The advantages of using SRB for bioremediation is the knowledge that they (i) possess a high metal-sequestering ability due to the presence of extracellular polymeric substances (EPS) that play a major role in the sorption of metals (Beech and Cheung, 1995; Braissant et al., 2007), (ii) are suitable for the treatment of high volume and low concentration complex wastewaters, (iii) are well recognised as principal inhabitants of deep geologic repositories, and have been shown to survive in such extreme ecosystems, which are anoxic and irradiated (Pederson et al., 2000; Haveman and Pederson, 2002; Chicote et al., 2004; Bruhn et al., 2009), (iv) metal removal by SRB is not limited to *ex situ* treatment in sulphidogenic bioreactors (Goncalves et al., 2007), but can also be applied *in situ* passive systems, such as artificial wetlands and, more recently, permeable reactive barriers (PRB) (Costa et al., 2008).

Metal ions uptake by biomass mainly depends on the components on the cell surface and the spatial structure of the cell wall. Peptidoglycan, teichoic acids and lipoteichoic acids are all important chemical components of bacterial surface structures. Some functional groups have also been found to bind metal ions, especially carboxyl group. In other studies, it has been shown that the O-, N-, S-, or P-containing groups also participate directly in the binding a certain metals (Darnall et al., 1986). Some active sites involved in the metal uptake are determined by using techniques of titration, infra-red and Raman spectroscopy, electron dispersive spectroscopy (EDS), X-ray photoelectron spectroscopy (XPS), electron microscopy (scanning and/or transmission), nuclear magnetic resonance (NMR), X-ray diffraction analysis (XRD), and XAFS (X-ray absorption fine structure spectroscopy) (Volesky, 2007).

2.5 METAL ADSORPTION BY BACTERIA

2.5.1 Factors Influencing Metal Ions Adsorption by Bacteria

Metal ions adsorption by bacterial biomass mainly depends on the metal involved and ionic charges of metal ion, the chemical composition of the metal ion solution and other external environmental factors such as solution pH, temperature, ionic strength, bacteria dosage, initial solute concentration and agitation rate (Gadd, 1986; Volesky, 1990; Vijayaraghavan and Yun,

2008). These factors do not only have an effect on the adsorptive properties of the bacterial surface reactive sites, but might also influence the stability of metal complexes (Benner et al., 1999). Therefore, an investigation of the effect of these factors on metal adsorption onto the microbial biomass is essential for the industrial application of biosorption, as it gives information about the performance of the process which is necessary for process design (Gadd, 2009).

Effect of pH

Solution pH seems to be the most important parameter in the adsorption of metals, as it affects the solution chemistry of the metals, the activity of the functional groups on the biomass cell surface and the competition of metallic ions in solution (Friis and Myers-Keith, 1986; Wang and Chen, 2006). The dependence of metal adsorption on solution pH has been reported in almost all biosorption systems examined, where at lower pH values, the biosorption capacity of metals is often reduced due to competition between cations and protons (H^+) for binding sites (Vijayaraghavan and Yun, 2008). In general, a pH range of 3-6 has been suggested as favourable for metal ion adsorption onto microbial biomass. This is because at higher pH values (>6), the formation of metal complexes due to chemical precipitation reactions may complicate the biosorption process. The increased adsorption capacity of various metals such as; Cd, Cu, Cr, Ni, Pb and Zn with increasing pH (3-6) has been reported. The observed metal ion adsorption increase with increasing pH has been attributed to the overall electronegative charge of the bacterial surfaces, which facilitate the complexation of metal ions onto the bacterial cell surface (Beveridge, 1981; Fein et al., 1997; Ngwenya et al., 2003; Yee et al., 2004; Johnson et al., 2007; Vasquez et al., 2007; Bueno et al., 2008; Calfa and Torem, 2008). However, there are exceptional cases, for example, the biosorption of some metal ions; for example, Ag^+, Hg^{2+} and $AuCl_4^-$, has been shown to be pH-independent and which is explained by the formation of covalent complexes with N and S-containing ligands (Darnall et al., 1986).

Effect of temperature

Temperature is an important parameter for the equilibrium and kinetic adsorption of metals onto microbial biomass, as it can have an effect on the stability of the metal complexes and the ionization of the bacterial cell wall moieties (Sag and Kutsal, 1995). In literature, both an increase in equilibrium metal adsorption with increasing temperature, and temperature

independent metal adsorption onto bacterial cell surfaces has been reported. For example, in a study by Zouboulis and co workers (2004), an increase in the equilibrium adsorption capacity for Cr onto *Bacillus licheniforms* was observed with increasing temperature (25-50°C), while the adsorption of Cd on the same bacterial biomass was not significantly affected when the temperature was increased. In a study by Ginn and Fein (2009), almost similar Cd and Pb adsorption trends as a function of temperature (5-80°C) were observed for the bacterial species; *Bacillus subtilis* and *Pseudomonas mendocina*. The effect of temperature on Cd adsorption capacity, speciation and thermodynamic stability of the important Cd surface complexes was negligible. Similarly, minimal temperature effects were also observed for the extent of Pb adsorption onto bacteria at above pH 5. However, increasing the temperature had a significant effect on speciation of the important Pb surface complexes, whereby stability constants increased with increasing temperature. Based on the studies cited above, it is apparent that the effect of temperature on metal ion adsorption onto bacterial surfaces is inconclusive, and varies with both the metal ions involved, bacterial species of interest and other environmental conditions such as pH.

Effect of ionic strength

Numerous authors have investigated the effect of ionic strength on the adsorption of different metals such as Cd, Cs, Eu, Hg, Pb and Zn onto different bacterial species, where the extent of metal adsorption decreased with increasing ionic strength. The observed decrease in the extent of metal adsorption at higher ionic strength solutions, has been ascribed to: (1) the competition between the metal ions and the electrolyte cations for the adsorption sites on the bacterial cell surface; (2) the decrease of activities of the metal ions due to the increase of ionic strength; (3) the formation of ionic pairs or chelating compounds, and (4) the presence of salts may compress the electric double layer surrounding negatively charged surfaces, resulting in the release of the adsorbed metal ions species back into solution (Ledin et al., 1997; Daughney and Fein, 1998; Cox et al., 1999; Small et al., 2001; Yee et al., 2004; Borrok and Fein, 2005; Beolchini et al., 2006). On the contrary, the ionic strength independent adsorption of metals onto bacterial surfaces has also been reported. For example, in a study by Haas and Dichristina (2001), no variations in the extent of U adsorption onto the Gram negative bacterium, *Shewanella putrefaciens*, were observed over the ionic strength range of 0.02 to 0.1 M. In this case, the

independent adsorption of metal ions with increasing background electrolyte concentration has been interpreted to indicate that the sorption process is primarily non-electrostatic in nature (Stumm and Morgan, 1996). From these observations, it is apparent that the extent of metal adsorption at different ionic strengths varies with the metal adsorbed, and that the magnitude of electrostatic effects is not dependent on the bacterial species is involved. However, more research still needs to be done to draw any valid conclusions on the effect of ionic strength on the adsorption of metal ions onto bacterial biomass.

Effect of biomass to metal ion concentration ratio

The effect of metal to biomass ratio on the adsorption kinetics has been studied before. Generally, it has been suggested that metal adsorption increases with increasing bacteria-to-metal concentration ratio. However, the adsorbed metal ion quantity per unit weight of biosorbent (specific metal uptake) decreases with increasing the biosorbent concentration, and has been reported in a number of studies (Gadd et al., 1988; Fourest and Roux, 1992; Daughney et al., 1998; Esposito et al., 2001; Daughney et al., 2001). These results may be explained by the fact that at low metal concentrations and high biomass concentrations the ratio of the biomass sorptive surface to total metal available is high; hence, all metal may be interacted with biosorbent and removed.

2.5.2 Modelling the Kinetics of Metal Adsorption by Bacteria

In order to investigate the mechanism of biosorption and potential rate controlling step such as mass transport and chemical reaction processes, kinetic models have been used to test batch sorption experimental data (Sarkar et al., 2003). Kinetics studies of sorption in wastewater treatment are significant since (i) the data can be used for determining the residence time of a sorbate at the solid-solution interface, (ii) the rate of sorption can be used to deduce predictive models for column experiments, and (iii) these studies can be used in understanding the mechanisms and effect of different environmental factors on the sorption process. In the past decades, several mathematical models have been proposed to describe sorption data, which can generally be classified as sorption reaction models and diffusion models. Diffusion-based kinetic models are always constructed on the basis of three consecutive steps; (1) diffusion across the liquid film surrounding the adsorbent particles, i.e., external diffusion or film

diffusion; (2) diffusion in the liquid contained in the pores and/or along the pore walls, which is so-called internal diffusion or intra-particle diffusion; and (3) adsorption and desorption between the adsorbate and active sites, i.e., mass action (Lazaridis and Asouhidou, 2003). On the other hand, reaction-based kinetic models originating from chemical reaction kinetics are based on the whole sorption process without considering the above mentioned steps.

Reaction-based kinetic models

Numerous authors have applied reaction-based kinetic models to describe the reaction order of adsorption systems based on the sorption capacity of the sorbent (McKay and Ho, 1999; Ho and McKay, 2000; Aksu, 2001; Chen et al., 2008; Chegrouche et al., 2009). Kinetic models, such as the Lagergren's pseudo first order equation (Lagergren, 1898), and the pseudo second order equation (Ho and McKay, 1999), are among the most widely used kinetic models to describe the biosorption process, and they are listed in Table 2.2. The pseudo first-order rate expression of Lagergren is based on solid capacity, and requires that the equilibrium sorption capacity, q_{eq}, be known. In many cases q_{eq} is unknown and as adsorption tends to become unmeasurably slow, the amount sorbed is still significantly smaller than the equilibrium amount. For this reason it is necessary to obtain the real equilibrium sorption capacity, q_{eq}, by extrapolating the experimental data using a trial and error method. Furthermore in most cases the Lagergren first order equation does not fit well for the whole range of contact time and is generally applicable over the initial 20–30 minutes of the sorption process (Lagergren, 1898).

Table 2.2 Expressions for the most frequently used reaction rate models

Model	Equation	Parameter description	Reference
Lagergren first order	$\frac{dq_t}{dt} = k_1(q_e - q_t)$	q_t = concentration of ion species in the sorbent at time t (mg g^{-1}), q_{eq} = equilibrium concentration of adsorbed ionic species in the sorbent (mg g^{-1}) and k_1= biosorption constant of pseudo-first-order Lagergren equation (min^{-1})	Lagergren, 1898
Pseudo second order	$\frac{dq_t}{dt} = k_2(q_e - q_t)^2$	q_t = concentration of ion species in the sorbent at time t (mg g^{-1}), q_{eq} = equilibrium concentration of adsorbed ionic species in the sorbent (mg g^{-1}), and k_2 = biosorption constant of pseudo-second-order Lagergren equation (min^{-1} g mg^{-1}).	Ho and McKay, 1999

The pseudo second-order equation is also based on the sorption capacity of the solid phase. Contrary to the other model it predicts the behaviour over the whole range of adsorption and is in agreement with an adsorption mechanism being the rate controlling step. In addition, this model assumes that the sorption follows the Langmuir equation (Ho and McKay, 1999).

Diffusion-based models

It is well known that a typical liquid/solid adsorption involves film diffusion, intraparticle diffusion, and mass action. For physical adsorption, mass action is a very rapid process and is normally negligible for kinetic studies. Thus, for a solid-liquid sorption process, the solute transfer is usually characterized by either external mass transfer (boundary layer diffusion) or intraparticle diffusion or both (McKay, 1984). If external diffusion of metal cations (within the diffuse layers outside the sorbent) is the rate-limiting step then the external mass transfer model can be fitted into sorption data with some success. However, when intraparticle diffusion (transfer of metal cations from the adsorbent surface to the internal active binding sites) is the rate-limiting step, then sorption data can be described by the intraparticle diffusion model (Table 2.3).

Table 2.3 Expressions of the diffusion-based kinetic biosorption models

Model	Equation	Parameter description	Reference
External mass transfer model	$\ln \frac{C_t}{C_0} = -k_f \frac{A}{V} t$	C_0 = initial metal concentration (mg L^{-1}), C_t = metal concentration at time t (mg L^{-1}), A=external sorption area ($m^2 g^{-1}$), V= total solution volume (L), and k_f = the external diffusion coefficient (cm s^{-1}).	Mathews and Weber, 1976
Intraparticle model	$q_t = k_i t^{0.5}$	q_t = concentration of ion species in the sorbent at time t ($mg.g^{-1}$) and k_i = the intraparticle diffusion rate ($mg.g.min^{0.5}$).	Weber and Morris, 1963

2.5.3 Modelling Equilibrium Batch Biosorption: Isotherm models

Equilibrium isotherm models are simple mathematical equations, which give a good description of the experimental behavior of a biosorbent over a limited range of operating conditions (Gadd et al., 1988; Kratochvil and Volesky, 1998; Gadd, 2009). Traditionally, isotherm models have been used to describe the adsorptive patterns of trace metals onto soils and sediments, but they have also been used to evaluate the sorption performance of different biosorbents. The main

limitation of these models is their basis on constant temperature and pH conditions, and their inability to predict spatial variations (Fein, 2000). Table 2.4 shows some of the single-component isotherm models that have been frequently used. Among these, the Langmuir model and the Freundlich model are the most widely accepted and well documented. The basic assumption of the Langmuir sorption isotherm is that sorption takes place at specific homogeneous sites within the sorbent. It is then assumed that once a metal ion occupies a site, no further sorption can take place at that site (Langmuir, 1918). The Langmuir isotherm model incorporates two easily interpretable constants: q_{max} and b. The parameter q_{max}, provides essential information on the maximum metal uptake capacity of the sorbent, and is useful for comparing the differences in metal uptake capacities between various biosorbent and metal species (Kapoor and Viraraghavan 1995; Pagnanelli et al., 2002; Volesky and Holan 1995). Low values of b are reflected in the steep initial slope of a sorption isotherm, indicating a desirable high affinity. Thus, for good sorbents in general, one is looking for a high q_{max} and a low b value (Kratochvil and Volesky, 1998).

Table 2.4 Some of the frequently used single component isotherm models.

Isotherm	Equation	Parameter description	Reference
Langmuir	$q = \frac{bq_{\max}C_e}{1+bC_e}$	q is equilibrium metal sorption capacity; C_e is the equilibrium metal concentration in solution; q_{max} and b are Langmuir constants related to maximum sorption capacity (monolayer capacity) and bonding energy of adsorption, respectively.	Langmuir, 1918
Freundlich	$q = kC_e^{1/n}$	k is a biosorption equilibrium constant, representative of the sorption capacity; and n is a constant indicative of biosorption intensity.	Freundlich, 1906
Combination Langmuir-Freundlich	$q = \frac{bq_{\max}C_e^{1/n}}{1+bC_e^{1/n}}$	Parameters same as above. Assuming that the surface is homogeneous, but that the sorption is a cooperative process due to adsorbate–adsorbate interactions.	Sips, 1948
Redlich-Peterson	$q = \frac{aC_e}{1+bC_e^{n}}$	a, b, and n are the Redlich–Peterson parameters. The exponent n lies between 0 and 1. For n =1 the model converts to the Langmuir form.	Redlich and Peterson, 1959
Brunauer-Emmett-Teller (BET)	$q = \frac{BCQ^0}{(C_s - C)\left[1+(B-1)C/C_s\right]}$	C_s is the saturation concentration of the adsorbed component; B a constant indicating the energy of interaction between the solute and the adsorbent surface, and Q^0 is a constant indicating the amount of solute adsorbed forming a complete monolayer	Brunauer et al., 1938

The Freundlich isotherm model assumes that the uptake of metal ions occurs on a heterogeneous surface by multilayer adsorption and that the amount of sorbate adsorbed increases infinitely as the concentration increases (Freundlich 1906). Both these models represent the theoretical model for monolayer adsorption. However, these adsorption isotherms may exhibit an irregular pattern due to the complex nature of both the sorbent material and its varied multiple active sites, as well as the complex solution chemistry of some metallic compounds (Volesky and Holan, 1995). The Redlich–Peterson isotherm incorporates the features of both the Langmuir and the Freundlich isotherms. The Redlich–Peterson isotherm has a linear dependence on concentration in the numerator and an exponential function in the denominator (Redlich and Peterson, 1959). The BET model describes the multi-layer adsorption at the adsorbent surface and assumes that the Langmuir isotherm applies to each layer (Brunauer et al., 1938). A practical consideration to the problem of metal pollution is the presence of more than one metal pollutant rather than monometal situation. In such a scenario it becomes essential to study the effect of the presence of co-cations on the biosorption capacity of the biosorbent (Schiewer and Volesky, 2000; Veglio et al., 2003). Therefore, to describe the biosorption of two or multi-metal ions within a system, various multi-component isotherm models have been developed, and examples are shown in Table 2.5.

Table 2.5 Examples of multi-component adsorption models

Isotherm	Equation	Parameter description	Reference
Competitive Langmuir	$q_i = \frac{b_i q_{\max i} C_{e_i}}{1+\sum_{i=1}^{N} b_i C_{ei}}$	C_{ei} and q_i are the unadsorbed concentration of each component at equilibrium and the adsorbed quantity of each component per g of biomass at equilibrium, respectively. b_i and q_{maxi} are derived from the corresponding individual Langmuir isotherm equations.	Langmuir, 1918
Combination Langmuir-Freundlich	$q = \frac{b_i q_{\max i} C_{ei}^{1/n_i}}{1+\sum_{i=1}^{N} b_i C_{ei}^{1/n_i}}$	Parameters same as above.	Sips, 1948
Competitive Redlich-Peterson	$q = \frac{a_i C_{ei}}{1+\sum_{i=1}^{N} b_i C_{ei}^{n_i}}$	a, b, and n are the Redlich–Peterson parameters. The exponent n lies between 0 and 1. For n =1 the model converts to the Langmuir form.	Bellot and Condoret, 1993
IAST: Ideal Adsorbed Solution Theory	$\frac{1}{q_t} = \sum \frac{Y_i}{q_i^0}$	Y_i is the solute concentration of component i in the solid phase. q_i^0 is the phase concentration of a single adsorbed component in equations with C_i^0	Radke and Prausnitz, 1972

2.5.4 Surface Complexation Modelling

Surface complexation models (SCM) are based on the concept of surface charge generated from the amphoteric surface sites are capable of explaining the reaction with sorbing cationic or anionic species to form surface complexes (Volesky, 2003). In the past, SCMs were exclusively used for describing metal ion adsorption on pure mineral materials (Stumm et al., 1970; Davis and Kent, 1990; Dzombak and Morel, 1990; Stumm and Morgan, 1996). However, in recent years, surface complexation modeling has also been successfully applied to predict trends of ion sorption at the bacteria-water interface (Fein et a., 1997; Cox et al., 1999; Fowle and Fein, 1999; Daughney et al., 2001; Haas et al., 2001; Yee and Fein, 2001; Wightman et al., 2001; Ngwenya et al., 2003; Borrok and Fein, 2005; Ginn and Fein, 2009). Generally, models of bacterial surface protonation serve two purposes: firstly, to clarify the molecular-scale adsorption mechanisms that occur between aqueous solutes and the bacterial surface, and secondly, to enable quantitative geochemical modeling of mass transport in bacteria-bearing systems. However, the lack of agreement for a universal model accounting metal ion adsorption onto bacterial cell surfaces has hindered progress towards achieving both purposes (Borrok et al., 2005). SCMs can be broadly classified into two groups: electrostatic models, which take into account electrostatic effects, and models that neglect the electrostatic effects (non-electrostatic model – NEM). Numerous authors have demonstrated that either of the two classes of SCMs can be successfully used to describe the adsorption behavior of protons and metal ions onto bacterial cell surfaces (Brassard et al., 1990; Plette et al., 1995; Fein et al., 1997; Volesky and Yang, 1999; Cox et al., 1999; Martinez et al., 2002; Ngwenya et al., 2003; Borrok and Fein, 2005; Johnson et al., 2007, Ginn and Fein, 2009).

Electrostatic Models

Electrostatic models (e.g., (e.g., the constant capacitance model, diffuse layer model, and the triple layer model) all contain at least one coulombic correction factor to account for the effect of surface charge on surface complexation. These coulombic correction factors take the form of electrostatic potential terms, $e^{-F\psi}{}_i/RT$, where ψ_i is the surface potential in the i^{th} surface plane in the intrinsic conditional surface complexation constant expressions (Goldberg, 1995). Numerous authors have suggested that the application of electrostatic models to account for the hydrophobic and electrostatic interactions that occur between the bacterial surface and the

aqueous metal ions play an important role in proton-binding (Plette et al., 1995; van der Wal et al., 1997; Daughney and Fein, 1998; Daughney et al., 2002; Martinez et al., 2002). For example, numerous authors have successfully used the CCM approach, relating surface charge to surface potential using an arbitrarily assigned capacitance value, to describe the electrostatic effects of metal adsorption onto bacterial surfaces (Fein et al., 1997; Yee and Fein, 2001, Ngwenya et al., 2003, Haas, 2004, Ojeda et al., 2008; Ngwenya et al., 2009). The assumptions in the CCM are: (i) all surface complexes are inner-sphere complexes; (ii) the constant ionic medium reference state determines the activity of the aqueous species and therefore no surface complexes are formed with ions from the background electrolyte; (iii) one plane of charge represents the surface; (iv) the surface potential, ψ_o, is related linearly to the surface charge density, σ_o, (where o represents the surface plane), by the capacitance of the bacterial surface (Equation 2.1). This linear relationship is limited to high ionic strength conditions and generally cannot be extended to dilute electrolyte solutions. In the CCM, the intrinsic discrete acidity constant of a site is shifted, and its pH range of influence broadened, by an electrostatic potential, ψ, at the so-called bacteria/water interface as shown in Equation 2.2

.

$$\sigma_0 = \frac{CSa}{F}\psi_0 \qquad [2.1]$$

$$K_{\text{int}} = K \exp^{(-ZF\psi/RT)} \qquad [2.2]$$

Where C is the capacitance density (F m^{-2}), S is the surface area (m^2 g^{-1}), a is the suspension density (g L^{-1}), F is the Faraday constant (C mol_c^{-1}), σ_o has units of mol_c L^{-1} and ψ_o, has units of V, K_{int} is the intrinsic stability constant referenced to zero surface charge and zero surface coverage, Z refers to the charge of the adsorbing ion, R the molar gas constant, and T the absolute temperature.

One other electrostatic model that has been frequently used account for bacteria surface double layer interactions is the Donnan electrostatic model (Ohshima and Kondo, 1990; Plette et al., 1995; Wasserman and Felmy, 1998; Martinez et al., 2002; Yee et al., 2004; Burnett et al., 2006; Hetzer et al., 2006; Heinrich et al., 2008). This model invokes the assumption that the cell wall is

an ion-penetrabale volume composed of homongeneous cross-linked ionizable functional groups. In addition, this model assumes that all counter ions necessary to balance the bacterial surface charge are present within the hydrated bacterial cell wall volume and the Donnan volume can be estimated, directly measured, or empirically-derived (Marinsky and Ephraim, 1986). The deprotonation of these functional groups forms an electrical potential which extends across the membrane to the interface between the cell wall surface and bulk solution. However, the extent to which Donnan potential theory can describe metal sorption data remains poorly understood. Moreover, due to the large uncertainties associated with the estimation of bacterial cell geometry parameters, particularly bacteria consortia, the applicability of this model in describing metal adsorption data remain questionable (Borrok and Fein, 2005).

Non-Electrostatic Model (NEM)

The non-electrostatic model (NEM) excludes explicit electrostatic terms from the mass law equations for surface equilibria, such that all chemical and electrostatic interactions are implicitly included in the equilibrium constant for the reaction (i.e, the free energy of sorption). This approach treats surface functional groups in the same manner as dissolved ligands or complexing metal ions but without a separate activity coefficient correction for the surface complex (Davis and Kent, 1990). In addition, because of neglect of the electrostatic effects, the results generated are conditional on ionic strength and the stability constants determined represent apparent constants, not intrinsic constants (Cox et al., 1999). A number of researchers have successfully used the NEM approach to describe the protonation and metal ion adsorption reactions at the bacterial cell surface and water interface (Cox et al., 1999; Borrok et al., 2004; Borrok et al., 2005; Fein et al., 2005; Pagnanelli et al., 2006; Johnson et al., 2007; Tourney et al., 2008; Ginn and Fein, 2009), where experiments were conducted at constant ionic strength conditions; and neglecting the electrostatic effects on the bacterial cell surface. However, in another study, Borrok and Fein (2005) used the NEM approach in comparison to electrostatic models to demonstrate that the ionic strength effect on bacterial surface proton binding reactions (over the range of 0.01 M to 0.5 M) is often relatively small and not significantly greater than experimental and modeling uncertainties. It was concluded in this study that the use of electrostatic corrections that rely on curve-fitting procedures with no external verification of some of the input parameters, e.g., capacitance or Donnan values, may not be justifiable.

2.5.5 Metal Desorption

Desorption of loaded biomass enables re-use of the biomass, and recovery and/or containment of sorbed materials, although it is desirable that the desorbing agent does not significantly damage or degrade the biomass. While the regeneration of the biosorbent may be accomplished by washing the metal-laden biosorbent with an appropriate desorbent solution, including dilute mineral acids, alkalis, and complexing agents, however, the type and strength of this solution depend on the extent of binding of the deposited metal (Puranik and Paknikar, 1997). One commonly used procedure that is designed to partitioning different trace metals based on their chemical nature is sequential extraction (Tessier et al., 1979). Separating these fractions using sequential extraction methods makes it possible to study the speciation and possible association between metals and sorbent. Traditionally, sequential extraction has been widely used in soil and sediment studies; however, recently, it has also been used to chemically leach metals out of sludge samples, and various sorbents (De Rome and Gadd, 1987; Mattuschka and Straube, 1993; Pagnanelli et al. 2002).

Generally, single extractants may broadly be divided into three main classes: (i) weak replacement of ion salts ($MgCl_2$, $CaCl_2$, NH_4NO_3), (ii) dilute solutions of either weak acids (acetic acid) or strong acids (HCl, HNO_3) and (iii) chelating agents (DTPA, EDTA). The weak replacement ion salts are able to release into solution metals which are associated with the exchange sites on the solid-phase and hence can be considered as bioavailable. The chelating agents, such as DTPA and EDTA, form complexes with free metal ions in solution and thus reduce the activities of the free metal ions in solution. The use of strong or dilute mineral acids is probably the most common method of metal desorption, and has been widely demonstrated. For example, Chandrashekar et al. (1998) conducted experiments to investigate the recovery of Ca, Fe and Ni ions from the loaded waste fungal biomass of *Aspergillus species* as a function of HCl concentration. The results revealed that with increase in HCl concentrations, metal desorption increased and at 5M HCI, complete removal of Ca and Fe was achieved while about 78% Ni was desorbed. Generally, this technique is easy to apply, inexpensive, and require little data analysis.

2.6 APPLICATION OF MICROBIAL TECHNOLOGY IN NUCLEAR WASTE MANAGEMENT

2.6.1 Scientific Framework of Technology

The distribution and diversity of microorganisms inhabiting contaminated sites and of the genes that code for phenotypes facilitating metal–microbe interactions are critical elements in metal and radionuclide bioremediation (Bazansak et al., 1999). Both a familiarity with the physiology of the active microbial populations and an understanding of how the relevant microbial processes can be manipulated *in situ* are crucial for the implementation of successful remedial strategies (Barkay and Schaefer, 2001). Recently, numerous authors have reported the presence of a wide range of indigenous microorganisms including; anaerobic denitrifiers, fermenters, sulphate reducers and methanogens from irradiated ecosystems (Bruhn et al., 1999; Kovacova et al., 2002; Chicote et al., 2004). In recent studies, the biostimulation and bioaugumentation concepts have been successfully implemented in laboratory scale investigations to promote the *in situ* immobilization of U, Tc, Cr, and other harmful metals generated from the nuclear power industry (Kumar et al., 2007).Viable microbial populations have been found in the waters of spent nuclear fuel pools, walls of a pool storing nuclear materials at a Spanish nuclear power plant; (Chicote et al., 2004) and in an underground granitic rock nuclear waste repository in Canada, where a range of heterotrophic aerobic and anaerobic bacteria ranging from 10^1 to 10^6 cells/g dry weight buffer were found. Among these were approximately 10^2 sulphate reducing bacteria (SRB) cells and methanogenes per gram of dry weight buffer, in spite of the oligotrophic and radioactive environment (Kovacova et al., 2002; Sarro et al., 2005). The survival of these microorganisms in such conditions is due to their resistance to gamma radiation, UV, H_2O_2, and desiccation. These microorganisms have also been found to be capable of the selective accumulation of a range of metals and radionuclides including; Mn, Zn, Cs, U, and Co (Romanovskaia et al., 2002; Gadd, 2004).

Since then there has been ongoing research on the use of microorganisms, to treat radioactive waste of different radiation levels and origin. The SRB metal remediation concept is not new, however their occurrence in radioactive environments has aroused a renewed interest in their application for subsurface radioactive waste management, particularly, groundwater bioremediation. The main concept behind the bioremediation of contaminated groundwater is

through the *in situ* emplacement of an adsorptive coating with SRB as bio-adsorbents/detoxifying agents on the aquifer matrix to control radionuclides dispersion to the biosphere (Figure 2.4). The operational conditions and design of this subsurface microbial treatment technology is very similar to biological permeable reactive barrier (PRB) systems. A PRB is an engineered zone of reactive material placed in an aquifer that allows passage of groundwater while retaining or degrading the contaminants (Morrison et al., 2002). These techniques employ a wall of biological reactive media, installed in the path of a contaminated groundwater flow, to remove or treat groundwater contaminants *in situ.* The reactive media is permeable to the groundwater flow and as it moves horizontally through the barrier, driven by natural hydraulic gradients, a variety of natural microbiological processes remove the contaminants from the water. These processes include precipitation, biosorption, enzymatic reduction, or biodegradation. Details on the design and configurations for subsurface PRBs have been reviewed by numerous authors (Gibert et al., 2002; Amos and Younger, 2003).

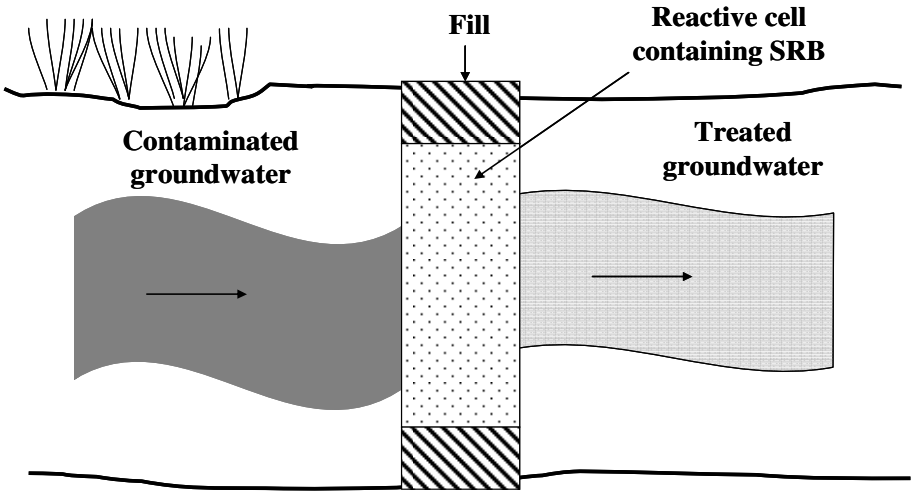

Figure 2.4: Elevated view of a permeable reactive barrier configuration for groundwater treatment. (Adapted from Gavaskar, 1999).

2.6.2 Prospects of Radionuclide Bioremediation in Passive Microbial Bioreactors

Passive bioreactors are preferred to traditional water treatment plant technologies because they allow higher metal removal at low pH and generate more stable sludge with lower operation costs and minimal energy consumption. By far, the remediation of groundwater contaminated as a result of radionuclide migration from repository sources remains one of the most intractable problems of environmental restoration, and as such one of the major challenges faced by the nuclear energy industry. Recently, innovative technologies, such as bioremediation, have been considered as one of the most promising solutions for the remediation of subsurface radionuclide contamination (Costa et al., 2008). The sustainability of the bioremediation system depends on a number of factors, which include; organic substrate sources and their degradation, effluent chemistry, microbiological diversity and activities and reactor configuration and hydraulics (Neculita et al., 2007). The mechanisms of metal removal for the passive bioreactor treatment system are very similar to biological permeable reactive barriers (PRBs). Therefore, in the context of PRB operation, natural biogeochemical processes form an integral basis for the successful operation of the bioremediation technology. Treatment in PRBs can be both abiotic and biotic; abiotic PRB treatment involves the use of neutralizing agents (such as lime), adsorbents and zero-valent iron (ZVI), which can be used as filling materials for metal sorption. On the other hand, in the biotic PRB system, natural microbial processes of SRB are exploited (Blowes et al., 2000; Gibert et al., 2002).

In microbial bioreactors, a wide range of reactions takes place which can remove metallic contaminants from water, and they include; precipitation in the form of sulphides, hydroxides, and carbonates; adsorption, surface precipitation, and polymerization on inorganic support, solid organic matter, bacteria, and metal precipitates are sorption mechanisms that can also occur. Adsorption of dissolved metals onto organic sites in the substrate material is an important process upon the start of a passive bioreactor (Pagnanelli et al., 2010). Over the years, metal adsorption onto microbial substrates (mainly, bacteria) has acquired great importance in existing efforts towards environmental bioremediation, therefore it should also be taken in account for future BPT and PRB designs to cater for a wider spectrum of metal/radionuclides, particularly those that cannot be precipitated into insoluble precipitates. Currently, this technology has been successfully used for the treatment of chlorinated aliphatic hydrocarbons, remediation of

chromium VI and the treatment of acidic mine drainage. Efforts for the adoption of this technique for subsurface radioactive waste management are still in the research phase.

2.6.3 Challenges and Future Perspectives

For *in situ* bioremediation to be successful, it is vital that the right microbes are in the right place with the right environmental factors for degradation to occur. In some cases, microbial metabolism of contaminants may produce toxic metabolites, therefore resulting in further environmental pollution. Consequently, bioremediation as a scientifically intensive procedure must be tailored to the site-specific conditions, which means that there, has to be feasibility studies on a small-scale before the actual clean-up of contaminated sites. However, demonstrated long term benefits of this technology compensate its limitations, and as such have paved the way for switching from the aggressive conventional spent fuel management practices into environmentally friendly and cost effective approaches. Development of novel and more efficient commercial bioremediation methods for spent fuel management are underway. In some countries, for example United States of America, these technologies are already in the testing phase and when integrated into existing waste management processes, they will greatly increase the efficiency and application of biological approaches in spent fuel management (Skeen et al., 2006).

The next generation bioremediation technologies include controlling and/or manipulating the subsurface microbiology via engineered bioremediation, relying on intrinsic bioremediation to prevent migration, and using *ex situ* bioprocesses in the treatment and separation of radionuclides from organic-metal waste mixtures. These may lead to the discovery of new physical mutagens that are more effective or have unique properties. These methods have the potential to reduce the cost of operations by several magnitudes, and simplify the overall process of SNF mgt. Some of the promising strategies for *in situ* metal bioremediation are biostimulation and bioaugumentation, and it has been reported that the addition of appropriate carbons sources to the contaminated aquifer effectively stimulates the growth of bacteria, responsible for controlling the migration of radionuclides *in situ* (Ortiz-Bernad et al., 2004).

CHAPTER 3

MATERIALS AND METHODS

3.1 CHEMICALS AND REAGENTS

All chemicals used were of analytical grade, and were purchased from Merck (South Africa), unless stated otherwise. All gases of highest purity standard were purchased from African Oxygen Limited (Afrox) (South Africa). Sr, Co and Cs stock solutions were prepared by dissolving 3.0429g of $SrCl_2.6H_2O$, 4.9383g of $Co(NO_3)_2.6H_2O$ and 1.267g CsCl, respectively, in 10mL HNO_3/distilled water solution (1:1) and then diluted to 1 L to give a final concentration of 1000 mg/L of each metal. Working concentrations and standard solutions were prepared by diluting the stock solution with distilled water to give the desired concentration. All glassware was soaked in 10% HNO_3 and rinsed with distilled water prior to and after use.

3.2 MICROORGANISM

A mixed sulphate reducing bacteria (SRB) starter culture previously isolated from a coal mine waste site was kindly supplied by Dr. Harma Greben (CSIR, Pretoria, South Africa). In previous studies, a range of radionuclides, have been shown to be present in coal samples. In addition, low to high radioactivity levels have also been detected around coal mines (Jamil et al., 1998; Jasinska et al., 1998). Therefore, the use of the present SRB cultures for Sr, Co and Cs uptake experiments was based on the hypothesis that the cultures are acclimatized to high metal and radionuclide concentrations. Initial kinetic sorption performance parameters for Sr, Co and Cs removal by growing SRB cultures were determined in batch anaerobic bioreactors (2L) incubated at 25±0.5°C with continuous stirring at 120 rpm. Further batch experiments were conducted in 100 mL serum bottles to evaluate the kinetic and equilibrium sorption parameters of the SRB cultures under non-growth conditions.

3.3 MEDIA

SRB enrichments were performed according to a procedure by Butlin et al. (1949) using medium B, a liquid medium containing sulphate, lactate and a trace of ferrous salt (Table 3.1). The media was sterilized using a Tomin TM-323 autoclave (Durawell Co. Limited, Taiwan). The microorganisms were incubated in the dark at 30±2°C with continuous stirring at 120 rpm. The anaerobic growth vessel was regularly flushed with 99.9% N_2 gas to maintain an anaerobic atmosphere. When considerable blackening of the medium had occurred (due to FeS formation), which took up to 28 days, the culture was examined to determine cell concentration using the total bacteria count (TBC) method. The enrichment procedure was repeated until the desired viable cell concentration was obtained. A 10 L stock culture bioreactor was started by aseptically transferring a 10% (v/v) of the enriched cultures into medium C. The stock culture was sub-cultured every 3-4 weeks by transferring the culture to freshly prepared medium C. This medium was selected on the basis of its lack of iron, as blackening of growth medium interferes with analytical procedures for metal biosorption experiments.

Table 3.1 Composition of media for SRB enrichment and growth.

Component	Composition per litre	
	Medium B	Medium C
Sodium lactate (60 % solution)	5 mL	6 mL
$MgSO_4.7H_2O$	2.0g	0.1 g
Na_2SO_4	-	4.5 g
NH_4Cl	1.0g	1.0 g
$CaSO_4$	1.0g	-
$CaCl_2.6H_2O$	-	0.06g
$FeSO_4.(NH_4)_2SO_4.6H_2O$	0.5g	-
Yeast extract	1.0 g	1.0 g
K_2HPO_4	0.5 g	-
KH_2PO_4	-	0.5g
$Na_2SO_3.7H_2O$	0.03g	-
Ascorbic acid	-	0.1 g
Sodium thioglycollate	-	0.1 g
Sodium citrate.$2H_2O$	-	0.1 g

3.4 BATCH SRB BIOREACTOR EXPERIMENTS

3.4.1 Bioreactor Configuration

The batch SRB bioreactor used for preliminary kinetic metal sorption experiments was a closed anaerobic system, which was constructed from a 2L Pyrex glass Erlenmeyer flask (Figure 3.1). Prior to bioreactor system assembly, the reaction vessel (bioreactor) was filled with 1.5 L medium C spiked with the target metal, and autoclaved together with the magnetic stirrer bar. The bioreactor was then immediately sealed with an airtight rubber stopper, and purged with high purity (99.9%) nitrogen gas to maintain anaerobic conditions. A 10% (w/v) zinc acetate solution was connected to reaction vessel to trap the hydrogen sulphide gas produced in the bioreactor. Samples were withdrawn using a sterile hypodermic syringe attached to a glass tube. Bioreactor mixing was achieved by means of an AM4 multiple heating magnetic stirrer (Velp Scientifica, Labex Pty Ltd, South Africa) in conjunction with stirrer bars.

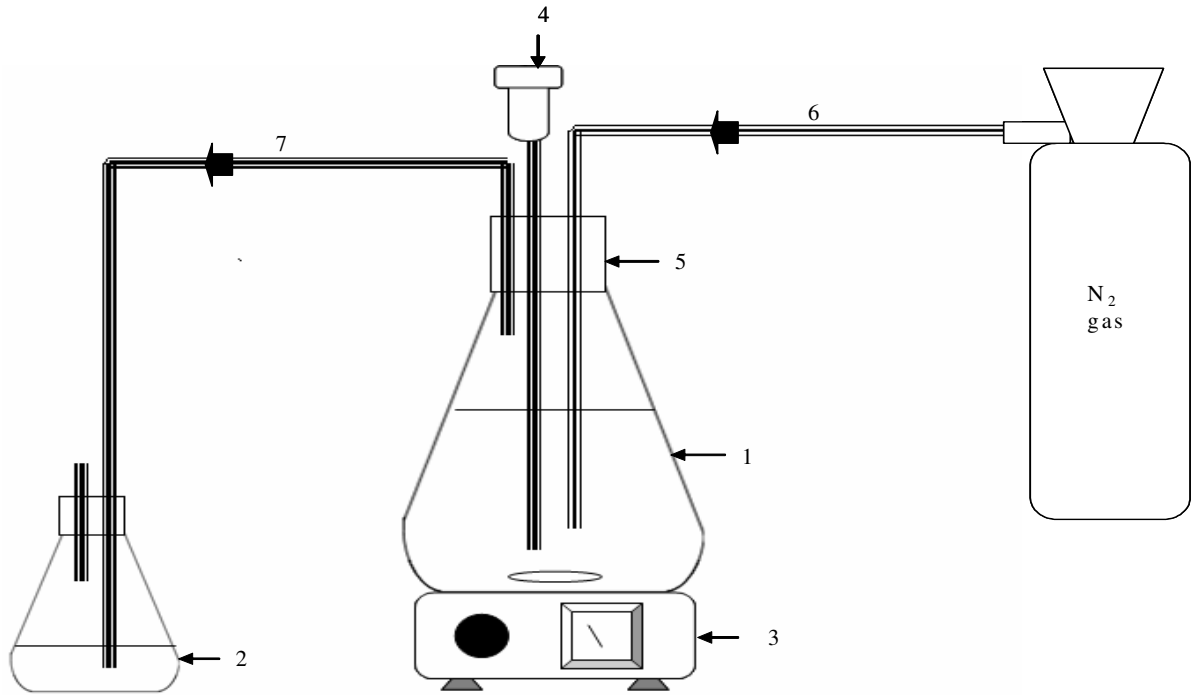

Figure 3.1: Schematic diagram of the laboratory-scale anaerobic SRB batch bioreactor. (1= anaerobic bioreactor, 2= 10% zinc acetate trap solution, 3= magnetic stirrer, 4= sampling syringe, 5= rubber stopper, 6= N_2 gas inlet and 7= H_2S gas outlet).

3.4.2 SRB Screening for Sr, Co and Cs Removal and Tolerance

Preliminary studies aimed at screening for selective Sr, Co and Cs removal and tolerance among individual cultures in the bacterial consortium were performed in a series of batch SRB bioreactors. Each of the batch bioreactors filled with growth medium supplemented with each metal at an initial concentration of 75 mg/L, were inoculated with a 5 mL culture sample containing 1.6×10^8 cells/mL of viable mixed SRB cells. All experiments were conducted in duplicate. The suspensions were incubated under optimal SRB growth conditions for up to 28 days. At the end of the incubation period, samples were removed for monitoring changes in the phylogeny of the original SRB as a result of exposure to the different metals. Prior to culture isolation in agar plates, enrichments for each sample were prepared as described before. SRB growth medium without metal but the bacterial inoculum (bacterial growth control) and medium with metal but without bacterial inoculum (abiotic control) served as controls.

3.4.3 Kinetics of Sr^{2+}, Co^{2+} and Cs^{+} Removal in the SRB Bioreactor

The removal of different initial Sr^{2+}, Co^{2+} and Cs^{+} concentrations (25-500 mg/L) and their effect on the growth and metabolism of the SRB consortium was also investigated. The suspensions were incubated under optimal SRB growth conditions for up to 14 days. Sampling was carried out daily over the entire incubation period, for sulphate, sulphide, residual metal concentration, pH analysis, as well as total biomass count. Prior to analysis, the samples were clarified by means of a Hermle Z 323 centrifuge (Memingen, Germany). Subsequent to centrifugation, the microbial component of bacterial suspensions was separated using a 0.22µm (Millipore, USA) filter paper. Results obtained were compared to with those from control experiments, consisting of bioreactors inoculated with viable SRB cells in the absence of Sr, Co and Cs, and bioreactors containing medium with metal but without bacterial inoculum (abiotic control). To determine the nature of the mechanism of Sr^{2+}, Cs^{+} and Co^{2+} removal from solution, metal-loaded SRB cells were subjected to a five-step desorption procedure (Tessier et al., 1979). Obtained results were compared with those obtained for Sr, Co and Cs removal by dead SRB cells (killed by autoclaving at 121ºC and 15 psi for 20 minutes).

3.4.4 Model Formulations for SRB Bioreactor Processes

The reaction schemes, rate equations and kinetic constants used for the biological processes; biomass population dynamics and sulphate reduction were adapted from literature. Different models have been proposed to describe the growth kinetics of a microbial population growing with a single limiting substrate. However, a study by Senn et al. (1994) has shown that out of several proposed, the Monod model (Monod, 1949) has been used extensively as the model parameters μ, μ_{max}, S and K_s have a biological meaning and are experimentally accessible. The Monod model describes the relationship between μ the specific growth rate) and S (substrate concentration) by a type of saturation kinetics as shown in Equation 3.1.

$$\mu = \mu_{\max} \frac{S}{K_s + S} \qquad [3.1]$$

Where: μ is the specific growth rate (1/h), μ_{max} the maximum specific growth rate (1/h), S the substrate concentration (mg/L) and K_s is the substrate affinity, i.e. the substrate concentration at which the cells grow at half maximum specific growth rate (mg/L).

To account for bacterial population growth, in the presence of a metal (inhibitor), a simple Monod's non-competitive inhibition kinetic model, incorporating an inhibition term, I, in which K_i is the inhibition coefficient, was used to model bacteria growth (Equation 3.2). Parameters for biological sulphate reduction in the presence of Sr^{2+}, Co^{2+} and Cs^{+} were estimated using the Pirt equation (Equation 3.3) as previously done by Kalyuzhnyi et al. (1998), and Robinson and Tiedje (1983). The sulphate concentration levels were assumed to be non inhibitory. Inhibition due to sulphide formation was assumed not significant as the sulphide concentration in the batch system at any time was much lower than the reported inhibition concentration (300–550 mg/L of sulphide is necessary to impart sulphide inhibition). The reactor was assumed to be completely mixed, and pH was kept constant in a narrow range (pH 6.8–7.2, unless stated otherwise). Thus, there was no inhibition associated acidic or alkaline conditions in the reactors. A second-order rate equation (Equation 3.5), based on the solute concentration, and incorporating an active biomass term was used to predict metal (Sr^{2+}, Co^{2+} and Cs^{+}) removal over time in the bioreactors.

$$\frac{dX}{dt} = \left(\frac{\mu_{\max} SX}{K_s + S} \right) \times I \qquad [3.2]$$

$$-\frac{dS}{dt} = \frac{1}{Y_{x/s}} \left(\frac{dX}{dt} \right) \qquad [3.3]$$

$$I = \frac{Ki}{Ki + C} \qquad [3.4]$$

$$-\frac{dC}{dt} = k_C CX \qquad [3.5]$$

where; μ_{max} is the maximum specific growth rate coefficient (1/h), K_s is the half saturation constant (mg/L), S is the concentration of substrate at time t (mg/L), $Y_{x/s}$ is the bacterial yield coefficient (mg of biomass produced per mg substrate utilized), X is the concentration of biomass at time t (mg/L), k_C is the second-order rate coefficient (L/mg/h) and C is the metal concentration at time t (mg/L).

3.4.5 Modelling Software

In this study, the computer program AQUASIM 2.0 (Reichert, 1998) was used for all bioreactor processes modeling. AQUASIM is a computer program for the identification and simulation of aquatic systems. The program can be used to calculate substrate removal in bioreactors for any user specified microbial system. AQUASIM extends the capabilities of conventional environmental simulation programs mainly in. two ways: (1) the program does not implement a specific model, but allow users to specify models as freely as possible and (2) it offers system identification tasks in addition to simulation. AQUASIM performs simulations by comparing calculated results with measured data, and such simulations are then used to validate model assumptions. Systematic deviations between calculated and measured values may suggest that additional important processes are to be considered or corrections are needed in the formulation

of processes. Another important functionality of AQUASIM is automatic parameter estimation for a given model structure using measured data. These estimations are done using the weighted least-squares technique. This is not only important for getting neutral estimates of parameters, but it is a prerequisite for efficiently comparing different models. Several calculations with several target variables, and universal as well as calculation-specific parameters, can be combined to a single parameter estimation process. This is a very important feature not present in most of the statistical software. This software has been successfully used by a number of researchers to describe SRB bioreactor processes (Kosseva and Hansford, 2001; Ristow and Hansford, 2001). The program AQUASIM estimated the best fit by minimizing the χ^2 values as shown in Equation 3.6. However, the goodness of fit χ^2 values may be subject to bias due to multivariate non-normality. If data from the model are similar to the experimental data, χ^2 will be a small number; if they are different, χ^2 will be a large number. For each metal set, the sensitivity of the kinetic parameters related to the SRB bioreactor processes; biomass, substrate and metal concentrations, was also computed using AQUASIM 2.0.

$$\chi^2 = \Sigma \frac{\left(S_{exp} - S_{mod}\right)^2}{S_{mod}} \qquad [3.6]$$

where: $S_{,mod}$ is the calculated (model) concentration at time t (mg/L), and $S_{,exp}$ is the experimental concentration at time t (mg/L).

3.5 KINETICS OF Sr^{2+}, Co^{2+} and Cs^{+} BIOSORPTION FROM AQUEOUS SOLUTION

3.5.1 Kinetic experiments

Kinetic sorption experiments for the effect of initial concentration, biomass concentration, metabolic state and pH on the removal of Sr^{2+}, Co^{2+} and Cs^{+} from single metal aqueous solutions were performed in 100 mL rubber-sealed serum bottles. The bacterial consortium used for the metal biosorption studies was reconstituted by combining all the bacterial isolates detected in both non-contaminated and contaminated bioreactors. The initial metal concentration and pH were varied between 25-500 mg/L and 2-9, respectively, and the biomass cell density was kept constant at 0.5 g/L. For the biomass concentration studies, cell density was varied between 0.5-3 g/L, while the initial metal concentration and pH were kept constant at 75 mg/L and 4,

respectively. To determine the effect of bacterial metabolic state, live and heat-killed bacteria cells were exposed to the different metals at an initial concentration of 75 mg/L and pH 4. SRB cells suspended in aqueous solution but without metal and aqueous metal solution but without bacterial inoculum (abiotic control) served as controls. In all experiments, samples (1 mL) were removed at timed intervals by sterile syringes for residual metal analysis. Metal concentration was determined by the AAS. The metal uptake capacity (q_{eq}) was calculated as:

$$q_{eq} = \frac{(C_{ini} - C_{eq})}{X} \qquad [3.7]$$

where: q_{eq} = metal uptake capacity (mg/g), C_{ini} = initial concentration of metal in solution (mg/L), C_{eq} = equilibrium concentration of metal in solution (mg/L), and X = dry weight of SRB added (g).

3.5.2 Kinetic Modelling

In an attempt to clarify the mechanism of Sr^{2+}, Co^{2+} and Cs^{+} removal from aqueous solution by SRB cells, and identify the main factors controlling sorption rate such as; mass transport, pore diffusion and chemical reaction processes, the first-order (Lagergren, 1898), pseudo-second-order (Ho and McKay, 1999), and external and intraparticle diffusion (Weber and Morris, 1963) kinetic models were evaluated.

The linearised pseudo-first and second order models can be expressed as follows:

$$\ln(q_{eq} - q_t) = \ln q_{eq} - k_1 t \qquad [3.8]$$

$$\frac{t}{q_t} = \frac{1}{k_2 q_{eq}^2} + \frac{t}{q_{eq}} \qquad [3.9]$$

where: q_t = concentration of ion species in the sorbent at time t (mg/g), q_{eq} = equilibrium concentration of adsorbed ionic species in the sorbent (mg/g), k_1= biosorption constant of pseudo-first-order Lagergren equation (min^{-1}) and k_2 = biosorption constant of pseudo-second-order Lagergren equation (min/ g/mg). The applicability of the pseudo-first and second order

models was determined by linear regression method, from which sorption parameters were determined.

For a solid-liquid sorption process, the solute transfer is usually characterized by either external mass transfer (boundary layer diffusion) or intraparticle diffusion or both. If external diffusion of metal cations (within the diffuse layers outside the sorbent) is the rate-limiting step then it has been shown that Equation 3.11 can be fitted into sorption data with some success.

$$\ln\frac{C_t}{C_{ini}} = -\mathrm{k_f}\frac{A}{V}\mathrm{t} \qquad [3.11]$$

where: C_{ini} = initial metal concentration (mg/L), C_t = metal concentration at time t (mg/L), A=external sorption area (m^2/g), V= total solution volume (L), and k_f = the external diffusion coefficient (cm/s). However, when intraparticle diffusion (transfer of metal cations from the adsorbent surface to the internal active binding sites) is the rate-limiting step, then sorption data can be described by Equation 3.12, as proposed by Weber and Morris in 1962;

$$q_t = k_i t^{0.5} \qquad [3.12]$$

where: q_t = concentration of ion species in the sorbent at time t (mg/g) and k_i = the intraparticle diffusion rate (mg.g.$min^{0.5}$).

The applicability of the external and intraparticle diffusion model was determined by linear regression method, from which sorption parameters were determined. For the external diffusion model, if the experimental data (a plot of $\ln(C_t/C_{ini})$ against time t), conforms to a linear plot with a high correlation coefficient (R^2), then external diffusion is the rate-limiting step. The external diffusion coefficient k_f (cm/s) can be calculated from the slope of the straight line obtained from Equation 3.10. On the other hand, if a plot of the experimental data (q_t against $t^{0.5}$) conforms to a linear plot and the line passes through origin, then intraparticle diffusion is the rate-limiting step (Webber and Morris, 1963). The intraparticle diffusion rate coefficient is given by the slope of the line.

3.6 MAXIMUM BIOSORPTION CAPACITY OF Sr^{2+}, Co^{2+} AND Cs^{+}

3.6.1 Equilibrium Sorption Experiments

Batch equilibrium sorption experiments were carried out using standard batch methodology as described by Volesky (1990). The equilibrium removal of Sr^{2+}, Co^{2+} and Cs^{+} from single and binary metal solutions was evaluated. For these studies, the bacterial consortium used was reconstituted combination of all the bacterial isolates detected in both non-contaminated and contaminated bioreactors. The initial concentration was varied between 25 and 1200 mg/L for single metal isotherms. The competitive removal of metal ions from binary metal solutions was carried out by adding equivalent initial concentrations of the target and competing metal ion ranging from 25 to 1200 mg/L. In all experiments, pH and SRB cell density were kept constant at 4 and 0.5 g/L, respectively. SRB cells suspended in aqueous solution metal but without metal and aqueous metal solution but without bacterial inoculum (abiotic control) served as controls. Samples (1mL) were removed by sterile syringes at equilibrium for residual metal analysis. Metal concentration was determined by the AAS.

3.6.2 Equilibrium isotherm modeling

The applicability of well established empirical models, such as the classical Langmuir (Langmuir, 1918) and Freundlich (Freundlich, 1907) equilibrium sorption isotherms in the present sorption process are evaluated. The Langmuir equation can be expressed as:

$$q = \frac{q_{max}\, bC_{eq}}{1 + bC_{eq}} \qquad [3.13]$$

This models incorporates two constants that are easy to interpret; q_{max}, the maximum sorbate uptake (mg/g), and *b,* the coefficient related to the affinity between the sorbent and sorbate. q = sorption uptake (mg/g). On the hand, the Freundlich equation can be expressed as:

$$q = kC_{eq}^{(1/n)} \qquad [3.14]$$

This model also incorporates two constants: k, which corresponds to the binding capacity; and n, which characterises the affinity between the bacterial sorbent and metal. C_{eq} = equilibrium concentration of the sorbate remaining in the solution (mg/L). In order to verify the good compliance of the experimental data to the empirical (Langmuir and Freundlich isotherms) models, a non linear regression method was used to construct model curves, from which equilibrium parameters were estimated.

3.7 ADSORPTION OF PROTONS AND Sr^{2+}, Co^{2+} AND Cs^{+} ONTO SRB CELLS

3.7.1 Preparation of Bacterial Adsorbent

A mixed SRB bacteria culture was obtained by combining all the bacterial isolates detected in both non-contaminated and contaminated bioreactors. The microorganisms were grown in stock in Postgate medium C for about 5-7 days, after which the actively growing bacteria cells were harvested and aseptically transferred to 2L rubber-sealed batch anaerobic bioreactors and allowed to grow in fresh Postgate Medium C. The cells were allowed to grow until mid-stationary phase (5-7 days). Equal volumes of liquid bacteria culture were dispensed into centrifuge tubes, and the bacteria were harvested from the growth media by centrifugation (6000 ×g, 15 minutes). Cells were repeatedly washed in deionized water to remove growth medium impurities. Metal cations that maybe present on SRB cell wall surfaces were stripped by soaking in 0.001M EDTA for 30 minutes, followed by intensive rinsing in deionized water. Finally cells were then subjected to two final rinses in a $NaNO_3$ electrolyte solution without an acid wash step to prevent any damage to the outer membrane of the gram negative species. The ionic strength of the electrolyte wash solution was varied according to that of the experiment in which the bacteria were to be used.

3.7.2 Metal Adsorption Experiments

Experiments for Sr, Cs and Co adsorption onto SRB cells were conducted under anaerobic conditions as a function of pH, ionic strength and temperature. Prior to use, the bottles were cleaned by soaking in two successive acid baths (10% v/v HNO_3) for 24 hours each, rinsed twice in ultra-pure water, and then dried in an oven at 105ºC. For each metal, a stock bacterial suspension consisting of a known mass of bacteria suspended in an electrolyte solution (0.1 M $NaNO_3$ or unless otherwise stated) was prepared. The stock bacterial suspension was then

supplemented with the target metal obtained from 1000 mg/L metal stock solution (prepared in 0.1 M $NaNO_3$) to yield the required initial concentration. The initial concentrations for Sr, Cs and Co were chosen based on calculations using MINTEQA2 (Allison et al., 1991) to circumvent premature metal precipitation with increasing pH. After the addition of the metal, the pH of the bacterial-metal stock suspension was recorded. The suspension was then divided into a series of 100 mL serum bottles, and the pH was adjusted to the desired value by adding small volumes of concentrated HNO_3 or NaOH solution. In all the experiments, the pH was allowed to drift, and the final pH of the suspension was recorded at the end of the equilibration period. After pH adjustment, the serum bottles were immediately sealed with airtight rubber stoppers, and incubated in a Labcon SPL-MP 15 Orbital Shaker (Labcon Laboratory Services, South Africa) at 100 rpm, and allowed to equilibrate for 3 hours at 25±0.5°C. All experiments were performed repeatedly in triplicates. At the end of the equilibration period samples were collected by sterile syringes equipped with a needle, which was inserted into the rubber stoppers. The collected sample was clarified by centrifugation. The clear supernatant was acidified to 1% v/v HNO_3 and stored at 4 °C before metal analysis.

3.7.3 Surface Complexation Modeling

In this study, FITMOD, a modified version of the computer program FITEQL 2.0 (Westall, 1982) was used to construct geochemical models describing proton interaction with the bacteria (Daughney et al., 2004). FITMOD incorporates a number of models; both nonelectrostatic and electrostatic double layer models. This program utilizes the proton balance approach to optimize protonation constants of the various functional groups on the bacterial surface. SRB titration experimental data obtained was plotted in terms of the concentration of deprotonated or protonated sites per mass of SRB (mol/g), using Equation 3.15.

$$[H^+]_{\text{added/released}} = (C_a - C_b - [H^+] + [OH^-])/m_b \qquad [3.15]$$

where: C_a, C_b, $[H^+]$ and $[OH^-]$ are the molar concentrations of acid, base, H^+ and OH^- species, respectively, and m_b is the weight of SRB cells (mg/L) in the suspension.

The mass law relationship in conjunction with the mole balance expressions was used to define the adsorptive process. A 1:1 metal/surface site stoichometry was used for all calculations, and equilibrium constants for aqueous metal hydrolysis were obtained from Baes and Mesmer (1979). This information was used to account for Sr, Co and Cs adsorption onto SRB cell surfaces according to Equation 3.16. Under equilibrium conditions partitioning between the solid surface and the aqueous phase is therefore quantified with the corresponding mass law (Equation 3.17).

$$M^{+} + R - A^{-} \Leftrightarrow R - AM \qquad [3.16]$$

$$K_{ads} = \frac{[R - AM]}{[M^{+}] \times [R - A^{-}]} \qquad [3.17]$$

where: M^{+} = target metal, R-A^{-} = deprotonated bacterial surface site, R-AM = metal-site complex, K_{ads} = thermodynamic equilibrium constant for the reaction, and brackets denote concentrations of the specified species.

The goodness-of-fit of the different models to the titration data is indicated by the overall variance, V(Y), which is calculated by FITMOD as shown in Equation 3.18. Values of V(Y) between 1 and 20 generally indicate an acceptable fit to the data (Daughney et al., 2004).

$$V(Y) = \frac{Y_{II}^{P\left(\frac{Y}{S_Y}\right)^2}}{n_p \bullet n_{II} - n_u} \qquad [3.18]$$

where: Y is the error in the mass balance calculations, S_Y is the default experimental error calculated by FITMOD, n_p is the number of data points, n_{II} is the number of chemical components for which both total and free concentrations are known, and n_u is the number of adjustable parameters.

3.8 ANALYTICAL PROCEDURES

3.8.1 Bacterial Culture Characterization

Gram Staining

Gram staining of SRB was carried out as described by Shimeld and Rodgers (1999). At mid-stationary phase, a 0.5 mL sample of sulphate reducing bacteria culture was aseptically withdrawn with a sterile syringe. The sample was smeared on a slide, soaked in a violet dye and then treated with iodine. The slide was then rinsed with alcohol and counterstained with safranine. The result was viewed on a phase microscope.

Phylogenetic Analysis

Culture isolation was carried out using a method by Butlin et al. (1949) in medium A, solidified by 2.3% agar. An aliquot of 9 mL of cooled liquid agar medium was mixed with 1 mL of culture dilution. The suspension was then incubated at 30ºC in an anaerobic jar. Individual colonies that developed were picked and cultured in the corresponding culture medium. The process of isolation was repeated several times until isolates were deemed to be pure. Genomic DNA was extracted according to the protocol described for the Wizard Genomic DNA purification kit (Promega). 16S rRNA genes were amplified by using primers Fd1 (5'-AGAGTTTGATCCTGGCTCAG-3') and Rd1 (5'-AAGGAGGTGATCCAGCC-3') and by using the following reaction conditions: 1 min at 94ºC, 30 cycles of 30 s at 94ºC, 1 min at 50ºC and 2 min at 72ºC, and a final extension step of 10 min at 72ºC.

PCR fragments were then cloned into pGEM-T-easy (Promega). Recombinant clones, with inserts of the correct length, were sequenced by using primers SP6 (5'-ATTTAGGTGACACTATAGAA-3') and T7 (5'-TAATACGACTCACTATAGGG-3') (Genome Express). The nucleotide sequences of the 16S rRNA genes were compared with reference sequences from the GenBank database. The 16S rRNA gene sequences of the strains were aligned with reference sequences of various *Desulfovibrio* species using programs provided by the Ribosomal Database Project II. Sequence alignment was verified manually using the program BIOEDIT. Positions of sequence and alignment uncertainty were omitted from the analysis. Pairwise evolutionary distances based on an unambiguous stretch of 1274 bp were computed by using the Jukes and Cantor (1969) method. The dendrogram was constructed by

using the neighbour-joining method. Confidence in the tree topology was determined by bootstrap analysis based on 100 re-samplings.

Scanning Electron Microscopy

Surface morphology of the present SRB culture was studied by the scanning electron microscope (SEM). SRB culture samples were filtered through a 0.22µm filter to obtain the cells. Filtered SRB cells were first fixed overnight in 2.5 % glutaraldehyde in 0.1M phosphate buffer (pH 7.0) solution. The fixative solution was decanted off and cells were then washed twice in phosphate buffer (0.1M, pH 7.0) for 10 minutes. Thereafter, the cells were dehydrated in a series of ethanol solutions, 30%, 50%, 70%, 80%, 90%, and twice in absolute ethanol, and each step lasted for 15 minutes. The samples were then dried in liquid CO_2 for 2 hours at critical point (31.1° and 73 atmospheres). Pieces of the membranes containing dried cells were cut into small squares and then mounted on stubs with double-sided tape, and then gold-coated for 30 minutes in a Large Desk II Cold Sputter Etch Coater. The prepared samples were then observed under a JEOL-JSM-840 scanning electron microscope.

Potentiometric titrations

Acid/base properties of SRB cells with regard to H^+ and OH^- ions were studied by potentiometric titrations. The titrations were performed using an automated titration system comprising of a burette system, glass electrode and a pH meter (Metrohm 718 STAT-Titrino model) according previously published procedures (Fein et al., 1997; Cox et al., 1999; Martinez et al., 2002; Ngwenya et al., 2003; Borrok and Fein, 2005; Johnson et al., 2007). Prior to titration, 0.3g (wet weight) SRB cells were suspended in 25 mL of the appropriate electrolyte solution which had been purged by N_2 bubbling for 60 minutes to eliminate CO_2. The suspension was immediately placed into a sealed titration vessel with continuous stirring at 140 rpm under N_2. Titrations were carried out by the gradual addition of pre-set small volumes of 0.1M NaOH or 0.1M HCl titrant (standardized against reagent grade $KC_8H_4O_4H$ and Na_2CO_3 respectively). The titrator was set to add successive base or acid after a stability of 0.1Mv/sec was attained. Three sets of duplicate SRB suspensions were first titrated with 0.1M HCl to about pH 4 and then titrated up to about pH 10 with 0.1M NaOH. SRB titration experiments were conducted at different ionic strengths (0.01M, 0.1M and 0.5M $NaNO_3$) and temperatures (5°C, 50°C and 75°C). A total organic carbon

(TOC) analysis was conducted on the bacterial suspensions to confirm the presence or absence of organic exudates, due to cell lysis. Blank titrations devoid of SRB cells were also performed for base and acid titration. Reversibility of the SRB acid/base behaviour was established by performing reverse titrations.

Fourier Transform Infrared Spectroscopy

The acid/base characterization was complemented by Fourier Transform Infra-Red (FTIR) spectroscopy analysis to confirm the presence of different cell wall functional groups. FTIR analysis of SRB cells was conducted according to a method described by Ojeda et al. (2008). The SRB cells equilibrated with a neutral (pH 6.5) electrolyte solution 0.1M $NaNO_3$. Triplicate SRB cell suspensions (in minimal volume of the electrolyte solution) were initially frozen at -20ºC and then freeze-dried. FTIR spectra of the freeze-dried samples of SRB were recorded on KBr pellets at room temperature using a Perkin Elmer FTIR GX spectrum 2000 (PerkinElmer, USA). The sample compartment was flushed with dry air to reduce interference of H_2O and CO_2. Data analysis focused on the 600-4000 cm^{-1} region.

3.8.2 Total Organic Carbon (TOC) Analysis

Total organic carbon analyses of samples were performed in accordance with Standard Methods of Examination of Water and Wastewater (APHA, 1994). Bacterial suspensions (100 mL) at different pH values (2-11), were centrifuged and the supernatant passed through 0.22µm filters to remove the microbial component. To prevent any organic compound losses, the clear extracts were stored in the dark at −20°C for not longer than 7 days until analysis time. The analysis of dissolved organic carbon was performed by means of a Shimadzu TOC-5000/5050 analyzer coupled to an ASI-V autosampler (Shimadzu Scientific Instruments, Inc., Tokyo, Japan). TOC analysis was performed using the 'acidify and sparge' method, otherwise known as Non-Purgeable Organic Carbon (NPOC) method. An overview of the instrument specifications and basic operation conditions used for TOC analysis is shown in Appendix 1. During the NPOC analysis, the sample is automatically injected into the total carbon reactor along with an oxidising agent (1.69 M $Na_2S_2O_8$) and, with 5% H_3PO_4 (v/v) to adjust the sample pH to 2-3. After pH adjustment, sparge gas is bubbled through the samples for 3 minutes to eliminate the inorganic carbon component. The total carbon remaining in the sample after sparging is

measured to determine the total organic carbon. The TOC concentration of the samples was estimated for a calibration curve constructed using potassium hydrogen biphthalate (KHP) working standard solutions with an organic carbon range of 2-12 mg/L. The zero standards (blanks) were prepared using Ultrapure Mill-Q water. All samples were analysed in duplicate.

3.8.3 Solid Phase Sr, Co And Cs Precipitates Analysis

Speciation Analysis

To determine the species distribution of the solid phase metal species, the bound metals were released from the SRB biomass using different desorbing agents of varying strengths according to a method by Tessier et al. (1979). SRB cells in aqueous solution not spiked with a metal served as a control.

Step I: To extract exchangeable species, 8 mL of 1M $MgCl_2$ solution (pH 6) was added to 2 g of the pellet obtained by centrifugation (7000g × 15 minutes). The mixture was stirred at 25ºC for 1 hour. The mixture was then centrifuged and the supernatant was used for metal analysis.

Step II: To extract species bound to carbonates, 10 mL of 0.1M sodium acetate adjusted to pH 5 using acetic acid was added to the residue obtained at step I. The mixture was stirred at 25ºC for 3 hours, and then centrifuged and the supernatant was used for metal analysis.

Step III: To extract species bound to oxides, 10 mL of 0.1M Hydroxyl ammonium chloride (pH 2) was added to the residue obtained from step II. The mixture was also stirred at 96ºC for 3 hours, and then centrifuged and the supernatant was used for metal analysis.

Step IV: To extract species bound to sulphide, 5 mL of 30% hydrogen peroxide adjusted to pH 2 with HNO_3 and 3 mL 0.02M HNO_3 was added to the residue obtained from step III. The mixture was stirred for 2 hours at 85ºC. This was followed by the addition of 5 mL aliquot of 3.2M ammonium acetate (pH 2) in 20% (v/v) HNO_3 to avoid adsorption of the extracted metal into the oxidized fraction. The mixture was stirred for a further 30 minutes at 85ºC and then centrifuged and the supernatant was used for metal analysis.

Step V: To extract residual strontium species, 2 mL each of H_2O_2, HNO_3 and Hydrofluoric acid were added to the residue obtained from step IV. The mixture was stirred at 96ºC for 3 hours, and then centrifuged and the supernatant was used for metal analysis.

3.8.4 Metal Concentration Analysis

Strontium

Total, solid-phase and dissolved Sr^{2+} concentrations were determined separately. Raw samples were centrifuged at 10 000 g for 20 minutes to obtain the dissolved and solid phase fractions. To determine the dissolved Sr^{2+} concentration, 2.5mL of the supernatant was dispensed into 10mL acid washed tubes to which 0.5mL of 30% H_2O_2 and 0.1mL of 70% trace metal grade HNO_3 were added and incubated at 60°C overnight. The resulting pellet was also subjected to the same acid digestion treatment. Following digestion or extraction, the volume of the solution was made up to 10mL, giving a 4× dilution factor. Strontium concentrations were determined at a wavelength of 460.7 nm in a nitrous oxide-acetylene flame using an AAnalyst400 Perkin Elmer AAS (Perkin Elmer, Shelton, USA) equipped with a 10 mA hollow cathode Sr lamp. Prior to sample analysis, the instrument was calibrated against a calibration and reagent blank (5% nitric acid solution in ultrapure water), as well as Sr^{2+} standards containing 0.2, 0.4, 0.6, 0.8, and 1.0 mg Sr/L). Linear calibration graphs were obtained over the concentration ranges 0–1.0 mg/L , with the correlation coefficient set at not less than 0.995 ($R^2 \geq 0.995$). Strontium ionization in this flame was suppressed by the addition of a potassium chloride solution to give a final concentration of 2 mg/L K^+ in all samples including the standards and blank. The lower detection limit for this procedure is estimated to be about 20 µg/L.

Cobalt

Total, solid-phase and dissolved Co^{2+} concentrations were also determined as described previously for Sr^{2+}. Cobalt concentrations were determined at a wavelength of 240.7nm in an air-acetylene flame using an AAnalyst400 Perkin Elmer AAS (Perkin Elmer, Shelton, USA) equipped with a 10mA hollow cathode Co lamp. Prior to sample analysis, the instrument was calibrated against a calibration and reagent blank (5% nitric acid solution in ultrapure water), as well as Co^{2+} standards of known concentrations. Linear calibration graphs were obtained over

the standard concentration ranges, with the correlation coefficient set at not less than 0.995 ($R^2 \geq 0.995$).

Cesium

Total, solid-phase and dissolved Cs^+ concentrations were also determined as previously described for Sr^{2+}. Cesium concentrations were determined at a wavelength of 852.1 nm in an air-acetylene flame using an AAnalyst400 Perkin Elmer AAS (Perkin Elmer, Shelton, USA) equipped with a 10 mA hollow cathode Cs lamp. Prior to sample analysis, the instrument was calibrated against a calibration and reagent blank (5% nitric acid solution in ultrapure water), as well as Cs^+ standards of known concentrations. Cesium ionization was also suppressed by the addition of a potassium chloride solution to give a final concentration of 2 mg/L K^+ in all samples including the standards and blank. Linear calibration graphs were obtained over the standard concentration ranges, with the correlation coefficient set at not less than 0.995 ($R^2 \geq 0.995$). The lower detection limit for this procedure is estimated to be about 0.005µg/mL.

3.8.5 Sulphate Concentration

The concentration of sulphate was determined using the turbidimetric method (APHA, 1994). Prior to analysis, samples were centrifuged (10 000 g for 15 minutes) to remove suspended solids. To a 5mL sample, 0.25mL of conditioning reagent (consisting of 50mL glycerol, 30mL concentrated HCl, 75g NaCl, 100mL ethanol and 300mL deionized water) was added, and mixed thoroughly. After that an excess amount of finely ground $BaCl_2$ was added and mixture was homogenized in a vortex for 1 minute. The absorbance of the mixture was measured at 420 nm. Sulphate concentration was calculated from a calibration curve ($R^2 \geq 0.995$) obtained from measurement of standard sulphate concentration in the range 2-20 mg/L, using a similar procedure for sulphate analysis.

3.8.6 Biomass Concentration

Viable SRB population

The three-tube most probable number (MPN) method was used for estimating the viable SRB population. Samples were first serially diluted by aseptically transferring 1 mL volumes into rubber-sealed culture tubes containing 9mL Postgate medium C. The culture tubes were then

incubated in the dark at 37℃ in a shaker at 200rpm for up to 28 days. Blackening of the medium due to FeS formation was regarded as a positive growth result. After the 28 days of incubation, the pattern of positive and negative tubes per dilution is noted, and then an MPN calculator was used to determine the most probable number of organisms.

Total SRB cell counts

The total bacteria count (TBC) method was used to estimate the total bacterial population. Bacteria were enumerated by direct counting using a Petroff-Hausser Counting Chamber (Labotech, South Africa) on a phase contrast Zeiss Axioskop II microscope (Zeiss, Germany).

Bacterial density (g dry/L)

For dry biomass determination, bacterial suspension aliquots of 30 mL were passed through a pre-weighed 0.22µm milli-pore filter. Prior to use, the filter was rinsed in ultrapure water to remove soluble salts that might be present in the filter. The biomass accumulated on the filter was dried at 80ºC for 48 hours and then weighed.

CHAPTER 4

Sr^{2+}, Co^{2+} and Cs^{+} REMOVAL IN A BATCH SULPHIDOGENIC BIOREACTOR

4.1 PROSPECTS OF RADIONUCLIDE REMEDIATION IN AN SRB BIOREACTOR

The present study evaluates the applicability of an SRB biomass as the reactive component in a metal bioremediation system aimed at controlling radionuclide dispersion in the environment. Due to their metabolic activities (which result in the production of biogenic ligands), reactive surface properties and ubiquitous distribution, SRB are considered to be principal microbial agents for controlling the dispersion of metals and radionuclides in the environment (Lovley and Phillips, 1992; Lloyd et al., 1999; Smith and Gadd, 2000; Ngwenya and Whitely, 2006). While the utilisation of SRB cultures for the bioremediation of water sources contaminated with Sr^{2+}, Co^{2+} and Cs^{+} as the ultimate solution is not completely fulfilling, however, it is the only practical solution worth exploring, considering that these microorgansisms have been found to be capable of surviving in irradiated environments (Bruhn et al., 2009). Engineered bioremediation (through biostimulation and bioaugumentation) has, in some instances been proposed as a potential strategy for the immobilization of various environmental contaminants in groundwater systems (Brown et al., 2006). However, the application of active (or growing) microbial cultures to contaminated sites is often complicated by unpredictable microbial activities due to the toxic effects of the metals and radionuclides. In addition, fluctuations in environmental conditions further present uncertainties in the performance of the culture in the contaminated environment.

Therefore, it is critical that the growth, metabolism and diversity dynamics of prospective metal bioremediation bacteria is thoroughly evaluated under contaminated environmental settings. In such cases, kinetic models for bacterial growth and biological substrate consumption become valuable aids for the design, operation and control of the chosen bioremediation strategies. Furthermore, the models become valuable research tools to improve our understanding of the fundamental microbial processes and interactions during metal bioremediation. According to

Mazidji et al. (1992), the broad non-specific impact of metals on microbial activity is manifested through two distinct modes of action; mortality of less tolerant bacterial species, leading to a decrease in total number of bacterial population and diversity, and the reduction of metabolic activities of the surviving bacterial culture. The former can be defined as the toxic effect of the metal, while the decrease in metabolic rate reflects the inhibitory effect of the metal. The present study presents findings on the toxic and inhibitory effects of Sr^{2+}, Co^{2+} and Cs^{+} on an SRB consortium by monitoring the changes in microbial diversity, biomass population and the sulphate reduction rates.

4.2 SRB CHARACTERIZATION AND SCREENING

4.2.1 Partial Characterization of the Initial SRB Consortium

In this study, a number of approaches were used to characterize the SRB consortium before and after exposure to increasing Sr, Co and Cs concentrations in a sulphidogenic bioreactor. Gram staining results indicated that the consortium was predominantly Gram-negative with a few Gram-positive species (Figure 1, Appendix 2). Surface morphology of SRB cells was studied with the scanning electron microscope (SEM). Under the SEM mainly subspherical and rod-shaped SRB cells occurring singly were observed, which is known for lactate as substrate (Figure 2, Appendix 2). The cells were approximately 0.5-1 µm in diameter and 1.7 – 2.5 µm long, which is in close agreement with literature values for SRB (Postgate, 1984; Motamedi and Pedersen, 1998). Phylogenetic analysis using the 16S rRNA fingerprinting technique of the original SRB consortium (control) indicated a dominance of only two genera, belonging to *Enterococcus* and *Staphylococcus* (Figure 4.1). The genus *Enterococcus* belongs to a group of bacteria that comprise of Gram-positive and produce lactic acid as the major metabolic end-product of carbohydrate fermentation. The ability of *Enterococcus* sp. to reduce sulphate into sulphide has been reported. The only difference between these microorganisms and SRB is that *Enterococcus* sp. reduce sulphate to synthesize sulphur containing organic compounds (cystein and methionin metabolism) and sulphide production is highly regulated due to its toxic effect which may contribute to cell death. On the other hand, SRB use sulphate as an electron acceptor to support growth under anaerobic conditions, a phenomenon known as sulphate respiration (Barton, 1992).

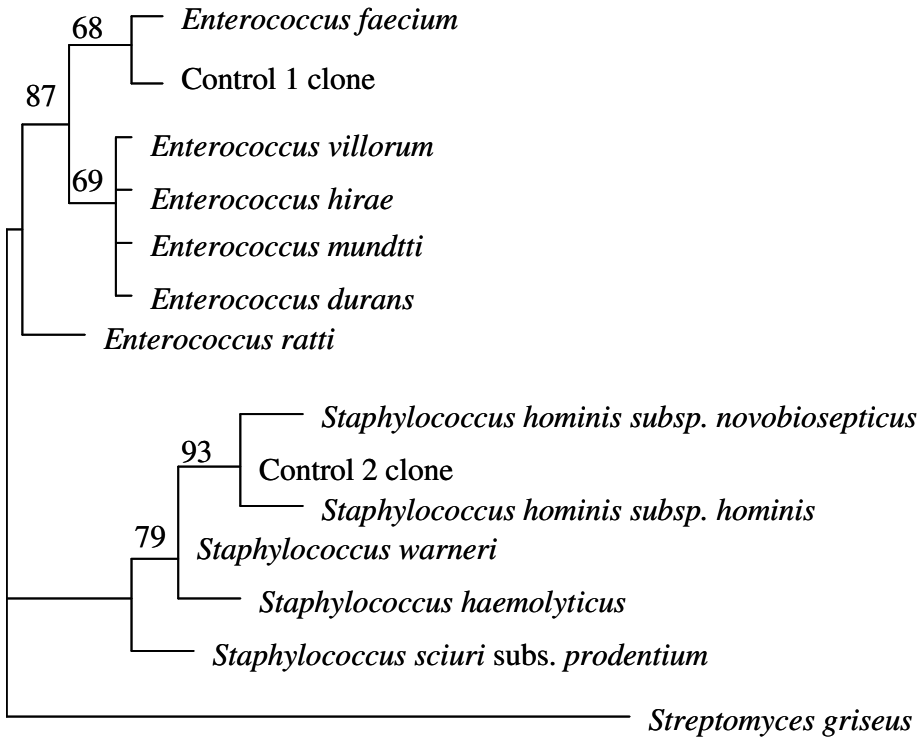

Figure 4.1: Phylogenetic tree of *Enterococcus* and *Staphylococcus* sp. related clones obtained from the original SRB culture (control). The cloned genes are named according to the isolate number.

4.2.2 Microbial Diversity Analysis in the Sr, Co and Cs Bioreactors

A number of researchers have reported the microbial removal of Sr^{2+}, Co^{2+} and Cs^{+} from contaminated aqueous streams (Small et al., 1999; HaiLei et al., 2007; Gao et al., 2010). However, there is lack of knowledge on the probable microbial diversity shifts that occur during Sr^{2+}, Co^{2+} and Cs^{+} bioremediation. Such results can help demonstrate the tolerance as well as applicability of individual microorganisms for selective removal of these metal ions. Previous results obtained from this study indicated that only two genera; *Enterococcus* and *Staphylococcus*, were present in the initial SRB culture, and no significant changes were observed in the SRB culture after a 28 day growth period. However, the presence of Sr^{2+}, Co^{2+} and Cs^{+} in the growth media resulted in the emergence of new bacterial strains representing 3 different genera, belonging to *Citrobacter*, *Paenibacillus* and *Stenotrophomonas* spp.,

respectively. The phylogenetic affiliations and gram-staining results of these isolates obtained from Sr^{2+}, Co^{2+} and Cs^{+} contaminated enrichments with their nearest phylogenetic neighbour in the GeneBank database are shown in Table 4.1. The emergence of these additional bacterial species can be attributed to their tolerance and ability to adapt to conditions of toxic Sr^{2+}, Co^{2+} and Cs^{+} concentrations. A detailed account on the growth and metabolism (sulphate reduction), as well as ability of the bacterial consortia detected in the different bioreactors for Sr^{2+}, Co^{2+} and Cs^{+} removal is presented at a later stage in this chapter.

Table 4.1 Phylogeny of the SRB isolates from Sr^{2+}, Co^{2+} and Cs^{+} contaminated bioreactors.

Clone	*Source*[1]	*Closest Match in GeneBank*[2]	*Similarity (%)*	*Gram staining result*[3]
Control 1	Coal mine wastewater	*Enterococcus faecium*	98	(+)
Control 2	Coal mine wastewater	*Staphylococcus hominis*	100	(-)
Sr1	Sr bioreactor	*Citrobacter* sp.	100	(-)
Sr2	Sr bioreactor	*Citrobacter farmeri*	97	(-)
Sr3	Sr bioreactor	*Citrobacter farmeri*	100	(-)
Sr4	Sr bioreactor	*Citrobacter* sp.	100	(-)
Co1	Co bioreactor	*Enterococcus faecium*	99	(+)
Co2	Co bioreactor	*Paenibacillus motobuensis*	99	(+)
Co3	Co bioreactor	*Paenibacillus motubuensis*	99	(+)
Co4	Co bioreactor	*Paenibacillus motobuensis*	99	(+)
Cs1	Cs bioreactor	*Enterococcus* sp.	99	(+)
Cs2	Cs bioreactor	*Enterococcus faecium*	99	(+)
Cs3	Cs bioreactor	*Stenotrophomonas maltophilia*	99	(-)

[1]Direct from coal mine wastewater or Sr^{2+}, Co^{2+} and Cs^{+} contaminated enrichments.
[2]Based on partial 16S rRNA sequences. Bootstrap = 100.
[3]Based on a method by Shimeld and Rodgers (1999), where (–) = Gram-negative and (+) = Gram-positive .

Microbial Diversity Shifts in the Presence of Strontium

Strontium exists in the environment in a variety of compounds, with the divalent cation, Sr^{2+}, as the most dominant species in contaminated groundwater systems (Brown et al., 2006). The biosorption of Sr^{2+} by bacteria has been reported by Small et al. (1999) and Ngwenya and Chirwa, (2010). However, this is the first study to demonstrate Sr^{2+} tolerance of individual microorganisms in an SRB consortium. Results obtained from this study revealed that cloned 16S rRNA gene sequences of bacterial enrichments obtained from Sr^{2+} contaminated bioreactors were closely affiliated to the marine SRB species belonging to genus *Citrobacter*. Figure 4.2

shows the phylogenetic affiliations of SRB clones isolated from Sr^{2+}contaminated enrichments and some known related bacteria based on partial 16S rDNA sequences. In particular, *Citrobacter farmeri* is a member of family *Enterobacteriaceae*, Gram-negative, obligate facultative and cocci-shaped anaerobe, which grows on lactate, acetate, pyruvate and hydrogen when provided sulphate as an electron acceptor. The ability of the *Citrobacter* sp. for sulphur and sulphate reduction has been reported (Odom and Singleton 1992; Sahrani et al., 2008; Qiu et al., 2010). *Citrobacter* sp. have been isolated from broad range substrate ecologies such as effluents from wastewater treatment plants, soil and aquatic habitats, as well as in microbial communities associated to biofilms that cause corrosion of oil pipelines (Holt et al. 1994; Nada et al. 2004; Neria-Gonzalez et al. 2006). These microorganisms have been used for the removal of a range of metals, including Pb, Cu, Cd, An, Am, U, La, Th (Macaskie and Dean, 1982; Macaskie et al., 1992; Sharma et al., 2009).

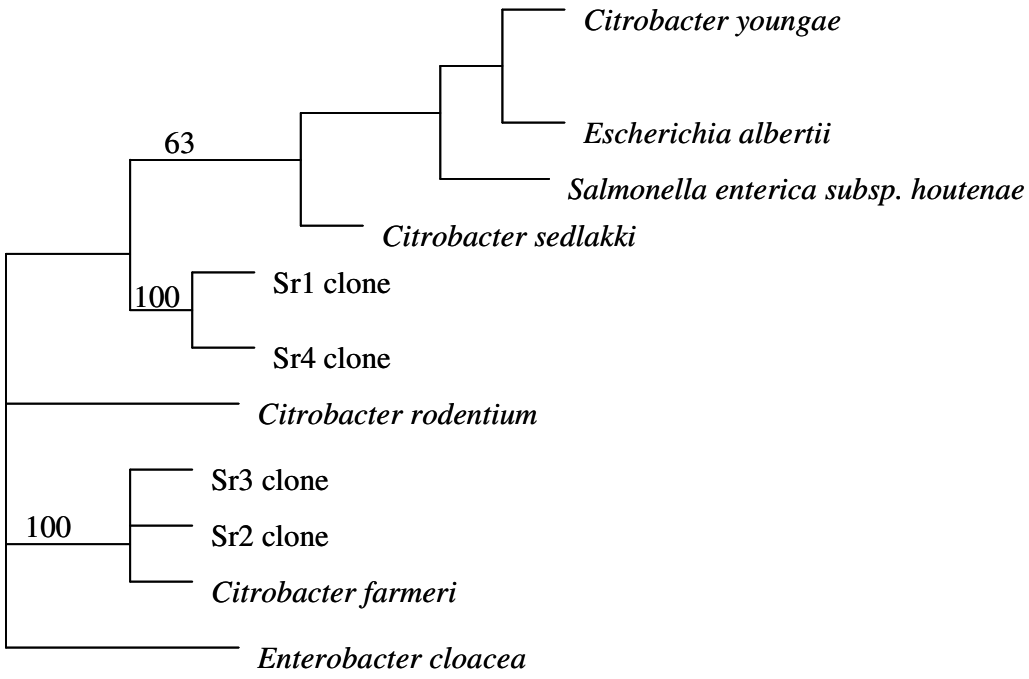

Figure 4.2: Phylogenetic tree of *Citrobacter* sp. related clones obtained from cultures grown in Sr^{2+} contaminated medium. The cloned genes are named according to the source/contaminating metal and isolate number.

Microbial Diversity Shifts in the Presence of Cobalt

The toxic and inhibitory effects of cobalt on the growth sulphate reducers have been studied before, as some SRB require the presence of a cobalt-containing, vitamin B_{12}-methyltransferase for carbon oxidation through the acetyl-CoA pathway (Weijma et al., 2000; Ekstrom and Morel, 2008). Results obtained in the present study indicated that the 16S rRNA gene sequences of SRB clones isolated from Co-contaminated bioreactors were closely related to *Paenibacillus* sp. and *Enterococcus* sp. *Paenibacillus* sp. are Gram-positive, facultative anaerobic bacteria that are related to *Bacilli* but differ in the DNA encoding their 16S rRNA. They have been shown to be capable of utilizing acetate as a carbon source (Nakamura, 1984). The phylogeny of *Paenibacillus* sp. and some known related bacteria based on 16S rDNA sequences are shown in Figure 4.3. The bacterium *Paenibacillus* has also been shown to be able to reduce colourless potassium tellurite to black metallic tellurium (Chien and Han, 2009). Similarly, the Co-reducing capability of these microorganisms has been recently reported by Gao and coworkers (2010).

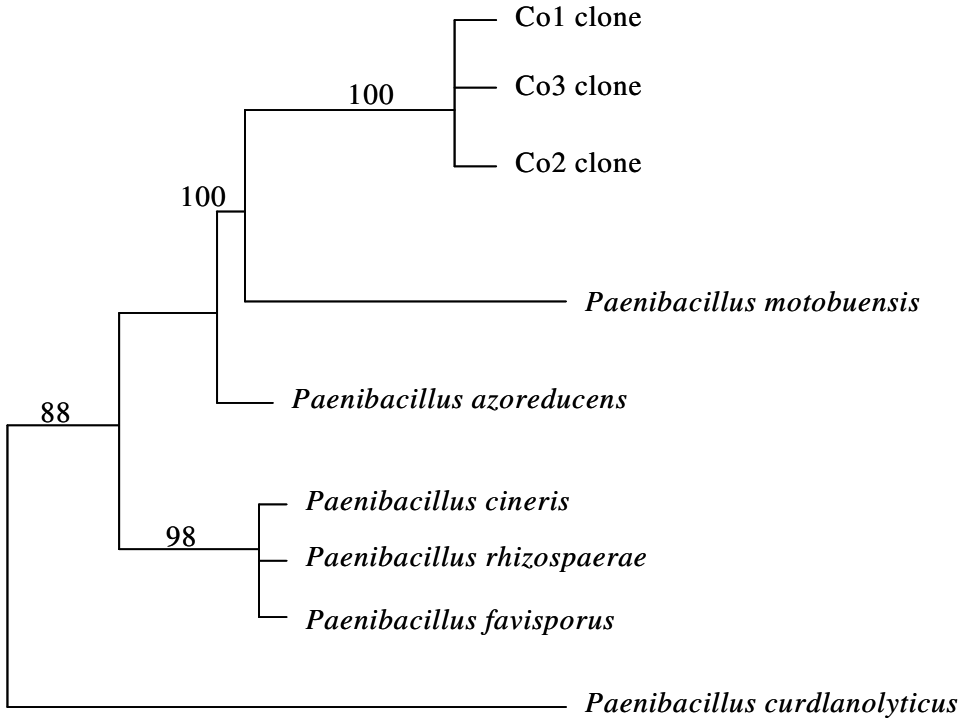

Figure 4.3: Phylogenetic tree of *Paenibacillus* sp. related clones obtained from cultures grown in Co^{2+} contaminated medium. The cloned genes are named according to the source/contaminating metal and isolate number.

Microbial Diversity Shifts in the Presence of Cesium

Phylogenetic analysis of bacterial isolates obtained from sulphidogenic bioreactors contaminated with Cs, indicated that the medium favored the growth of two main strains; *Enterococcus* sp. and *Stenotrophomonas* sp. Figure 4.4 shows the phylogenetic affiliations of the *Enterococcus* sp. isolated from Cs^+ contaminated enrichments and some known related bacteria based on partial 16S rDNA sequences. The biological effects of cesium on different living organisms are well documented (Avery et al., 1993; Lloyd and Macaskie, 2000). However, limited studies have been done on the resilience of individual microorganisms towards cesium. Therefore, results obtained from this study are crucial in establishing the applicability of specific growing bacterial cultures for cesium bioremediation. The observed results demonstrate that *Enterococcus* sp. (original bacterial isolate) is more resilient to Cs^+, compared to *Staphylococcus* sp.

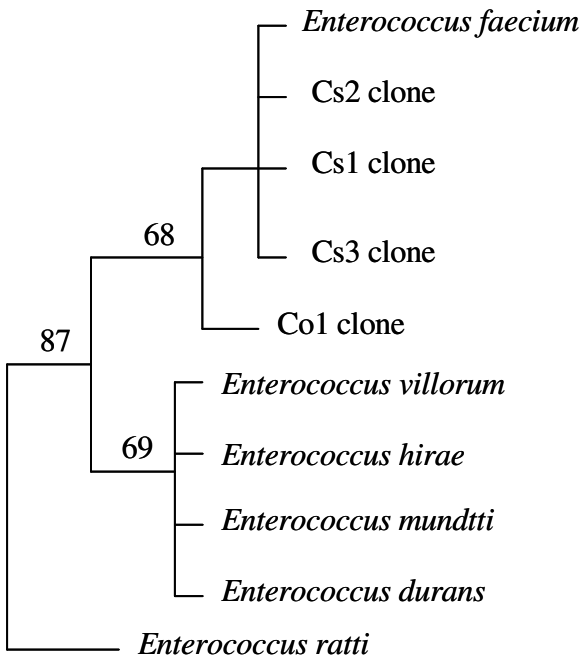

Figure 4.4: Phylogenetic tree of *Enterococcus* sp. related clones obtained from cultures grown in Cs^+ contaminated medium. The cloned genes are named according to the source/contaminating metal and isolate number.

This genus belongs to a group of Gram-positive bacteria, which produce lactic acid as the major metabolic end-product of carbohydrate fermentation. The metal removing capability of the *Enterococcus* sp., particularly, *E. faecium* has been reported recently (Yilmaz et al., 2010). The genus *Stenotrophomonas*, which is phylogenetically placed in the γ-Proteobacteriacea group, was first described with the type species *S. maltophilia*1. The phylogenetic affiliations of the *Stenotrophomonas* sp. isolated from Cs^+ contaminated enrichments and some known related bacteria based on partial 16S rDNA sequences are shown in Figure 4.5. *S. maltofilia* is found in diverse environments, including water, soil debris, raw milk, frozen fish and disinfection solutions used in hospitals (Garcia et al., 2002).

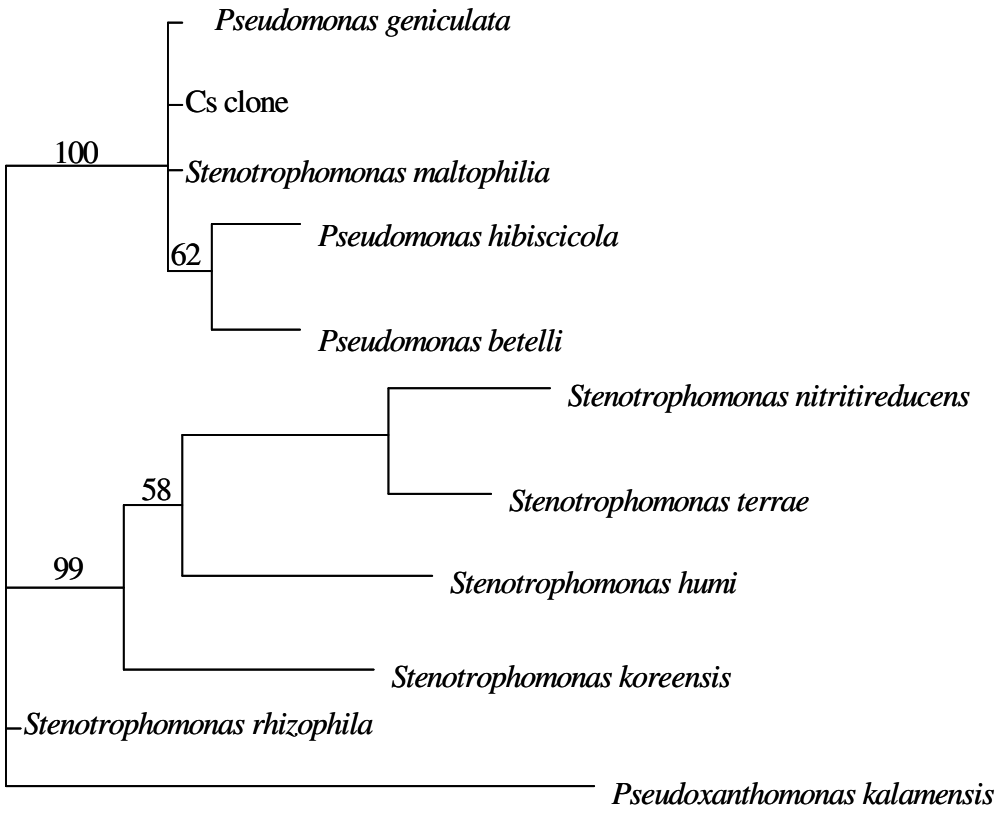

Figure 4.5: Phylogenetic tree of *Stenotrophomonas* sp. related clones obtained from cultures grown in Cs^+ contaminated medium. The cloned genes are named according to the source/contaminating metal and isolate number.

S. maltophilia, has extraordinary range of activities, including the breakdown of natural and man-made pollutants that are central to bioremediation and phytoremediation strategies. Like other Gram-negative bacilli, these microorganisms are tolerant to various toxic metals, such as Ag, As, Cd, Co, Hg, Pb, Zn, U and selenite (Botes et al., 2007; Ryan et al., 2009). Members of the genus *Stenotrophomonas* have also been reported to play an important ecological role in the nitrogen and sulphur cycles (Banerjee and Yesmin, 2002).

4.2.3 Mechanisms of Sr^{2+}, Co^{2+} and Cs^{+} Removal in the Bioreactors

Results obtained from this study showed no metal concentration loss in the absence of bacteria (abiotic control). Experiments were also conducted in a closed bioreactor system, which minimises metal losses/additions to and from the environment. Figure 4.6 shows the distribution of Sr^{2+}, Co^{2+} and Cs^{+} species on bacterial cells after exposure to a medium containing 75 mg/L of each metal. Results obtained suggest that Sr^{2+} removal occurred mainly through biosorption as about 68% of the solid phase Sr^{2+} was found to be occurring in the exchangeable fraction, gives an indication of the amount of Sr^{2+} that is bound to cell surface functional groups by relatively weak electrostatic interaction, and can be released by ion-exchange processes (Dahl et al., 2008). Similarly, high metal concentrations were obtained in the exchangeable fractions of both soil amended with sewage sludge and sulphide-rich tailings of a mine (Nyamagara, 1998; Carlsson et al., 2002). The remainder of the solid-phase Sr^{2+} was a result of a chemical precipitation due to the presence of ligands in the medium, including sulphate (resulting in the formation of insoluble strontium sulphate), as well as products of both sulphate reduction and carbon oxidation. About 22% of the Sr^{2+} was bound to carbonates, 4% bound to oxides and hydroxides, 3% sulphides and the remainder occurring as an immobile fraction. The mechanisms of Sr^{2+} removal by other microorganisms, e.g. *Aspergillus niger* has been studied. The experimental data obtained showed that immobilised *A. niger* was effective in removing Sr^{2+} from aqueous solution. Analysis of the Sr^{2+} precipiates by FTIR analysis showed that Sr^{2+} removal was facilitated by the presence of surface amide groups I and II (Pan et al., 2009). Regardless of the metabolic state of the SRB cells, the results obtained clearly demonstrated that the different bacterial surface chemical functional groups played a significant role in determining the mode and extent of Sr^{2+} removal in the bioreactor. The unique and strong Sr^{2+} complexing ability organic ligands present on the SRB cell surface is detailed in Chapter 5.

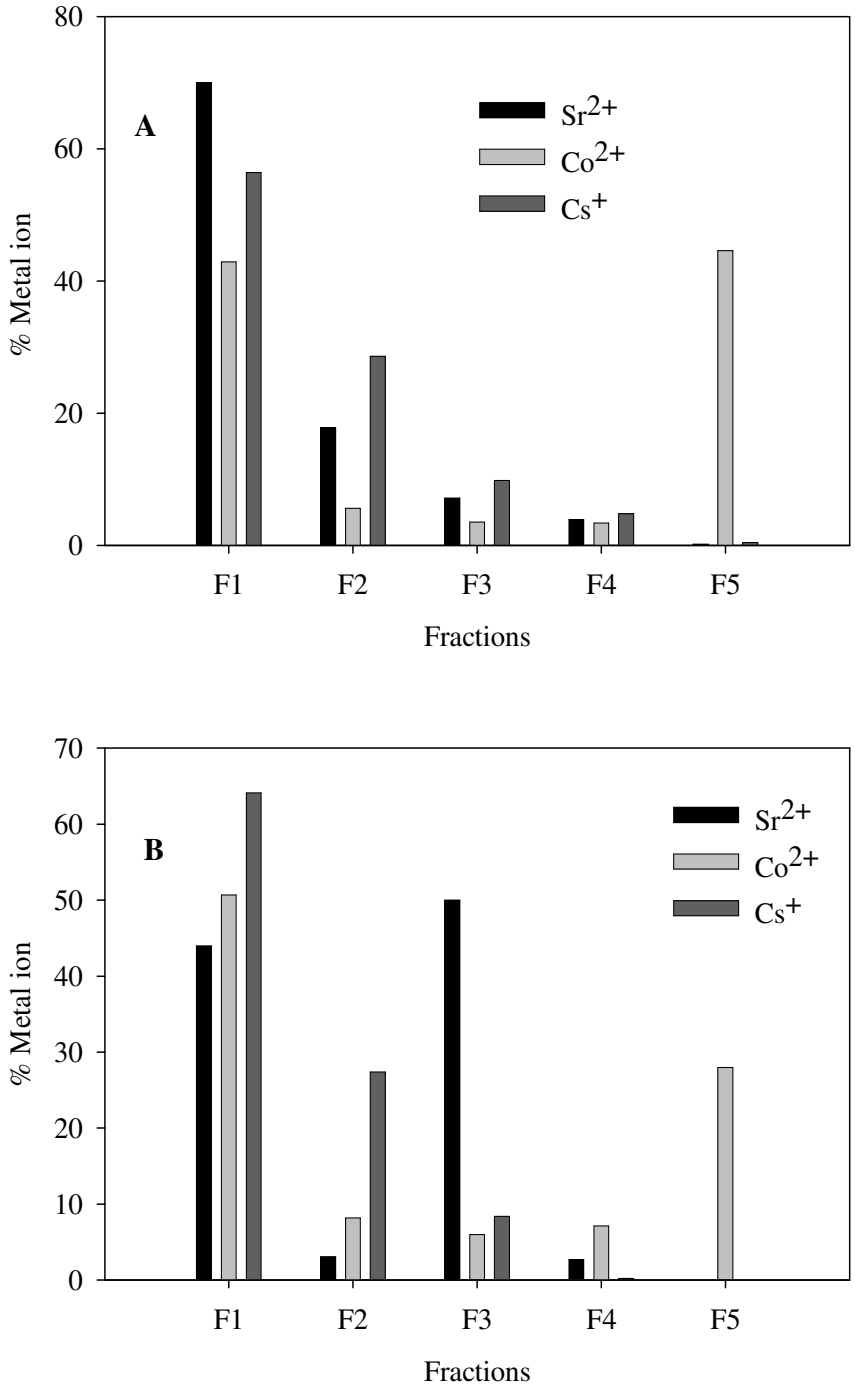

Figure 4.6: Partitioning of Sr^{2+}, Co^{2+} and Cs^{+} species on viable (A) and dead (B) SRB biomass. F1 = exchangeable, F2 = carbonates, F3 = oxides, F4 = sulphide/organics, and F5 = residual fraction.

However, the metabolic state of the bacteria had a significant effect on the mechanism and fate of Co^{2+} in the bioreactor. Under growth conditions, the Co^{2+} in the medium is ultimately accumulated both inside (45%) and outside the cell (43%). The dual mechanism of metal removal from solution by the bacterial cells has been reported before (Ho and McKay, 2000; Aksu, 2001; Goncalves et al., 2007). Initially metal sorption occurs through a rapid sorption phase, where the metal ions bind to the surface through the formation of ionic bonds, which is followed by a slower, metabolism-dependent phase, where the metal is accumulated inside the cell. The extent of Co^{2+} intracellular accumulation and adsorption is represented by the immobile fraction (F5) and the exchangeable fraction (F1), respectively. Cobalt is a metabolically essential metal required by most living organisms, including bacteria. Therefore, most Co-assimilating organisms possess specialized energy-dependent systems, which transport the metal into the cell, resulting in its intracellular accumulation (Ekstrom and Morel, 2008). Similarly, in the present study, bioaccumulation accounted was the main mechanism of Co^{2+} removal by live cultures as compared to the non-viable SRB cultures. The remainder of the Co^{2+} in the medium was removed from solution through the formation of metal-ligand complexes, which was observed, in both live and dead SRB cultures.

The accumulation of cesium by different life forms is well documented (Avery et al., 1993; Lloyd and Macaskie, 2000). Cs^{+} is chemically similar to the biologically essential alkali cation K^{+}, and enters into the cells of biosorbents through K^{+} transporters. Alternatively, in the absence of Cs^{+} transport across membranes, extracellular adsorption of the cation on the cell surface occurs. Similarly, in the present study Cs^{+} uptake from solution by SRB biomass (dead or alive) occurred manly through surface adsorption reactions, as most of the sorbed metal was released by an ionic desorbing agent. The observed extracelluar adsorption of Cs^{+} exhibited by the present culture can be attributed to the ability of the SRB potassium ion transporters to discriminate between the toxic cesium cation and biologically essential potassium cation. The resistance of live SRB cultures for Cs^{+} uptake are also be further demonstrated by the slight differences in the percentage amount of Cs^{+} released by the different desorbing agents, as compared to dead SRB cells. Similar results have been obtained in experiments for the accumulation of cesium by the bacterium *Thermus sp*. TibetanG7 (HaiLei et al., 2007).

4.3 SIMULATION OF SULPHIDOGENIC BIOREACTOR PROCESSES

4.3.1 Modelling Approach

Kinetics of SRB growth and biological sulphate reduction

Batch experiments were conducted to estimate the kinetic parameters associated with SRB growth and metabolism in the presence of increasing Sr^{2+}, Co^{2+} and Cs^{+} concentrations. The approach by Kalyuzhnyi et al. (1998) formed the basis for modeling the kinetics of SRB growth and biological sulphate reduction (BSR) in the bioreactors. The Monod model provides a link between bacterial growth and substrate utilization. According to this model, bacterial growth phenomena can be described satisfactorily with four parameters; two kinetic parameters: the maximum growth rate (μ_{max}) and half velocity concentration (K_s), and two stoichiometric parameters: the yield coefficient ($Y_{x/s}$) and substrate (sulphate) concentration (Kovarova-Kovar and Egli, 1998). Since it is anticipated that the presence of metal ions might have negative effects on SRB cell activities, the Monod was modified by the addition of an inhibition term, I, (Equation 3.3), to incorporate the toxic and inhibitory effects of Sr^{2+}, Co^{2+} and Cs^{+}. The present model neglected cell decay because of the relatively short experimental durations.

Kinetics of Metal Uptake by Microbial Biomass

Results obtained in this study indicated that Sr^{2+}, Co^{2+} and Cs^{+} removal occurred in the presence of both active (alive) and non-active (heat-killed) SRB biomass, and metal ion removal occurred mainly through biosorption processes, with the exception of Co^{2+} where additional metal uptake through bioaccumulation also occurs. During metal uptake, the mobile metal ion (metal ion in solution) concentration is in equilibrium with the immobile metal ion concentration on the bacterial cells. Therefore, a linear relationship is assumed between the two. Thus, the decrease in dissolved metal concentration in the bioreactors was accounted for by a simple pseudo second-order rate law equation (Equation 3.4), incorporating a total biomass term (X) which accounts for both the active (alive) and non-active (heat-killed) SRB biomass in the bioreactors. Since, the sulphate concentration in the bioreactors was typically 2-7 orders of magnitude higher that the initial metal concentration, the formation of insoluble $SrSO_4$ at lower initial Sr^{2+} concentrations was assumed to be minimal.

4.3.2 Model Calibration and Parameter Estimation

Experimental and model data sets (S_0, S, X_0, X, C_{ini}, C and t) were obtained from a study of SRB growth and metabolism in the presence of Sr^{2+}, Co^{2+} and Cs^{+} at various concentrations (25-500 mg/L) in batch experiments, where sulphate, biomass and metal concentrations were measured over time. The model was calibrated using sets of data for each metal at an initial metal concentration of 75 mg/L. Model simulations of bacterial population, biological sulphate reduction and metal removal in the bioreactors were implemented in the computer program for simulation of aquatic systems, AQUASIM 2.0 (Reichert, 1998). The initial conditions and model input values for parameters used for the simulation of SRB bioreactor processes are shown in Appendix 3. Monod kinetic parameters were determined by fitting the experimental data to the equations described in Section 3.5.4 by using a non-linear chi-square method, which minimizes the residual sum of squares between the experimental data and calculated values.

4.3.3 Simulation of SRB Bioreactor Processes in the Presence of Strontium

Kinetics of SRB Growth in the Presence of Sr^{2+}

Table 4.2 shows the optimised Monod kinetic parameters for SRB growth in the presence of increasing initial Sr^{2+} concentrations. Fairly constant kinetic parameters were obtained, indicating that the model was precise in simulating SRB growth in the presence of Sr^{2+} as an inhibitor. Model fits improved with increasing inhibitor (initial Sr^{2+}) concentration, suggesting that the model is more applicable at higher initial Sr^{2+} concentrations where SRB growth inhibition is well defined. Similarly, there a good agreement was observed between the experimental data and model predictions (Figure 4.7). However, the model failed to capture the initial short (24 hours) acclimitisation (lag) phase of the bacterial consortium.

Table 4.2 Optimised Monod parameters for SRB population growth in the presence of Sr^{2+}.

C_{ini} (mg/L)	X_0	μ_{max} (1/h)	K_s (mg/L)	$Y_{x/s}$ (mg/mg)	K_i (mg/L)	χ^2
25	46	0.981	466.9	0.0758	0.616	918.8
75*	48	0.987	466.9	0.0735	0.616	611.5
100	47	0.989	462.4	0.0738	0.616	408.8
300	56	0.986	466.8	0.0749	0.616	298.6
500	48	0.982	466.1	0.0749	0.616	68.8

* = data used for model calibration and parameter estimation

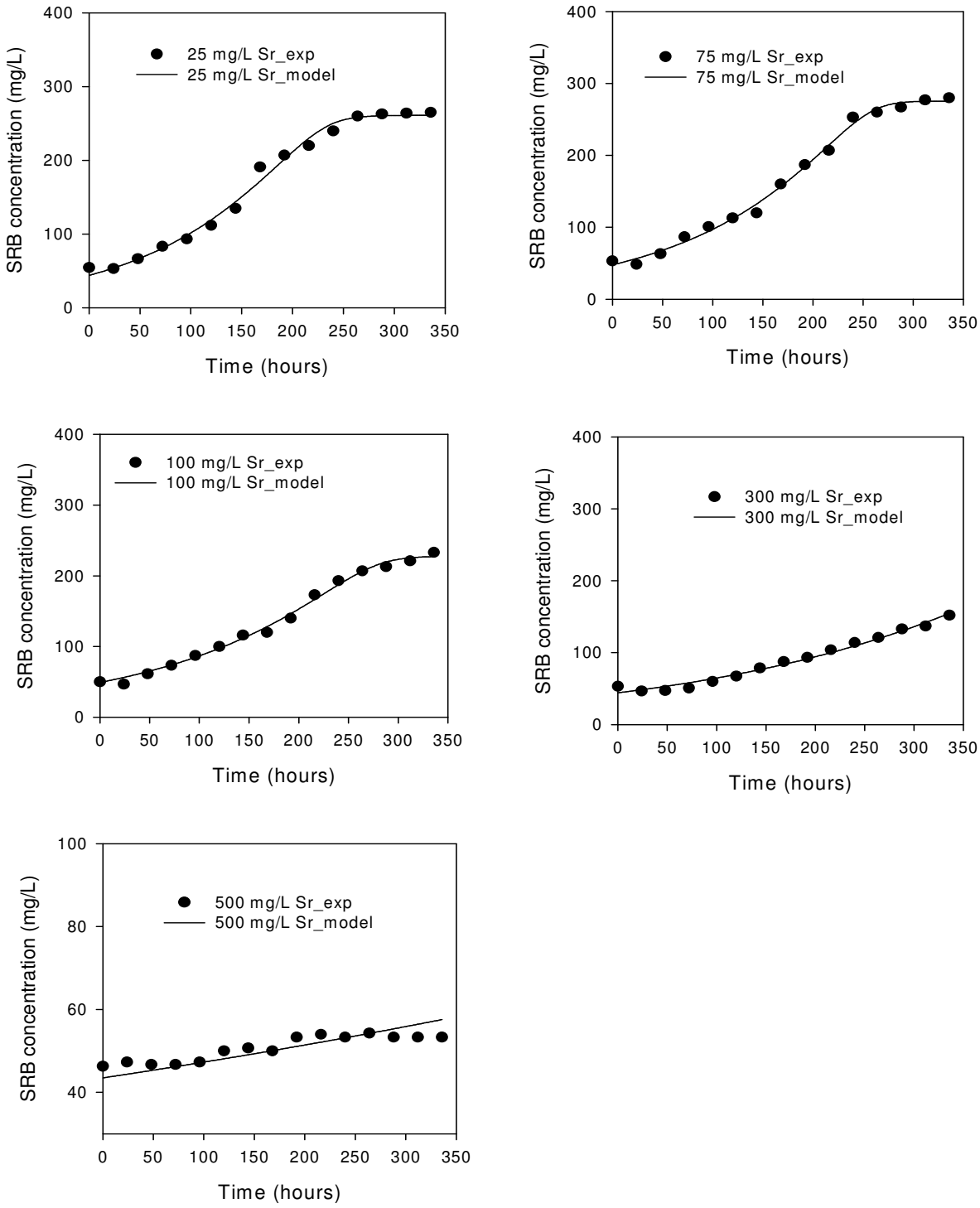

Figure 4.7: Experimental and model predicted growth of an SRB biomass in a batch bioreactor in the presence of different initial Sr^{2+} concentrations.

Both the experimental observations and model simulations indicated that after the short acclimitisation phase, there was a longer exponential phase (up to 250 hours) followed a stationary phase. However, it was evident that increasing the initial Sr^{2+} concentration prolonged the acclimatization phase and delayed the outset of the exponential phase. Generally, the bacterial concentration multiplied remarkably (up to five times) in the presence of Sr concentrations of ≤ 100 mg/L, after which an increase in initial concentration significantly lowered microbial growth. In this case, the toxic and inhibitory effects of the metal were inevitable as neither biosorption nor precipitation lowered the available Sr^{2+} concentration to a level tolerable for SRB growth. Despite the presence of high Sr^{2+} concentrations, it should be noted that despite positive SRB growth was maintained in all bioreactors. However, the SRB biomass growth rate decreased with increasing Sr^{2+} concentrations. These results further demonstrate the resilience of *Citrobacter* spp. towards Sr^{2+}.

Kinetics of Biological Sulphate Reduction in the Presence of Sr^{2+}

Table 4.3 shows the Monod kinetic parameters for biological sulphate reduction in the presence of increasing initial Sr^{2+} concentrations and the corresponding initial SRB concentrations. The obtained goodness of fit (χ^2) values indicate that increasing the initial Sr^{2+}concentration resulted poor model fits. These parameters also suggest that the toxic (growth retardation) effect of Sr^{2+} is well defined compared to its inhibitory effect, as lower inhibition coefficients were obtained for the biological sulphate reduction process. Comparisons between experimental observations and model simulations show marked model misfits (Figure 4.8), which can be attributed to the unpredicted decrease in sulphate concentration due to the chemical precipitation of sulphate (Sr^{2+} reaction with sulphate), which is not accounted for by the present model.

Table 4.3 Optimised Monod parameters for biological sulphate reduction in the presence of Sr^{2+}.

C_{ini} (mg/L)	X_0 (mg/L)	S_0 (mg/L)	μ_{max} (1/h)	K_s (mg/L)	$Y_{x/s}$ (mg/mg)	K_i (mg/L)	χ^2
25	46	3034	0.982	466.9	0.0732	0.354	51864.8
75*	48	3027	0.985	466.6	0.0730	0.356	27400.9
100	47	3013	0.989	466.9	0.0730	0.356	45181.3
300	56	3114	0.988	467.0	0.0735	0.356	99586.5
500	44	2912	0.988	469.0	0.0730	0.357	751165.6

* = data used for model calibration and parameter estimation

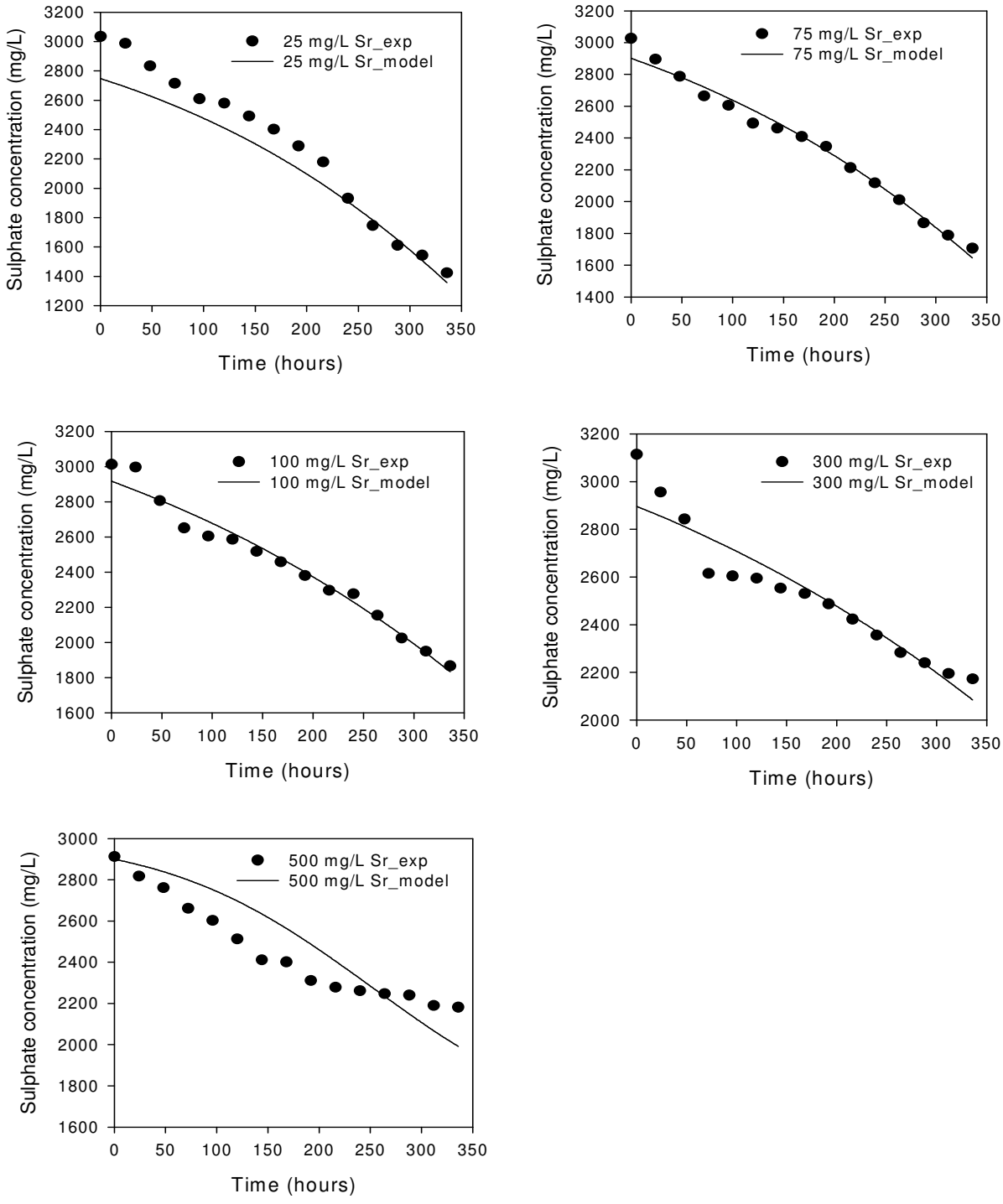

Figure 4.8: Experimental and model simulations of sulphate reduction in a batch SRB bioreactor in the presence of different initial Sr^{2+} concentrations.

The obtained results also reveal that the efficiency of biological sulphate reduction (BSR) was dependent on the initial Sr^{2+} and biomass concentration, where increasing the initial Sr^{2+} concentration resulted in the reduction viable biomass and consequently the metabolic (sulphate reduction) potential of the surviving SRB cultures (previously identified as *Citrobacter* sp.). For example, at an initial Sr^{2+} concentration of 25 mg/L, the sulphate concentration decreased from 3034 to 1501 mg/l, corresponding to a sulphate reduction rate of about 4.56 mg/L/h, compared to a rate of 2.18 mg/L/h observed at an initial Sr^{2+} concentration of 500 mg/L. The sulphate reduction capability of *Citrobacter* sp. is well documented (Odom and Singleton 1992; Barton 1995; Sahrani et al., 2008; Qiu et al., 2010).

Kinetics of Sr Removal in the Bioreactors

The kinetic parameters obtained for the removal of Sr^{2+} (25-500 mg/L) by a growing SRB biomass at biomass initial concentration (X_0) in the range 43.5-56.0 mg/L are shown in Table 4.4. Results obtained indicate that the parameter k_C (rate coefficient) is not a true constant as its value changes with increasing initial concentration. This is not surprising considering that the rate of metal removal from solution is dependent on both the metal and biomass concentration at any given time. High Sr^{2+} concentrations retard SRB growth, consequently limiting Sr^{2+} removal from solution. The model fits improved with decreasing initial metal concentration, implying that the model predictions are more valid for Sr^{2+} uptake at lower initial concentrations. Figure 4.9 shows the uptake kinetics of by the growing SRB biomass, where a comparison is made between the model predictions and experimental observations. The increased difficulties in model fits with increasing initial Sr^{2+} concentrations is a direct result of the premature chemical precipitation of Sr^{2+} due to the formation of $SrSO_4$, as previously reported.

Table 4.4 Optimised kinetic parameters for Sr^{2+} removal by growing SRB cells in a bioreactor.

C_{ini} *(mg/L)*	X_0 *(mg/L)*	k_C *(×10^{-3})*	*Metal removal capacity (%)*	χ^2
25	46	9.73	100	4.73
*75	48	9.88	100	122.4
100	47	2.44	100	1612.1
300	56	0.104	64	73940.1
500	44	0.0111	40	95029.0

* = data used for model calibration and parameter estimation

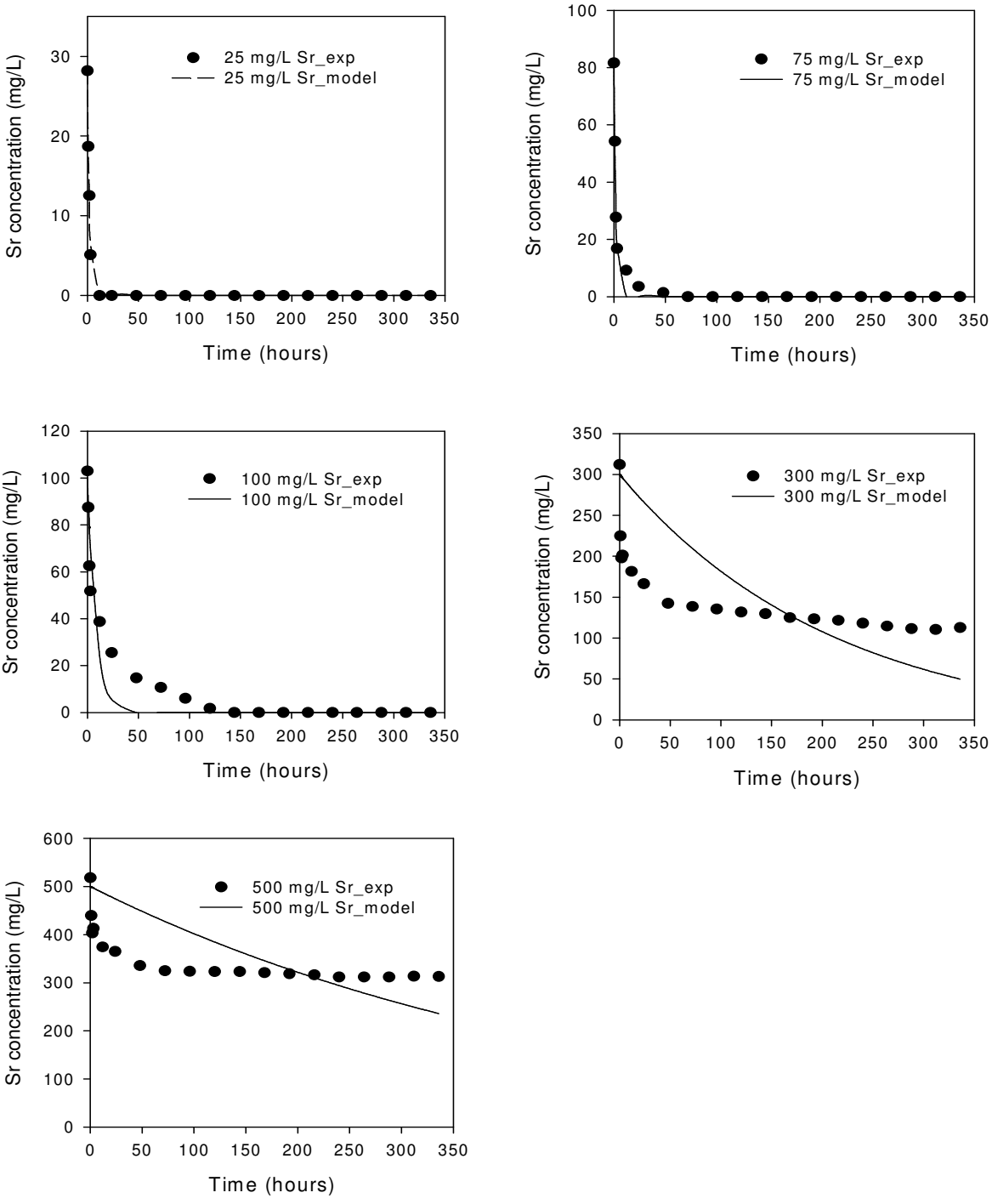

Figure 4.9: Experimental and second-order model plot showing the removal of different Sr^{2+} initial concentrations by a growing SRB consortium in a batch bioreactor.

Generally, in all bioreactors experimental and model simulations an initial fast Sr^{2+} removal rate, which then slows down with time in accordance with the outset of the stationary bacterial growth phase, after which no additional metal removal occurs was observed. This is a common phenomenon for most metal biosorption processes reported in literature (Ho and McKay, 1998; Ho and McKay, 2000; Aksu, 2001). Results obtained also indicated that the overall Sr^{2+} uptake (%) decreased with increasing initial concentration due to increased metal toxicity effects. Complete Sr^{2+} uptake was attained in the first 12, 72 and 144 hours at initial concentrations of 25, 75 and 100 mg/L, respectively. This study is among the first to report on the removal of Sr^{2+} by growing bacterial cultures. Results obtained demonstrate that SRB bioreactors inoculated with active bacterial species belonging to the genus *Citrobacter* hold a promise towards development of *in situ* Sr^{2+} bioremediation technologies.

4.3.4 Simulation of SRB Bioreactor Processes in the Presence of Cobalt

Kinetics of SRB Growth in the Presence of Co^{2+}

Results obtained show that Co^{2+} was less toxic to the present SRB culture compared to Sr^{2+}, as higher maximum growth rates (μ_{max}) and lower growth inhibition coefficient (Ki) was observed (Table 4.5). A good correlation between the experimental data and model simulations was observed, and model fits slightly improved with increasing initial concentration. The effect of cobalt on the growth and metabolism (sulphate reduction) of pure SRB cultures has been studied, where decreased growth rates and metabolic activities were observed in the presence of high Co^{2+} concentrations (Weijma et al., 2000; Ekstrom and Morel, 2008). Similarly, results obtained from this study also show that initial Co^{2+} concentration ≥300 mg/L retarded the growth of the SRB consortium (Figure 4.10).

Table 4.5 Optimised Monod parameters for SRB population growth in the presence of Co^{2+}.

C_{ini} (mg/L)	X_0	μ_{max} (1/h)	K_s (mg/L)	$Y_{x/s}$ (mg/mg)	K_i (mg/L)	χ^2
25	50	1.50	455.0	0.0772	0.352	1810.6
75*	50	1.50	456.2	0.0779	0.358	2182.3
100	50	1.53	456.9	0.0780	0.358	2745.3
300	50	1.51	455.1	0.0780	0.356	2955.5
500	50	1.51	455.1	0.0778	0.358	5534.5

* = data used for model calibration and parameter estimation

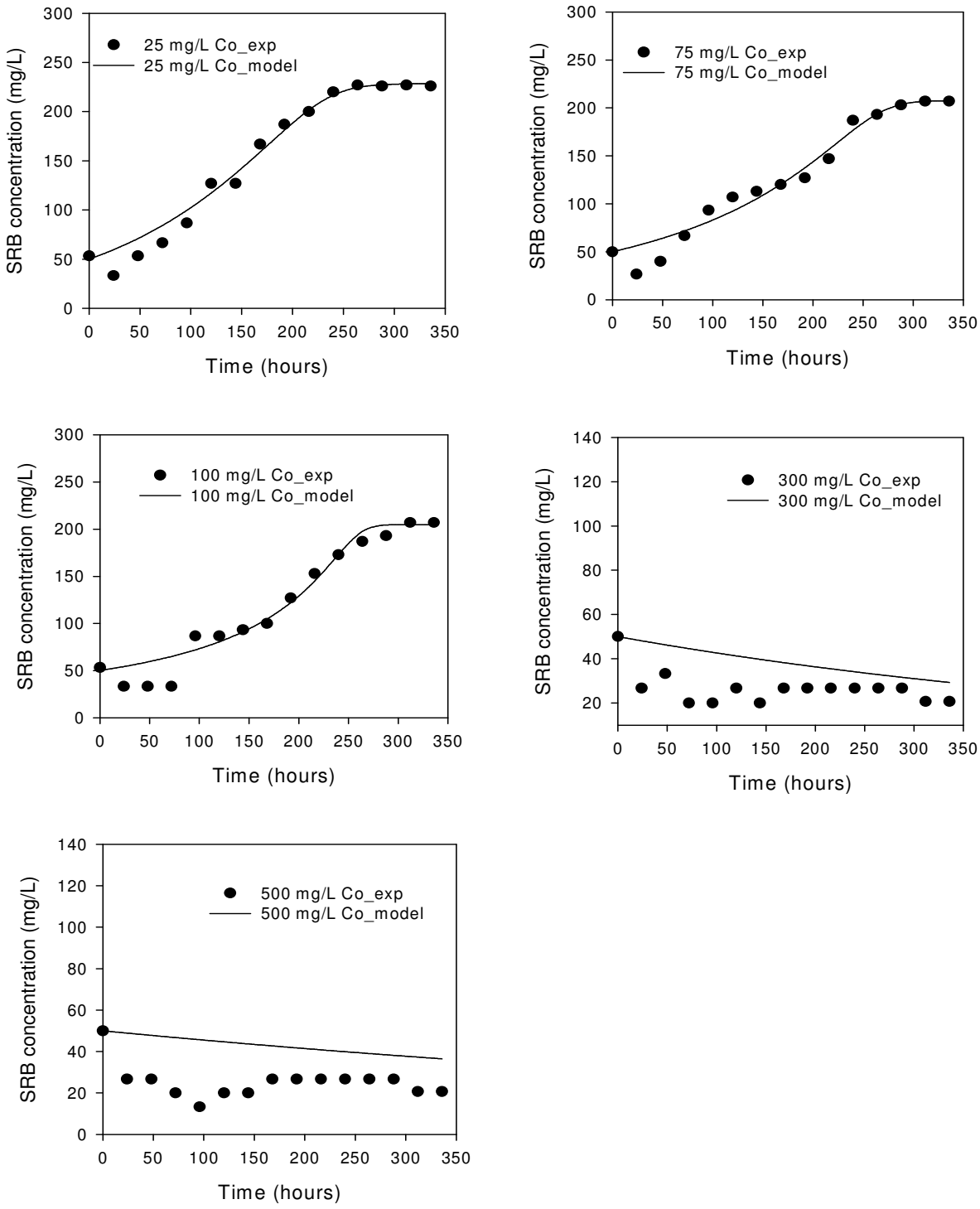

Figure 4.10: Experimental and model predicted growth of an SRB biomass in a batch bioreactor in the presence of different initial Co^{2+} concentrations.

Experimental observations for SRB growth showed that the presence of Co^{2+} in the growth media resulted in a brief initial decline in SRB concentration, which the present model failed to simulate. This phase was followed by a longer exponential phase which lasted up to 250 hours, and lastly a stationary phase, which the were both simulated well by the mode. Generally, positive SRB growth was only recorded at initial Co^{2+} concentrations ≤100 mg/L, after which increasing the initial concentration resulted in growth retardation. Therefore, the poor model simulations observed at higher concentrations (≥300 mg/L) can be attributed to the inadequacy of the model to simulate negative bacterial growth. These results demonstrate the sensitivity of *Paenibacillus* sp. towards high initial Co^{2+} concentrations.

Kinetics of Biological Sulphate Reduction in the Presence of Co^{2+}

Table 4.6 shows the optimised Monod kinetic parameters for biological sulphate reduction by SRB cultures in the presence of increasing initial Co^{2+} concentrations. When the experimental data was fit into the sulphate reduction equation, an improvement in model fit was observed with increasing initial Co^{2+} concentration. The parameters obtained reflect that the inhibitory effect of Co^{2+} on sulphate reduction was less compared to Sr^{2+}, as indicated by the lower sulphate reduction inhibition coefficients. Lower inhibition coefficients (K_i values) were obtained for sulphate reduction, compared to those obtained for SRB growth, suggesting that the toxic (growth retardation) effect of Co^{2+} is superior to its inhibitory effect. This remark is substantiated by experimental sulphate reduction studies at higher initial Co^{2+} concentrations (≥300 mg/L), where positive metabolic activity (sulphate reduction) was observed (Figure 4.11).

Table 4.6 Optimised Monod parameters for biological sulphate reduction in the presence of Co^{2+}.

C_{ini} (mg/L)	X_0 (mg/L)	S_0 (mg/L)	μ_{max} (1/h)	K_s (mg/L)	$Y_{x/s}$ (mg/mg)	K_i (mg/L)	χ^2
25	50	3030	1.50	457.0	0.0779	0.172	44118.3
75*	50	3045	1.50	456.8	0.0778	0.173	14408.7
100	50	3000	1.50	456.1	0.0777	0.172	10297.0
300	50	3030	1.53	455.0	0.0776	0.172	18262.5
500	50	3060	1.50	456.0	0.0776	0.172	16575.6

* = data used for model calibration and parameter estimation

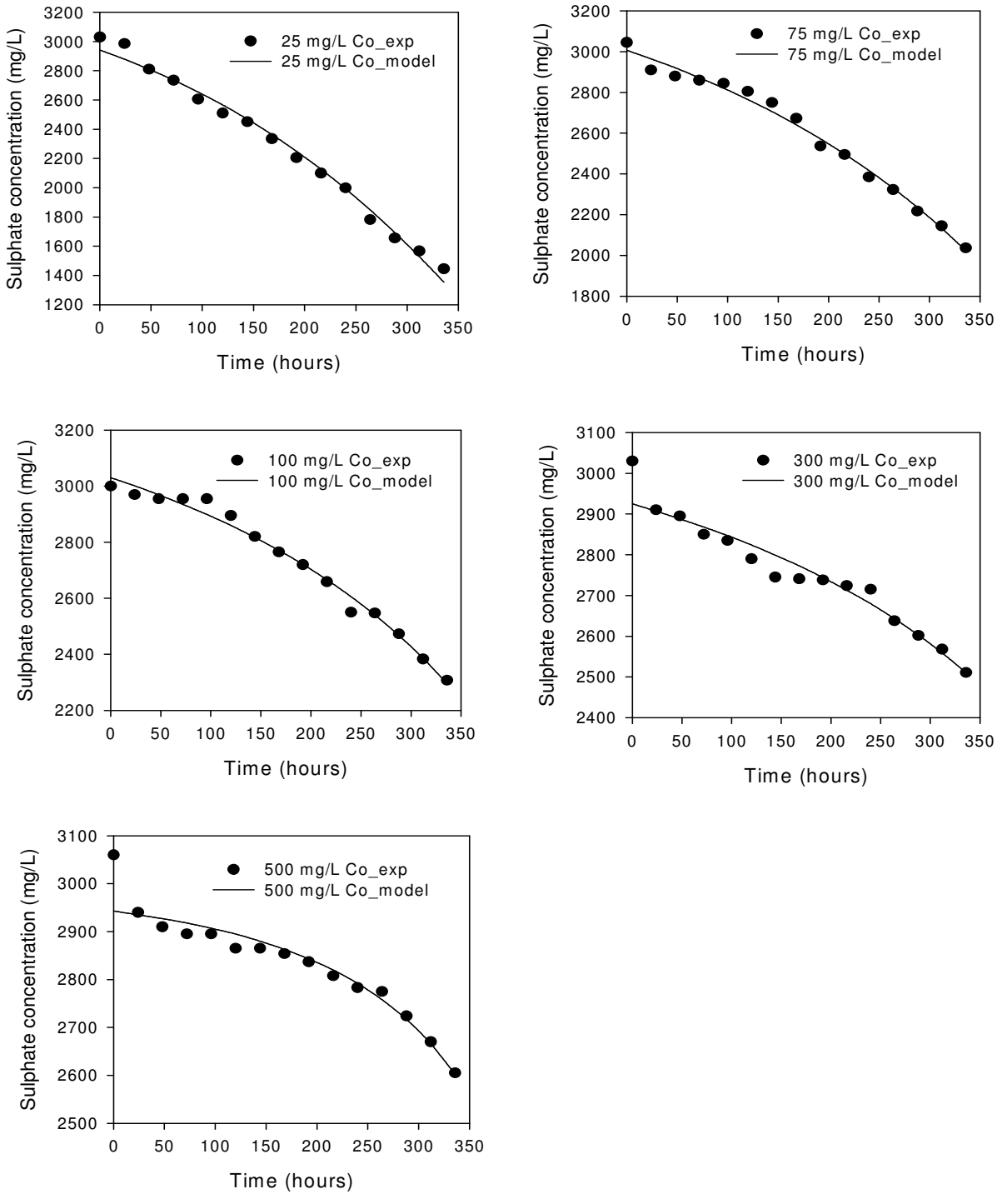

Figure 4.11: Experimental and model simulations of sulphate reduction in a batch SRB bioreactor in the presence of different initial Co^{2+} concentrations.

With regards to metabolic rate efficiency of the consortium, sulphate reduction rates (mg/L/h) of 4.79, 3.93, 3.41, 2.80 and 1.34 were obtained in the presence of 25, 75, 100, 300 and 500 mg/L Co^{2+}, respectively. In view of these findings, it is not clear whether both Co-tolerant bacterial species (*Paenibacillus* sp. and *Enterococcus* sp.) were involved in the observed gradual decrease of sulphate in the bioreactors. While *Paenibacillus* sp. are known to be capable of utilizing acetate as a carbon source (Nakamura, 1984), further studies are necessary to validate their ability or inability to reduce sulphate into sulphide. On the other hand, *Enterococcus* sp., have been shown to be capable of reducing sulphate into sulphide (Barton, 1992). In summary, the underlying prerequisite for successful utilization of active microorganisms for effective Co^{2+} bioremediation is that the initial Co^{2+} should be kept at a minimum.

Kinetics of Co^{2+} Removal in the Bioreactors

Table 4.7 shows the optimised kinetic parameters for Co^{2+} removal by a growing mixed SRB consortium. The goodness of fit (χ^2 values) of the model gradually improved with decreasing initial Co^{2+} concentration. The second-order rate coefficient (k_C) in the range 1-9 was obtained at initial Co^{2+} concentration ≤300 mg/L. However, increasing the initial Co^{2+} concentration to 500 mg/L decreased the rate coefficient, and poor model fit. Accordingly, a lower removal rate was observed at an initial Co^{2+} concentration of 500 mg/L. Generally, the batch experiments showed a 100%, 74%, 69%, 13% and 6% removal of the total Co^{2+} concentration at initial concentrations of 25, 75, 100, 300 and 500 mgL^{-1}, respectively. These results further emphasise that low initial Co^{2+} concentrations have less negative effects on SRB growth and metabolism. Similarly, the experimental data and model simulations also showed that the removal of Co^{2+} by the cultures was dependant on the initial concentration (Figure 4.12).

Table 4.7 Optimised kinetic parameters for Co^{2+} removal by growing SRB cells in a bioreactor.

C_{ini} *(mg/L)*	X_0*(mg/L)*	k_C *(×10^{-5})*	*Metal removal capacity (%)*	χ^2
25	50	8.85	100	135.7
*75	50	4.98	74	212.6
100	50	7.11	69	354.5
300	50	1.44	13	303.0
500	50	0.578	6	494.7

* = data used for model calibration and parameter estimation

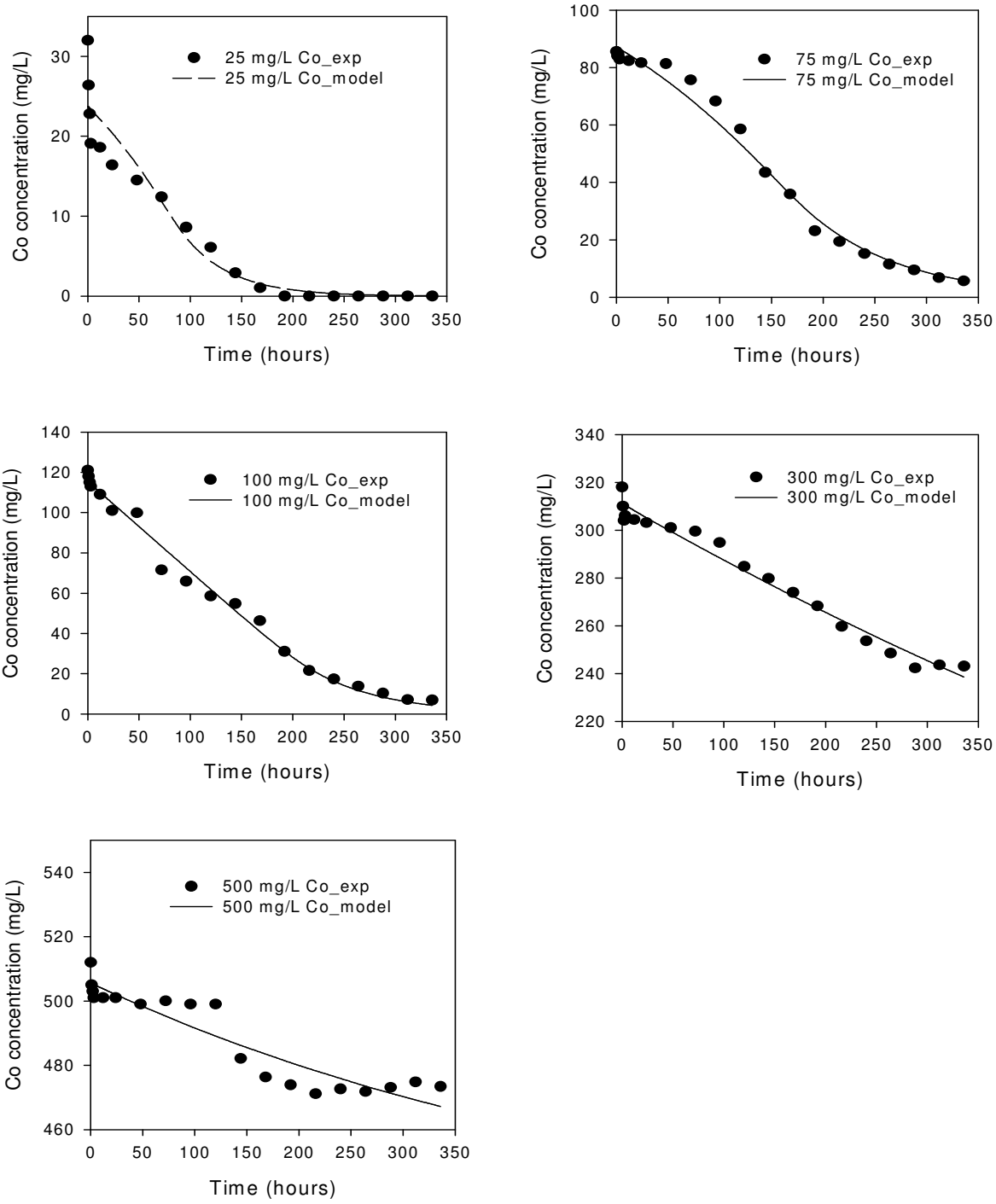

Figure 4.12: Experimental and second-order model plot showing the removal of different Co^{2+} initial concentrations by a growing SRB consortium in a batch bioreactor.

It is evident that increasing the initial Co^{2+} concentration, the Co^{2+} removal capacity of the SRB consortium was lowered to a level corresponding to the observed growth and metabolic activity of the surviving cultures. The removal of Co^{2+} through enzymatic reduction and bioprecipitation (as CoS and $CoCO_3$) in the presence of SRB cultures has been reported (Krumholz et al., 2003). Since SRB possess specialized Co^{2+} assimilation mechanisms, the metal is then ultimately accumulated inside the cell (Weijma et al., 2000; Ekstrom and Morel, 2008; Gao et al., 2010). In accordance with these observations, results obtained in this study indicated that a portion of the Co^{2+} in solution was removed through bioaccumulation. However, in addition to bioaccumulation and biopreciptation, results obtained in this study indicated that a significant portion of the Co^{2+} in solution was removed by biosorption.

4.3.5 Simulation of SRB Bioreactor Processes in the Presence of Cesium

Kinetics of SRB Growth in the Presence of Cs^+

Table 4.8 shows the optimized Monod parameters for SRB growth in the presence of increasing initial Cs^+ concentrations. While parameter optimization was successful, there was no clear trend in the model fits with an increase/decrease in initial Cs^+ concentration. However, the best model fit was obtained at higher initial Cs^+ concentration, suggesting that the present Monod inhibition model is more valid at higher initial Cs^+ concentration (≥100 mg/L) where the toxic effects can be successfully simulated. Lower inhibition (K_i) coefficients were obtained in the presence of Cs^+ in the bioreactors, compared to Sr^{2+} and Co^{2+} suggesting that Cs^+ is less toxic to the SRB consortium. Accordingly, a high maximum specific growth rate (μ_{max}) was observed. At lower initial Cs^+ concentrations (≤100 mg/L), the experimental data obtained suggested that the SRB consortium did not reach stationary phase for the duration of the experiments, while the model predicted that stationary phase was reached after 264 hours of exposure (Figure 4.13).

Table 4.8 Optimised Monod parameters for SRB population growth in the presence of Cs^+.

C_{ini} (mg/L)	X_0 (mg/L)	μ_{max} (1/h)	K_s (mg/L)	$Y_{x/s}$ (mg/mg)	K_i (mg/L)	χ^2
25	47	9.281	492.7	0.0626	0.0571	3008.9
75*	49	9.287	492.8	0.0626	0.0571	720.5
100	47	9.281	492.9	0.0627	0.0571	5518.1
300	49	9.289	492.9	0.0627	0.0571	1254.0
500	55	9.298	492.1	0.0627	0.0572	250.1

* = data used for model calibration and parameter estimation

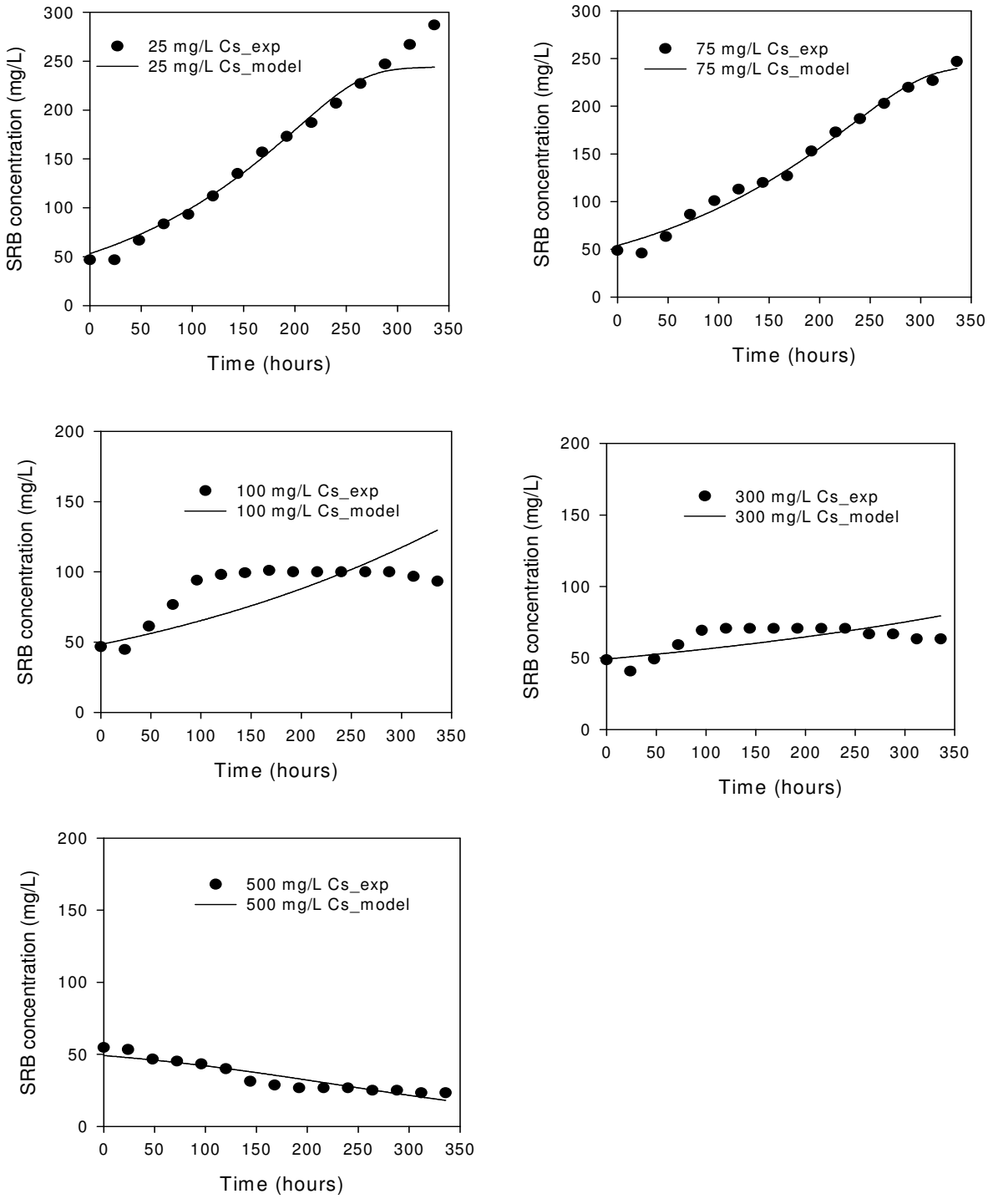

Figure 4.13: Experimental and model predicted growth of an SRB biomass in a batch bioreactor in the presence of different initial Cs^{+} concentrations.

This discrepancy can be attributed to the low toxicity of Cs^+, suggesting that it was not necessary to modify the Monod model with an inhibition term. The low toxicity of Cs^+ towards live microbial cells has been reported. However, its presence in high concentrations can dramatically decrease the uptake of essential growth micronutrients K^+ and Na^+, and these elements, thereby retarding vital microbial processes and growth (Avery, 1995). Therefore, the increased Cs^+ tolerance displayed by the present SRB consortium may result from sequestration of Cs^+ in vacuoles or changes in the activity and/or specificity of transport systems mediating Cs^+ efflux, rendering it less toxic to the microorganisms identified as belonging to *Enterococcus* sp. and *Stenotrophomonas* sp.

Kinetics of Biological Sulphate Reduction in the Presence of Cs^+

Table 4.9 shows optimised Monod parameters for sulphate reduction in the presence of increasing initial Cs^+ concentrations. The obtained results indicate that Cs^+ had a lesser effect on the metabolic activities (sulphate reduction) of the SRB consortium, compared to Sr^{2+} and Co^{2+}, as lower inhibition coefficient (K_i) values were obtained. Model fits improved with increasing initial concentration. However, visual comparisons between the experimental data and model simulations showed a poor correlation, particularly at an initial concentration of 500 mg/L (Figure 4.14). While the experimental data evidently displayed the inhibitory effect of Cs^+ at this concentration, the model predicted a less inhibitory effect. Since Cs^+ is chemically similar to the biologically essential alkali cation, K^+, it enters into the cells of living organisms through the K^+ transporter system. If present in high concentrations, the sequestered Cs^+ can act as a replacement for the essential alkali cation, K^+, thus causing undesirable biological effects on the bacterial cell (Avery, 1995).

Table 4.9 Optimised Monod parameters for biological sulphate reduction in the presence of Cs^+.

C_{ini} (mg/L)	X_0 (mg/L)	S_0 (mg/L)	μ_{max} (1/h)	K_s (mg/L)	$Y_{x/s}$ (mg/mg)	K_i (mg/L)	χ^2
25	47	3034	6.35	499.3	0.0628	0.0283	40115.4
75*	49	3027	9.30	495.0	0.0647	0.0282	17106.0
100	47	3054	9.97	492.7	0.0618	0.0283	10909.7
300	49	3041	9.98	492.4	0.0620	0.0283	9228.5
500	55	3120	9.96	495.7	0.0622	0.0283	8815.4

* = data used for model calibration and parameter estimation

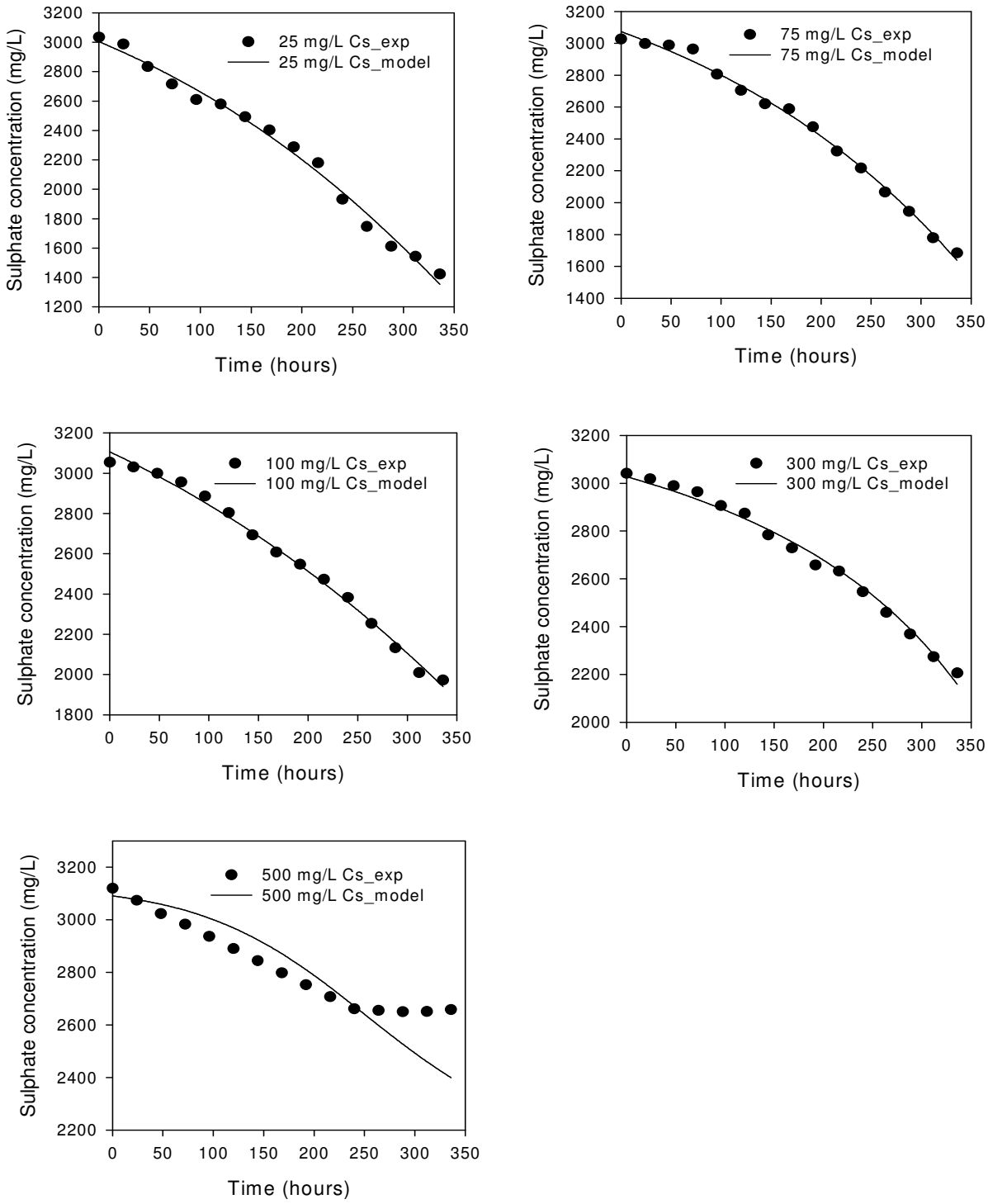

Figure 4.14: Experimental and model simulations of sulphate reduction in a batch SRB bioreactor in the presence of different initial Cs^+ concentrations.

The precise intracellular target(s) for Cs^+-induced toxicity and inhibitory effects have yet to be clearly defined, although certain internal structures, e.g. ribosomes, become unstable in the presence of Cs^+ and Cs^+ is known to substitute poorly for K^+ in the activation of many K^+-requiring enzymes (Avery, 1995). In summary, it can be assumed that the observed reduction of sulphate in the bioreactors was a direct result of the metabolic activities of the two Cs-tolerant isolates, *Enterococcus* sp. and *Stenotrophomonas* sp., due to low toxicity of Cs toxicity. However, the sulphate reduction efficiency of the SRB consortium decreased with increasing initial Cs^+ concentration.

Kinetics of Cs^+ Removal in the Bioreactors

Table 4.10 shows the optimized parameters for Cs^+ uptake by a growing SRB consortium. From this table it is clear that an increase in initial Cs^+ concentration resulted in poor model fits. The parameter, k_C (second-order rate coefficient) and the corresponding Cs^+ removal capacity of the SRB biomass decreased with increasing initial Cs^+ concentration. The low Cs^+ removal capacities at higher (≥300 mg/L) can both be attributed to both the toxic and inhibitory effects of Cs^+, which retard SRB growth and metabolism. Comparisons between the experimental data and model plots indicate that the model satisfactorily simulated removal at initial Cs^+ concentrations ≤75 mg/L (Figure 4.15). At initial concentration ≥300 mg/L, the model predicted a faster rate than was observed in Cs^+ removal experiments. Similarly, there was an evident dependence of Cs^+ removal on SRB concentration. At low initial Cs^+ concentrations of 25 and 75 mg/L, complete removal was observed within the first 24 hours and after 240 hours, respectively.

Table 4.10: Optimised kinetic parameters for Cs^+ removal by growing SRB cells in a bioreactor.

C_{ini} *(mg/L)*	X_0 *(mg/L)*	k_C *($\times 10^{-4}$)*	*Metal removal capacity (%)*	χ^2
25	47	8.00	100	105.7
*75	49	1.33	100	162.1
100	47	0.783	68	1003.4
300	49	0.304	38	3404.9
500	55	0.117	18	6447.5

* = data used for model calibration and parameter estimation

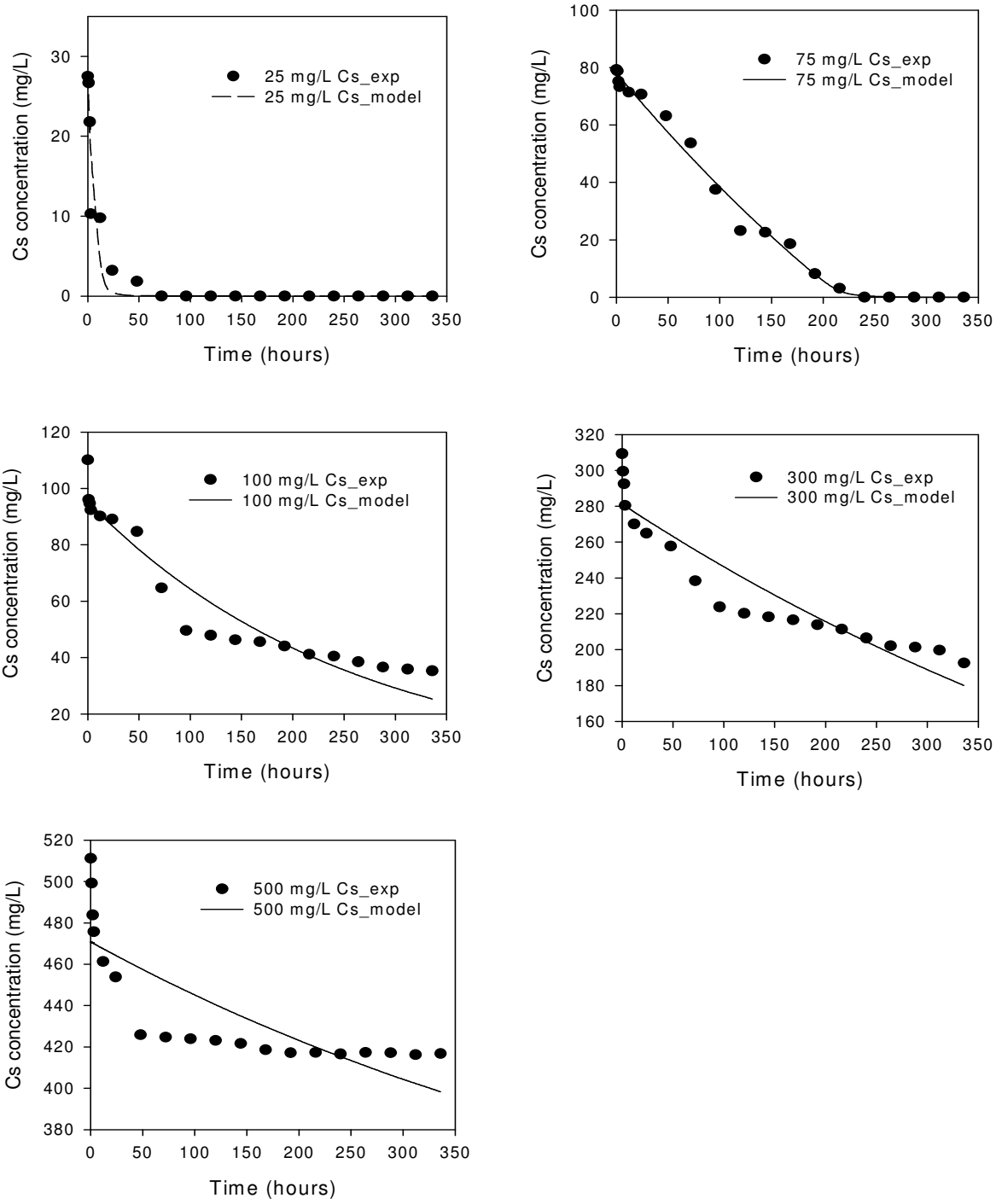

Figure 4.15: Experimental and second-order model plot showing the removal of different Cs^{+} initial concentrations by a growing SRB consortium in a batch bioreactor.

Cs^+ exists almost exclusively as the monovalent cation Cs^+ in the natural environment. Although Cs^+ is a weak Lewis acid that exhibits a low tendency to form complexes with ligands, its chemical similarity to the biologically essential alkali cation K^+ facilitates high levels of metabolism-dependent intracellular accumulation (Lloyd and Macaskie, 2000). However, previous results obtained in this study showed that limited Cs^+ removal bioreactors occurred through bioaccumulation. The low microbial Cs^+ bioaccumulation observed in this study can be attributed to presence of competitive cations, e.g. K^+, Na^+, NH_4^+ and H^+, in the medium, whose presence have been reported to decrease its significantly (Avery, 2004). The distinct chemical properties of Cs^+, indicate that different approaches are required for biological Cs^+ removal to those which are generally adopted for other metals/radionuclides. However, its low toxicity eliminates one potential problem in the use of live/growing cells for its removal. The inherent differences in Cs^+ uptake capacities of different microorganisms appear to be largely attributable to differences in the affinity of monovalent cation transport systems for Cs^+. The application of rigorous screening procedures involving the use of autoradiography has great potential for isolation of microorganisms with particularly high affinities for Cs^+ (Avery, 1995).

4.3.6 Sensitivity Analysis

The sensitivity test, computed in AQUASIM 2.0 (Reichert, 1998), was performed to evaluate the relative importance of parameters on the Monod model output. The parameters of interest were the kinetic and stoichiometric parameters, including X, C_{ini}, K_i, K_s, $Y_{x/s}$ and μ_{max}. A 1% change in a given model input parameter was applied, while the others were kept constant, and the effect of the change on the model was evaluated. From the plot, it is clear that minor adjustments in the parameters; K_i, K_s, $Y_{x/s}$ and μ_{max} are critical to the model output. The model sensitivity to the parameters K_i and μ_{max} increases from zero and reaches a maximum at 240 hours then decreases again to zero, exhibiting the behaviour of the absolute value of the sensitivity function (Reichert, 1998). On the other hand, the model sensitivity to the parameter $Y_{x/s}$, remained at zero until after 240 hours, after which it increased reaching a maximum at 312 hours. Relatively, the model was less sensitive to the parameter K_s, suggesting that this constant is of minor significance to reactor performance. The dependence of the biomass concentration (X) on the initial metal concentration (C_{ini}) is identifiable, as such is an important aspect that has to be taken into consideration for evaluating the performance of bioremediation bioreactors utilizing growing biomass.

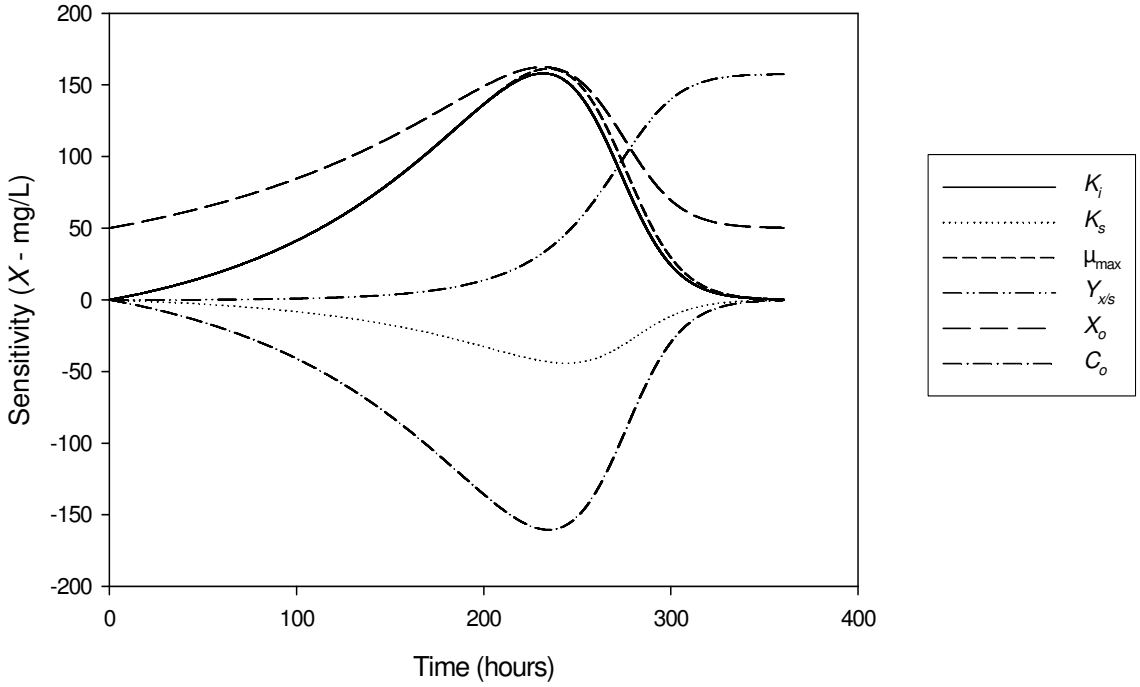

Figure 4.16: Time course of the sensitivity functions of SRB biomass concentration (*X*) at an initial metal concentration of 75 mg/L with respect to other kinetic parameters.

4.4 SUMMARY

In the original SRB consortium, microorganisms belonging to two genera; *Enterococcus* and *Staphylococcus* were detected. However, exposure to media containing Sr^{2+}, Co^{2+} and Cs^{+} led to the emergence of new bacterial strains; *Citrobacter, Stenotrophomonas* and *Paenibacillus* sp. The presence of Sr^{2+} in the growth medium resulted in the complete eradication of the original consortium members, and the emergence of *Citrobacter* sp. These microorganisms demonstrated a unique high Sr^{2+} tolerance, which permitted positive bacterial growth and metabolism, as well as high metal removal capacities in the presence of Sr^{2+} concentrations of up to 500 mg/L. However, there was an obvious dependence of bacterial activities (growth and sulphate reduction) on the initial Sr^{2+} concentration, where an increase in metal concentration corresponded to a decrease in bacterial activities. Likewise, Sr^{2+} removal from solution was

dependent on the bacterial concentration, as complete Sr^{2+} removal was observed where the toxic and inhibitory effects of the metal on the culture was low. This study is the first to demonstrate high Sr tolerance among the *Citrobacter* sp., and it can be assumed this trait is genetically intrinsic as the microorganisms were not pre-exposed to Sr. Results from this study also provide strong evidence *Paenibacillus* sp. and *Enterococcus* sp., isolated from the Co-contaminated SRB bioreactors are resilient towards Co^{2+} and facilitate its removal through biosorption and bioreduction. However, initial Co^{2+} concentration ≥300 mg/L had a detrimental effect on the growth and metabolism of the SRB consortium. As a result, the metabolism-dependent Co^{2+} removal (bioreduction) capacity of the cultures was also lowered. At such high concentration it can be assumed that biosorption processes supersede bioreduction. On the other hand, the presence of Cs^{+} resulted in the replacement of *Staphylococcus* sp. with *Stenotrophomonas* sp., while *Enterococcus* sp were retained. The bacterial isolates obtained from the Cs^{+}-contaminated sulphidogenic bioreactors displayed a high degree of Cs^{+} tolerance, as a prolonged exponential growth phase was observed.

Microbial Cs^{+} removal from solution occurred mainly through biosorption processes, and the removal capacity decreased with increasing initial concentration. Although Cs^{+} is a weak Lewis acid that exhibits a low tendency to form complexes with ligands, complete removal was observed at initial concentration ≤75 mg/L, suggesting that the present SRB consortium may possess extremely hydrophilic binding sites that promote the uptake of Cs^{+} onto bacterial cells. In summary, through experimental and model simulations, we have been able to demonstrate the interrelationships between SRB activities (growth, metabolism and diversity) and individual fission product cations removal from solution. Results obtained indicate that satisfactory (up to 100%) metal removal can be attained, where the toxic and inhibitory effects of the metal on the bacterial culture are minimal. Generally, the sensitivity of the original SRB culture towards the different metals was in the order Sr>Co≥Cs. It is evident that the biosorption mechanism and cell capability can also be influenced by chemical and physical properties of the target metal ion itself, thereby determining cell viability (Veglio and Beolchini, 1997). Therefore, elucidation of mechanisms active during bacterial metal sequestration is essential, in order to establish consistency, and for successful exploitation of the phenomenon in realistic settings of industrial wastewater treatment.

CHAPTER 5

KINETIC AND EQUILIBRIUM STUDIES FOR Sr^{2+}, Co^{2+} and Cs^{+} UPTAKE ONTO SRB CELLS

5.1 BACKGROUND

Theoretically, metal sorption by bacteria is assumed to be a function of: (i) cell surface properties, such as charge and orientation of the functional groups on the cell surface; (ii) metal speciation in the aqueous phase; and (iii) release of metal-complexing exudates (Volesky and Holan, 1995). In addition, metal sorption also depends on the metal involved and the composition of the system, for instance, pH, ionic strength, temperature, metal to bacteria ratio (Gadd, 1986; Volesky, 1990; Daughney and Fein, 1998; Wang and Chen, 2007; Vijayaraghavan and Yun, 2008). However, up till now, metal sorption by bacteria (under constant or different experimental conditions) is still poorly understood (Vijayaraghavan and Yun, 2008). To enhance our understanding on biosorption, knowledge of the thermodynamic and kinetic aspects of the sorption process should be established so to know more about its performance and mechanisms. From a mechanistic point of view, the prediction of the sorption mechanism or rate-limiting step is crucial for interpretation of the experimental data. Biosorption kinetics are significant as the data can be used for determining the equilibration time of the biosorption process, as well as in understanding the mechanisms and effect of different environmental factors on the biosorption process (Sarkar et al., 2003). In an attempt to clarify the mechanism of Sr^{2+} , Cs^{+} and Co^{2+} removal from aqueous solution by SRB cells, and identify the main factors controlling sorption rate such as; mass transport, pore diffusion and chemical reaction processes, the pseudo-first-order, pseudo-second-order (Lagergren, 1898), and external and intraparticle diffusion (Weber and Morris, 1963) kinetic models were evaluated. On the other hand, the classical Langmuir (Langmuir, 1918) and Freundlich (Freundlich, 1907) equilibrium sorption isotherms were used to evaluate the overall biosorption performance of the bacterial biosorbent.

In order to clarify the molecular-scale adsorption reactions that occur between aqueous solutes (protons and Sr^{2+}, Cs^{+} and Co^{2+}) and the bacterial surface, and quantify metal adsorption onto the bacterial cell surfaces, a surface complexation modeling approach was used. Prior to SCM

development, preliminary biomass characterization studies were carried out using a combination of Gram-staining, SEM, phylogenetic analysis, potentiometric titrations and FTIR analysis. Biomass characterization results on Gram-staining result, morphological and phylogenetic nature of the present culture were discussed in the previous Chapter. Forward and reverse titration curves of the bacteria showed that the present SRB consortium displayed a significant buffering behaviour over the pH range 3.5-10.3 (Figure 3, Appendix 2). The significant buffering may be due to the presence of different functional groups on the bacterial surface consuming the added base by donating protons, as there was no evidence of saturation observed. FT-IR spectroscopy provides chemical information about the biomolecular composition of whole bacterial cells. Since this technique probes the whole cell, so that the structures uniquely associated with the cell wall cannot be assessed in isolation of all of the cytoplasm, results obtained are for bacterial characterization purposes due to the high specificity of the obtained spectra. The FTIR spectrum obtained indicated the presence of different functional groups, including organic sulphates, hydroxyl, aromatic phosphates and phosphodiester, primary and secondary amines and carboxylic groups (Table 2, Appendix 2). These results serve as a guidance for the identification of the different possible mechanisms (physical adsorption, complexation, ionic exchange, surface micro-precipitation) operating at the cell surface-metal solution interface, and aid the identification of the active sites on bacterial cell wall(Haas, 2004).

5.2 KINETIC STUDIES OF Sr^{2+}, Cs^{+} AND Co^{2+} BIOSORPTION

5.2.1 Effect of Initial Concentration

The effect of initial concentration on the kinetics of Sr^{2+}, Cs^{+} and Co^{2+} biosorption from aqueous solution was investigated at a concentration range of 25-500 mg/L. The results obtained from experimental controls, which consisted of SRB cells suspended in aqueous solution without metal and aqueous metal solution but without bacterial inoculum (abiotic control), showed that metal losses due to abiotic processes was insignificant, and that the SRB cells did not release any metal ions into solution. Therefore, the observed metal removal was due to uptake by the bacterial cells. When the experimental data for Sr^{2+}, Cs^{+} and Co^{2+} sorption at different initial concentrations were analysed with the Lagergren pseudo-first-order kinetic model, poor model fits were obtained (Table 5.1). This is because this model fails to account for the slower phase of metal biosorption (Ho and McKay, 1998; Ho and McKay, 2000; Aksu, 2001).

Table 5.1 Pseudo-first order model parameters for the effect of initial concentration on the kinetics of Sr^{2+}, Cs^{+} and Co^{2+} removal in single metal solutions.

C_o	Sr^{2+}			Co^{2+}			Cs^{+}		
(mg/L)	q_{eq}	$K_1(\times10^{-2})$	R^2	q_{eq}	$K_1(\times10^{-2})$	R^2	q_{eq}	$K_1(\times10^{-2})$	R^2
25	12.7	1.22	0.780	16.4	1.08	0.964	3.32	0.88	0.525
75	35.9	1.64	0.835	36.0	1.49	0.946	33.1	1.66	0.819
100	30.0	1.51	0.823	27.1	1.13	0.949	35.5	1.08	0.962
300	190.6	1.83	0.958	58.6	1.50	0.938	81.5	1.66	0.939
500	330.3	2.11	0.950	192.5	1.97	0.917	9.67	1.20	0.689

However, good conformity between experimental data and model results was observed upon analysis with the pseudo-second-order kinetic model, suggesting that the adsorption is the rate controlling step (Ho and Mckay, 1998). Generally, the equilibrium metal uptake capacity (q_{eq}) of the bacteria increased with increasing initial concentration, clearly demonstrating that the initial concentration was the driving force for the mass transfer of Sr^{2+}, Cs^{+} and Co^{2+} onto the bacteria (Table 5.2). The adsorption rate constant (k_2) for Sr^{2+} and Cs^{+} decreased with increasing initial concentration. These observations imply that the biosorption of these metal ions is concentration dependent, where at higher initial concentrations; the ratio of available adsorption sites to metal ions is less and as the binding sites saturates the rate of biosorption declines. Similar results have been reported elsewhere in literature (Aksu, 2001; Shaukat et al., 2005; Chen et al., 2008; Chegrouche et al., 2009; Ahmadpour et al., 2010). The experimental and model representations of the data for removal of Sr^{2+}, Cs^{+} and Co^{2+} by SRB at different initial concentration are shown in Figure 5.1.

Table 5.2 Pseudo-second order model parameters for the effect of initial concentration on the kinetics of Sr^{2+}, Cs^{+} and Co^{2+} removal in single metal solutions.

C_o	Sr^{2+}			Co^{2+}			**Cs^{+}**		
(mg/L)	q_{eq}	$k_2(\times10^{-4})$	R^2	q_{eq}	$k_2(\times10^{-4})$	R^2	q_{eq}	$k_2(\times10^{-4})$	R^2
25	40.3	33.2	0.998	28.3	10.0	0.994	13.0	82.8	0.999
75	135.1	11.4	0.999	78.4	9.38	0.999	77.6	10.1	0.999
100	147.1	1.34	0.999	78.1	13.3	0.999	92.3	9.39	0.998
300	256.4	1.65	0.997	93.7	5.01	0.994	128.4	3.15	0.994
500	370.3	0.798	0.995	188.9	1.13	0.979	66.7	10.4	0.999

A

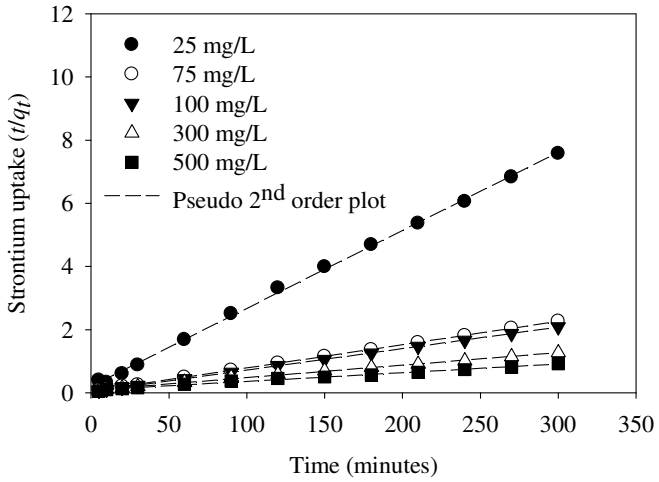

B

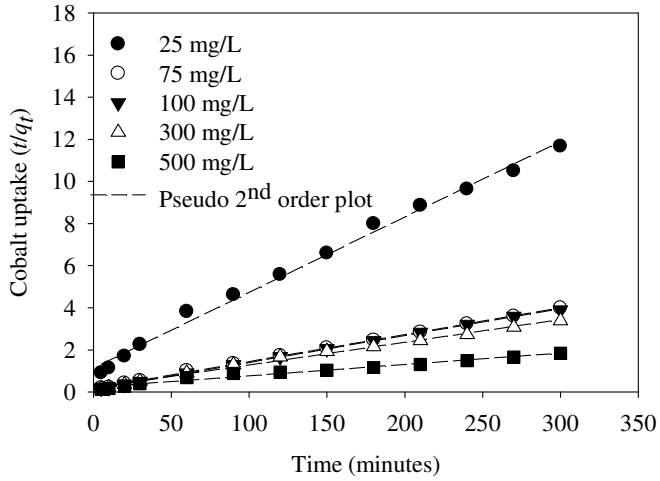

C

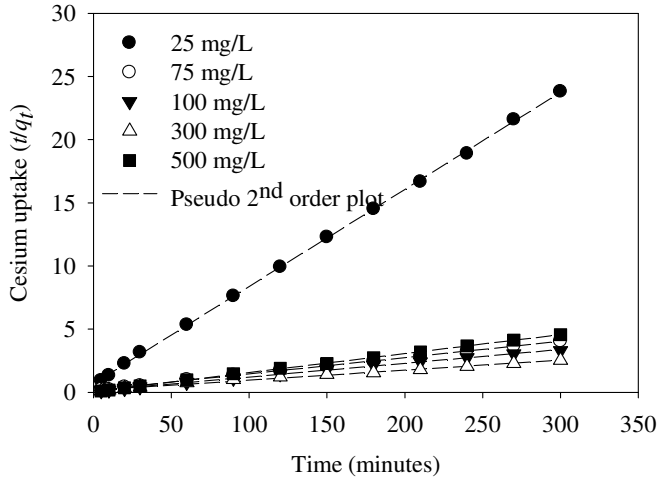

Figure 5.1: Pseudo-second-order model plot for the effect of different initial metal concentrations on the removal of Sr^{2+} (A), Co^{2+} (B) and Cs^{+} (C) from solution by SRB.

The conformity of the data to the second-order rate model suggests that the present biosorption process occurred through electrostatic electron exchange between the bacterial sorbent and the metal. Generally, the uptake of metals by SRB was observed in the order Cs<Co<Sr. The obtained results suggest that the present metal removal process is a second-order reaction. It can therefore be assumed that the rate limiting step of the metal removal process is chemisorption. When the data was analysed with the diffusion (external and intraparticle) models, it was apparent that the sorption of Sr^{2+}, Cs^{+} and Co^{2+} occurred only on the external surface of the SRB cells. The external diffusion model shows excellent correlation with the experimental sorption data, with high correlation coefficients obtained as shown in Table 5.3. This suggests that metal sorption is probably a surface process occurring on the exterior of the sorbent particle. These results are in agreement with earlier observations by Ho and McKay (2000) and Mullen et al. (1989), where chemical sorption was determined to be the underlying mechanism for metal removal from solution. The external diffusion coefficient (k_f) values decreased with an increase in the initial metal concentration. This may be due to the lower competition for the sorption surface sites at lower concentration. At higher concentrations, the competition for the surface active sites will be high and consequently lower sorption rates are obtained.

Table 5.3 External diffusion parameters for the effect of initial concentration on the kinetics of Sr^{2+}, Cs^{+} and Co^{2+} removal in single metal solutions.

C_o	Sr^{2+}		Co^{2+}		Cs^{+}	
(mg/L)	k_f ($\times 10^{-4}$)	R^2	k_f($\times 10^{-4}$)	R^2	k_f($\times 10^{-4}$)	R^2
25	5.91	0.971	2.00	0.982	1.18	0.923
75	5.36	0.985	2.18	0.972	2.09	0.955
100	4.09	0.988	1.91	0.942	2.09	0.979
300	1.55	0.974	0.727	0.962	0.727	0.973
500	1.00	0.911	0.455	0.922	0.364	0.964

5.2.2 Effect of pH

Solution pH is a measure of the concentration of H+ in solution, and H+ can compete with the cations in aqueous solution for sorption sites on the cells. Hence lower pH (high H+ concentration) leads to less adsorption of other cations. In addition, pH also affects the surface charge of the adsorbent, degree of the ionization, and speciation of the adsorbate (Choudhary and Sar, 2009). Speciation of Sr^{2+}, Cs^{+} and Co^{2+} at pH 2-9 was determined using the chemical speciation model MINTEQ (Allison et al., 1990). At an initial concentration of 75 mg/L and pH range 2-9, results obtained showed that most of Sr (99.8%) and Cs (99.96%) species in solution were present in their highly dissociated forms (Sr^{2+} and Cs^{+}, respectively). Only about 0.2% and 0.04% existed as $SrCl^{+}$ and CsCl, respectively. This observation strongly suggests that both cations undergo limited hydrolysis, which is in agreement with earlier findings by Baes and Mesmer (1976).

With regard to cobalt speciation, both initial concentration and pH played a significant role in the speciation of Co^{2+} in solution. Generally, an increase in pH resulted in the decrease in the highly dissociated Co species. At low pH (pH 2-4), Co species were present as 99.7% Co^{2+} and 0.3% $CoNO_3^{+}$. At near neutral pH (pH 5-7) slight precipitation occurred as Co species were distributed as follows: 99.68% Co^{2+}, 0.3% $CoNO_3^{+}$ and 0.016% $CoOH^{+}$. Increasing the pH to 8 resulted in Co^{2+} precipitation due to the formation of $Co(OH)_2$ (0.12%), whereas the rest of the Co species were distributed as follows: ~97% Co^{2+} and 2% $CoOH^{+}$. Further increase in pH to 9, resulted in increased precipitation with approximately 10% of the initial concentration present as $Co(OH)_2$, 77% as Co^{2+}, 0.3% as $CoNO_3^{+}$, 13% $CoOH^{+}$ and 0.1% as $Co_4(OH)_4^{4+}$. These findings are also in agreement with earlier studies on Co^{2+} hydrolysis reported in literature (Baes and Mesmer, 1976).

The pseudo-second-order model provided the best fit for effect of pH on Sr^{2+}, Cs^{+}, and Co^{2+} removal by SRB, and the obtained parameters are shown in Table 5.4. Higher removal capacity was coupled to lower rate constants for Sr^{2+}. Similarly, the fit of the data to the pseudo-second-order model is in agreement with a mechanism where adsorption is the main rate controlling step. Comparisons between experimental and model data for removal of Sr^{2+}, Cs^{+} and Co^{2+} by

SRB at different pHs (2-9) is shown in Figure 5.2. Sr^{2+} sorption by SRB was pH independent as there were minimal differences in the uptake capacities at different pH ranges. The low initial Sr^{2+}concentrations resulted in an almost similar removal capacity at the different pH values. The present SRB culture has demonstrated a unique high Sr^{2+} binding at the different pH values. Cs^{+} removal, on the other hand was dependent on the solution pH. High Cs^{+} removal was observed between pH 2 and 6, and thereafter an increase in pH resulted in decreased uptake. This is a common feature whenever sorption is pH dependent as functional groups with low pKa values such as a carboxyl (pKa 3.0–4.0) with other side chain carboxyl groups (pKa 4.0–4.5) become deprotonated with increasing pH. The deprotonation of bacterial surface sites generates a net negative charge at the surface, which favours the binding of cationic species (Fein et al., 1997; Douglas and Beveridge, 1998). Similarly, for Cs^{+}, the pH dependent uptake can be attributed to the deprotonation of cell wall functional groups that occurs with increasing pH, progressively resulting in increased Cs^{+} uptake capacity until all the binding sites are saturated. Solution pH thus influences the main mechanism of removal of cations from solution, and consequently the sorption capacity of the cationic species from solution.

Table 5.4: Pseudo-second order model parameters for the effect of pH on the kinetics of Sr^{2+}, Cs^{+} and Co^{2+} removal in single metal solutions.

pH	Sr^{2+}			Co^{2+}			Cs^{+}		
	q_{eq}	$k_2(\times10^{-4})$	R^2	q_{eq}	$k_2(\times10^{-4})$	R^2	q_{eq}	$k_2(\times10^{-4})$	R^2
2	134.6	6.374	0.998	78.6	9.202	0.999	76.4	10.9	0.999
4	132.5	6.191	0.997	78.7	9.076	0.999	75.5	9.81	0.999
6	137.1	4.845	0.996	82.3	8.846	0.998	77.0	10.3	0.999
7	137.8	5.044	0.996	85.8	14.7	0.999	76.3	8.77	0.998
8	138.9	4.751	0.996	91.1	8.26	0.998	73.4	11.0	0.999
9	139.8	4.873	0.996	119.1	4.247	0.996	65.5	9.42	0.999

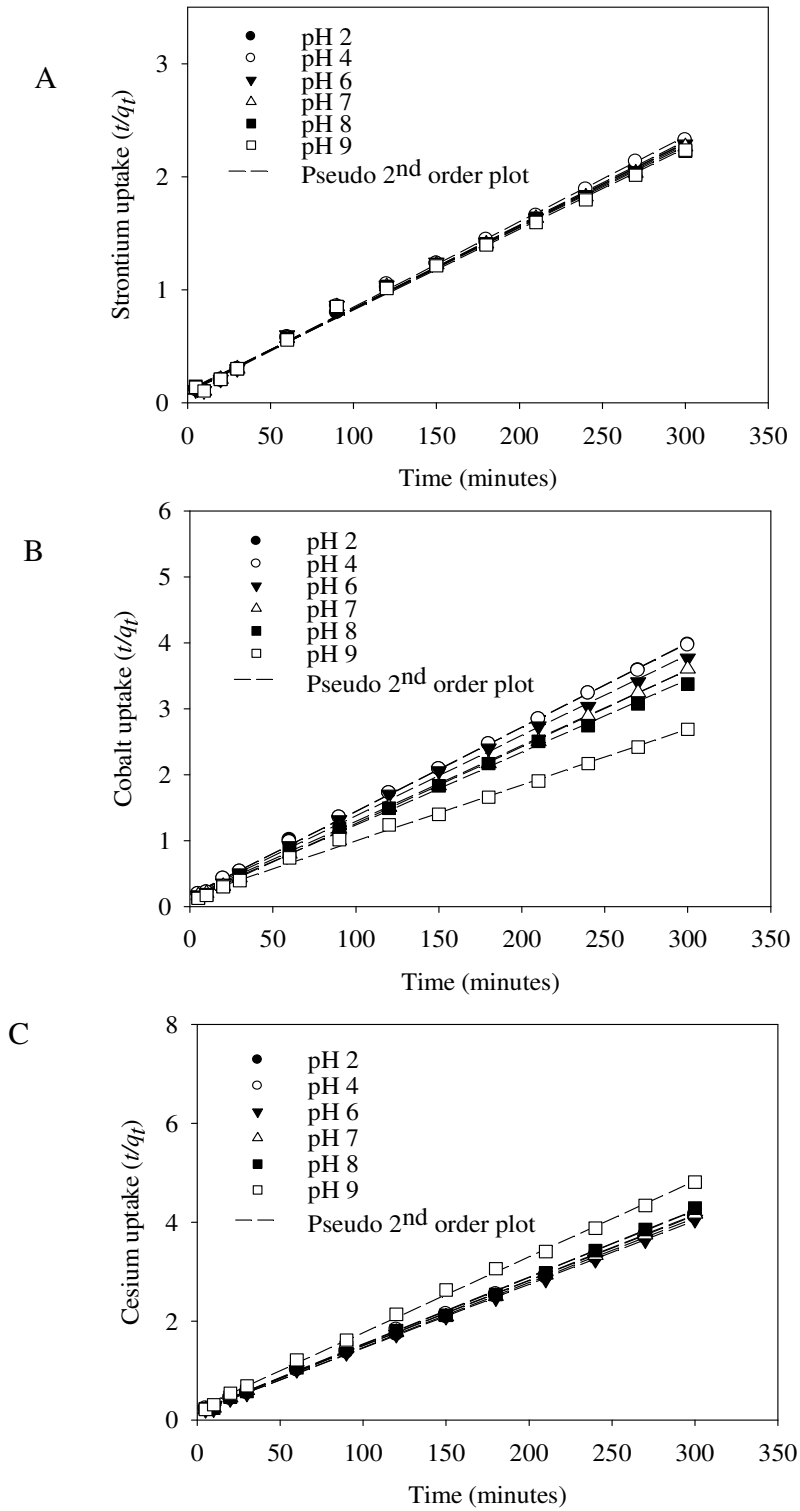

Figure 5.2: Pseudo-second-order model plot for the effect of pH on the removal of Sr^{2+} (A), Co^{2+} (B) and Cs^{+} (C) from solution by SRB.

5.2.3 Effect of Sorbent Dose

The 'best fit' of the experimental data obtained was again obtained when the data was analysed using the pseudo-second order model. Table 5.5 is a summary of the parameters obtained for the effect of sorbent dose on the sorption kinetics of Sr^{2+}, Cs^{+} and Co^{2+} from aqueous solutions at a fixed initial concentration of 75 mg/L and pH 4.

Table 5.5 Pseudo-second order model parameters for the effect of sorbent dose on the kinetics of Sr^{2+}, Cs^{+} and Co^{2+} removal in single metal solutions.

Dose (gL^{-1})	Sr^{2+}			Co^{2+}			Cs^{+}		
	q_{eq}	$k_2(\times10^{-4})$	R^2	q_{eq}	$k_2(\times10^{-4})$	R^2	q_{eq}	$k_2(\times10^{-4})$	R^2
0.5	10.7.7	23.8	0.999	78.3	9.76	0.999	80.0	7.01	0.999
1.0	57.6	24.0	0.999	78.4	9.93	0.999	77.6	10.2	0.999
2.0	29.9	32.4	0.996	82.0	9.52	0.998	91.2	10.7	0.998
3.0	21.5	21.1	0.970	86.0	14.0	0.999	126.4	3.76	0.993

Figure 5.3 shows the comparisons between experimental and model data for removal of Sr^{2+}, Cs^{+} and Co^{2+} by SRB at different initial SRB dosage. Evidently, an increase in the biomass concentration resulted in an increased equilibrium metal uptake, and similar results have been reported by a number of authors, including; Gadd et al. (1988); Fourest and Roux (1992); Daughney et al. (1998); Esposito et al. (2001); Daughney et al. (2001); Burnett et al. (2007) and Ahmadpour et al. (2010). This can be attributed to the increased surface area, which in turn increases the number of binding sites (Esposito et al., 2001). A higher cell concentration is also expected to be accompanied by an increased accumulation of cellular metabolites, which further facilitate metal ion precipitation. However, in order to achieve a cost effective sorption process without drastically reducing the metal uptake efficiency, a lower biomass could be used. Additionally, in some cases increasing the biomass concentration does not necessarily result in remarkably increased metal uptake as larger amounts of biomass have been found to interfere with metal binding sites as they tend to agglomerate (Gadd et al., 1988).

A

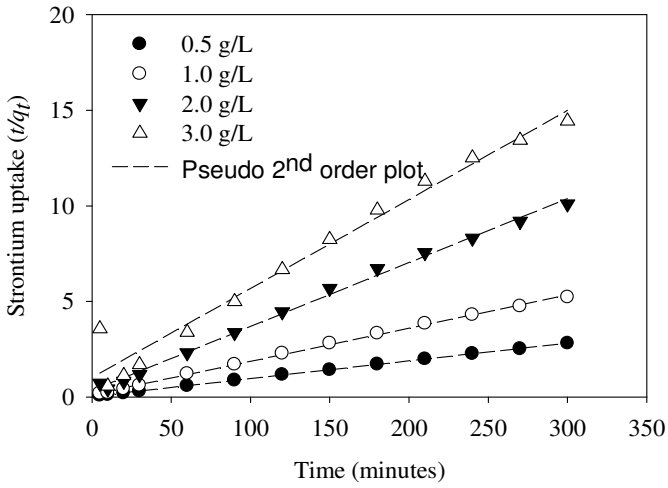

B

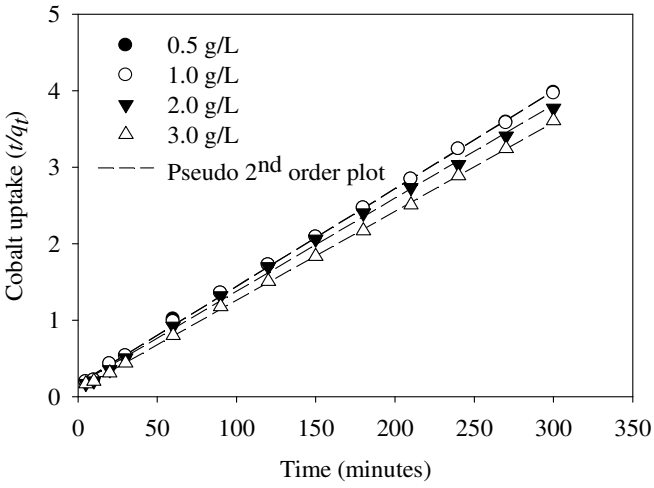

C

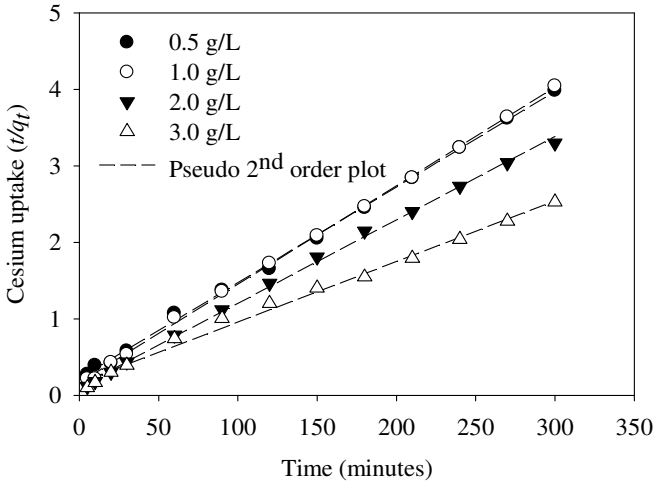

Figure 5.3: Pseudo-second-order model plot for the effect of sorbent dose on the removal of Sr^{2+} (A), Co^{2+} (B) and Cs^{+} (C) from solution by SRB.

5.2.4 Effect of Metabolic State

To determine the effect of metabolic state on Sr^{2+}, Cs^{+} and Co^{2+} uptake, each SRB biomass type (at a biomass density of 1 g/L) was exposed to an aqueous solution containing the target metal at an initial concentration of 75 mg/L. Kinetic parameters obtained after analysis of the data by the pseudo-second order model are shown in Table 5.6. The results obtained suggest that the effect of metabolic state on Sr^{2+}, Cs^{+} and Co^{2+} biosorption also follows a pseudo-second order process, since there was a precise match between the experimental and the calculated q_{eq} values, and higher correlation coefficient values. These results support an earlier suggestion that chemical sorption is the main rate-controlling step.

Table 5.6 Pseudo-second order model parameters for the effect of metabolic state on the kinetics of Sr^{2+}, Cs^{+} and Co^{2+} removal in single metal solutions.

Metabolic State	Sr^{2+}			Co^{2+}			Cs^{+}		
	q_{eq}	$k_2(\times10^{-4})$	R^2	q_{eq}	$k_2(\times10^{-4})$	R^2	q_{eq}	$k_2(\times10^{-4})$	R^2
Heat-killed	72.1	9.5	0.999	36.9	26.0	0.998	47.6	14.9	0.999
Growing	130.9	7.37	0.997	76.3	6.16	0.990	55.6	13.7	0.996
Non-growing	114.4	14.3	0.998	73.7	10.8	0.998	68.6	11.8	0.996

At the end of the incubation period, a higher Sr^{2+} uptake efficiency (86%) was achieved with growing SRB cells, followed closely by resting cells (77%), and lastly heat-killed SRB cells (48%). There was a close match between the experimental data and model data (Figure 5.4), and the similarity in the sorption capacities (q_t) by growing and resting SRB biomass for the first 90 minutes of incubation suggest that during the initial phases of sorption living SRB cells employ almost similar sorption mechanisms for metal ions uptake. The additional sorption observed thereafter in the growing cells can be attributed to other metabolism-related Sr^{2+} precipitation strategies discussed in the previous chapter. For instance, as part of their metabolism actively growing SRB cells produce biogenic ligands which are responsible for further precipitation of metal ions into insoluble forms. The sorption process by dead cells was characterized by a rapid initial uptake in the first 30 minutes of incubation, and thereafter a slow phase until equilibrium was reached, a common phenomenon also reported in other studies (Choi and Yun, 2004; Lu et al., 2006). Evidently, live cells have consistently displayed high metal removal capacities, whereas non-viable bacteria cells performed poorly (Parmar et al., 2000).

A

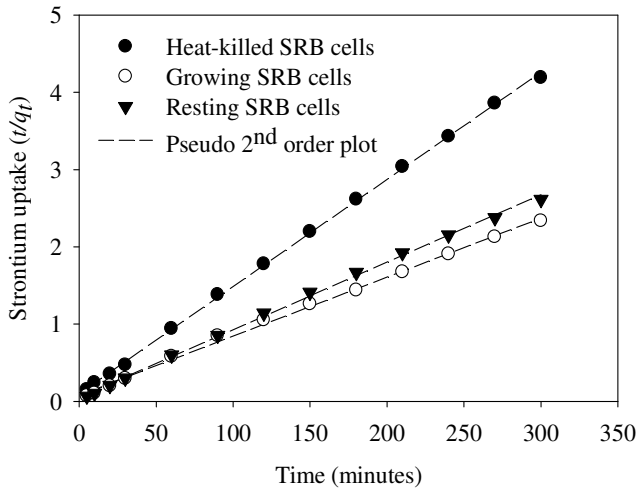

B

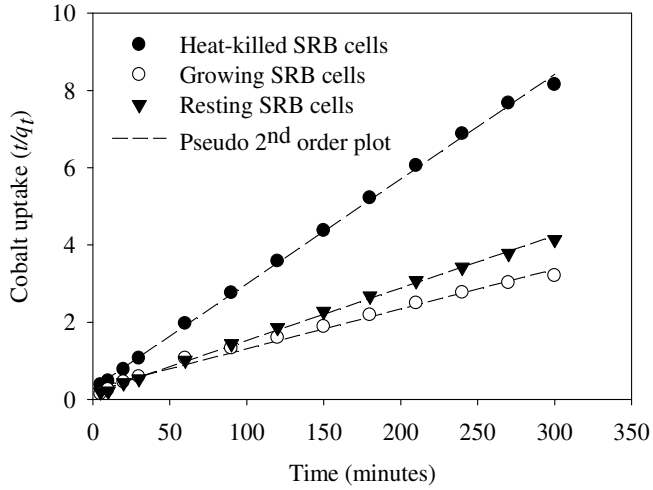

C

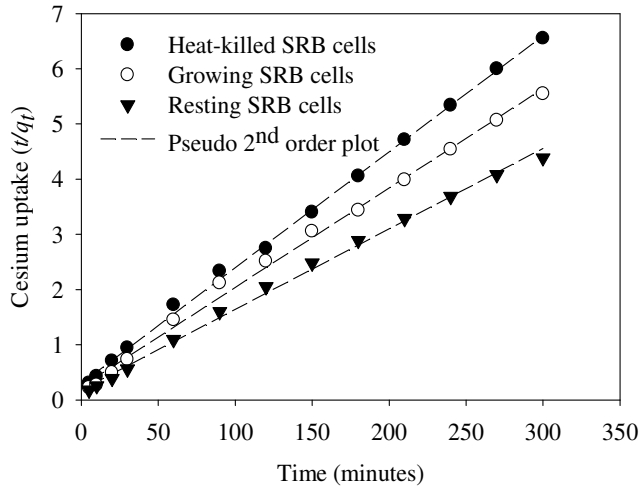

Figure 5.4: Pseudo-second-order model plot for the effect of metabolic state on the removal of Sr^{2+}(A), Co^{2+} (B) and Cs^{+} (C) from solution by SRB.

5.3 EQUILIBRIUM Sr^{2+}, Co^{2+} and Cs^{+} BIOSORPTION

5.3.1 Sr^{2+}, Co^{2+} and Cs^{+} Biosorption from Single Metal Solutions

Equilibrium sorption isotherms are empirical models that provide basic information on a given system and are useful for comparing different biosorbents and affinities of different metal ions for the same biosorbent (Gadd, 2009). The Langmuir isotherm model provided the best fit for the equilibrium data for Sr^{2+}, Co^{2+}, and Cs^{+} removal from single metal systems by SRB as shown by the higher R^2 values than in the Freundlich model (Table 5.7). However, the parameters obtained from experimental data analysis with the Freundlich give an indication of the non-heterogenecity of the sites involved in the sorption process, as n>1, suggesting a monolayer sorption process.

Table 5.7 Langmuir and Freundlich model parameters for the removal of Sr^{2+}, Cs^{+} and Co^{2+} in single metal solutions.

Metal ion	Langmuir model			Freundlich model		
	q_{max} (mg g^{-1})	b ($\times 10^{-2}$)	R^2	k	n	R^2
Sr^{2+}	405.5	1.95	0.974	52.3	3.28	0.955
Cs^{+}	192.9	1.55	0.995	13.0	2.19	0.981
Co^{2+}	203.3	1.19	0.961	16.2	2.57	0.882

The Langmuir model allows the determination of a very important parameter, the maximum sorption capacity (q_{max}), which is useful for comparison of sorption capabilities. Consequently, the results for the equilibrium sorption process for Sr^{2+}, Co^{2+}, and Cs^{+} in single metal systems are discussed based on the parameters obtained from the Langmuir model plots. The maximum removal capacity (q_{max}) was almost double for Sr^{2+} compared to Cs^{+} and Co^{2+}. Similarly, the binding affinity coefficient (b) was higher for Sr^{2+} compared to Cs^{+} and Co^{2+}. The SRB culture in this study exhibited a superior Sr^{2+} binding capacity, compared to other studies in literature as shown in Table 5.8. Comparisons between the experimental data and the Langmuir and Freundlich isotherm model plots are shown in Figure 5.5. The isotherm model plots obtained for the removal of Sr^{2+}, Co^{2+} and Cs^{+} from single metal systems by SRB suggest that the sorption process conforms to a monolayer binding process, since the best fit was obtained with the Langmuir model (Kratochvil and Volesky, 1998).

Table 5.8 Equilibrium sorption performances of various sorbents for Sr^{2+}, Co^{2+} and Cs^{+} uptake from aqueous solution.

Metal ion	q_{max} (mg g^{-1})	Sorbent	Reference
Sr^{2+}	**405.5**	**SRB consortium**	**This study**
	140.0	Pakistani coal	Shaukat et al., 2005
	55.0	*Bacillus sp.*	Tajer et al., 2007
	26.67	*Cystoseira indica*	Dabbagh et al., 2007
	12.89	*Amaranthus spinosus*	Chen, 1997
Cs^{+}	**192.9**	**SRB consortium**	**This study**
	14.5-71.9	Marine algae species	Jalali-Rad et al., 2004
	28.6	*Bacillus polymyxa*	Shevchuk and Klimenko, 2009
Co^{2+}	468.75	*Oscillatoria sp*	Ahuja et al., 1999
	203.3	**SRB consortium**	**This study**
	190	*Rhizopus sp*	Suhasini et al., 1999
	8.42	Sludge	Van Hullebusch et al., 2004

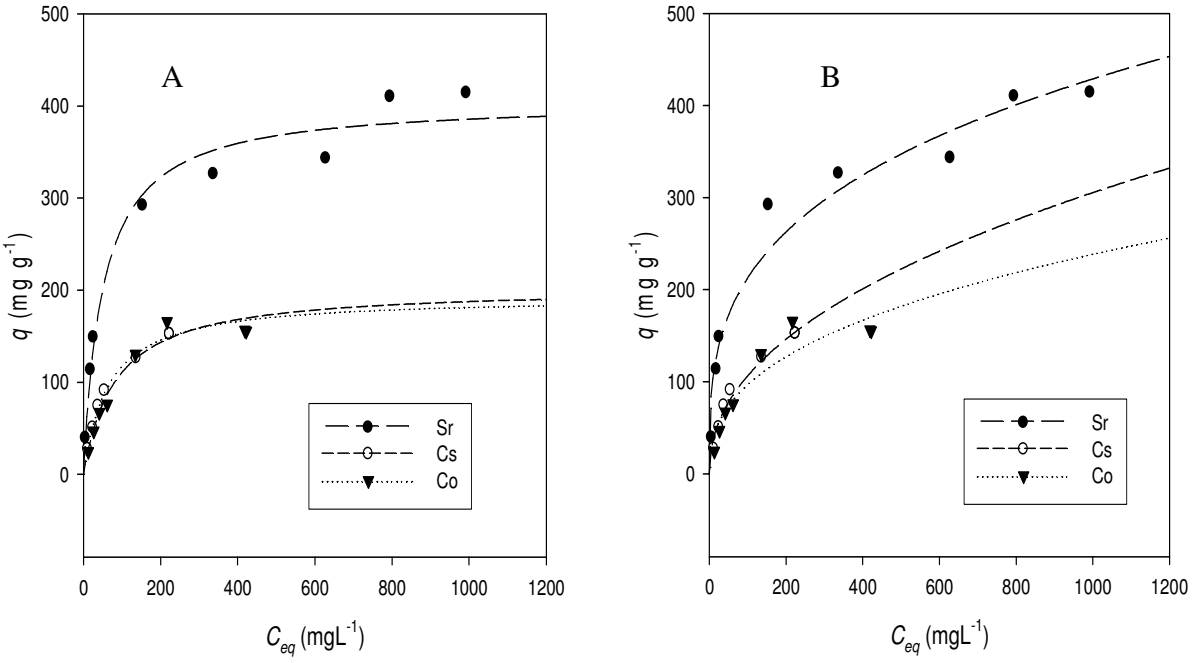

Figure 5.5: Langmuir (A) and Freundlich (B) isotherm plots for Sr^{2+}, Co^{2+} and Cs^{+} sorption by SRB at a biomass density of 0.5 g/L. (pH = 4 and temperature = 25°C).

5.3.2 Competitive Binding of Sr, Cs And Co in Binary Metal Solutions

The effect of a secondary metal ion on metal uptake by SRB was investigated in binary metal solutions to investigate the specificity of the uptake process. The Langmuir isotherm model was used to interpret the binary-component equilibrium sorption data, and the parameters obtained are shown in Table 5.9. The results show a 33% and 34% loss in the Sr^{2+}removal capacity (q_{max}) in the presence of Cs^{+} and Co^{2+}, respectively. In the presence of Co^{2+} and Sr^{2+}, the Cs^{+} removal capacity was lowered by 55% and 45%, respectively. Among the binary systems investigated, Co^{2+} uptake was the most sensitive to the presence of Cs^{+}, where a 76% reduction of the sorption capacity (q_{max}) was observed. However, in the presence of Sr^{2+}, only a 9% loss of removal capacity was observed. With regard to the results, the following inferences can be made: (1) the present SRB culture demonstrated a high Sr^{2+} affinity. This is evident in all the binary metal solutions investigated in this study, (2) specialized binding-sites/processes specifically for divalent metals (Sr^{2+} and Co^{2+}) removal may exist. This is supported by minimal inhibitory effects by the presence of a second cation, with the exception of the Co-Cs system, (3) No specific binding sites for Cs^{+} may exist. This is indicated by the inhibition of Cs^{+} removal, in the presence of other cations. A similar phenomenon of competitive biosorption has been reported for the binary adsorption of Pb^{2+} and Cu^{2+} onto *Aspergillus flavus*, where it was shown that the biosorption capacities of the metal ions in the binary metal mixture were lower than that of noncompetitive conditions (Akar and Tunali, 2006). Similarly, the same observations were made for the competitive adsorption of Cd^{2+} and Pb^{2+} (Fan et al., 2008). The results clearly demonstrate the antagonistic effect of multiple metal ions in a biosorption system, which is a result of the competition for adsorption sites on the cell surfaces and/or the screening effect by the competing metal ions.

Table 5.9 Equilibrium sorption parameters for Sr^{2+}, Cs^{+} and Co^{2+} uptake from binary systems.

Metal system	Component	Langmuir			Freundlich		
		q_{max} (mg g^{-1})	$b(\times 10^{-2})$	R^2	k	n	R^2
Sr-Cs	Sr^{2+}	277.8	5.72	0.985	42.7	3.20	0.871
	Cs^{+}	107.5	3.06	0.938	18.0	3.34	0.670
Cs-Co	Cs^{+}	131.6	2.52	0.958	15.6	2.76	0.794
	Co^{2+}	49.3	3.40	0.986	7.55	2.89	0.847
Co-Sr	Co^{2+}	185.2	2.19	0.950	27.9	4.09	0.601
	Sr^{2+}	274.8	7.41	0.974	44.8	3.16	0.889

5.4 ADSORPTION OF PROTONS AND Sr^{2+}, Co^{2+} AND Cs^{+} ONTO SRB CELL SURFACES

5.4.1 Surface Complexation Modelling Approach

A number of acid-base surface complexation models (SCM) have been applied to predict the identities and concentrations of functional groups involved in metal adsorption on the bacterial surfaces (Fein et al., 1997; Daughney et al., 2001; Haas et al., 2001; Yee and Fein, 2001; Ngwenya et al., 2003).In this study, the titration experimental data was analysed with the nonelectrostatic model (NEM). This model neglects the effects of the bacterial surface electric field, and has been successfully used to invoke up to four discrete sites on bacteria surfaces of individual and mixed bacterial cultures (Borrok and Fein, 2005; Fein et al., 2005; Pagnanelli et al., 2006; Johnson et al., 2007). Although, our experiments were conducted at different ionic strengths, the rationale of using the NEM approach is based on the findings by Borrok and Fein (2005). In their study, it was concluded that the effect of ionic strength (over the range of 0.01 M to 0.5 M) on the apparent proton binding reactions is relatively small and not significantly greater than experimental and modelling uncertainties of using electrostatic models. Therefore, application of the NEM approach is an initial step to define the type, and quantify and compare the magnitude of ionic strength effects on the SRB cell surfaces to those of other bacterial species/consortia that have been studied before. Experimental titration data was reported as H^{+} added per gram (wet weight) bacteria, calculated using Equation 3.15. An example of an input file for computation of the number of apparent proton binding constants (pK_a) and their concentrations on the surfaces of the bacterial consortium is shown in Appendix B1. All apparent proton binding constants (pK_a) reported in this study were corrected for ionic strength and temperature effects using the Davies equation (Appendix 4b). Apparent stability constants for the adsorption of Sr^{2+}, Co^{2+} and Cs^{+} onto the surfaces of the bacterial consortium were computed from the experimental data obtained, which was entered into the FITMOD program as shown in Appendix B3.

5.4.2 Modelling the Acid-base Properties of SRB

Results from acid–base titrations of bacterial suspensions allow the determination of the absolute concentrations and deprotonation constants of specific proton-active surface sites on the cell walls (Daughney and Fein, 1998). The titration curves obtained in this study indicate that the

present SRB consortium displayed a significant buffering behaviour over the pH range (pH 3.5-10.3) studied due to the presence of different functional groups on the bacterial surface consuming the added base by donating protons (Figure 5.6). There was no evidence of saturation observed with respect to proton adsorption. The experimental potentiometric titration curves obtained are similar in shape and position to each other as well as to those determined previously for a number of individual bacterial and mixed bacterial species (Haas et al., 2001; Yee and Fein, 2001; Ngwenya et al., 2003; Haas, 2004; Borrok et al., 2004; Borrok and Fein, 2005). The positions of the titration curves of the bacterial consortium also changed slightly as a function of ionic strength from 0.01 to 0.5 M. These results are in agreement with findings by other authors for the titration of bacteria consortia (Borrok et al., 2004; Borrok and Fein, 2005; Johnson et al., 2007). Regardless of the ionic strength of the medium, a four-site non-electrostatic model (NEM) yielded an excellent fit to the experimental titration data compared to fewer discrete sites fit of the same model (Table 5.10).

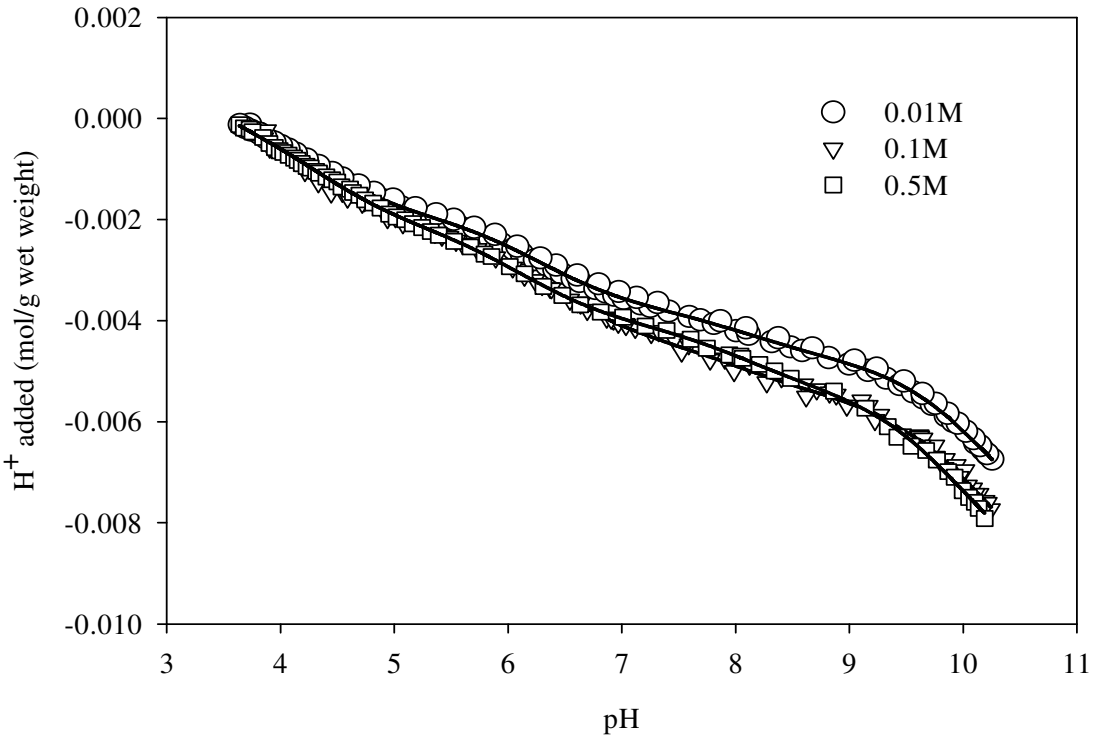

Figure 5.6: Potentiometric titration data of a viable SRB consortium reported as H+ added per gram (wet weight) in 0.01 M, 0.1 M and 0.5 M $NaNO_3$ and 25°C. Data shown are averages of three replicates performed at each ionic strength.

Since the NEM neglects the electrostatic effects on the bacterial cell surface, therefore, the proton binding constants reported are conditional on the ionic strength conditions in which the experiments were conducted. The apparent proton binding constants (pK_a) for the four NEM sites were each assigned to a corresponding functional group according to published literature. Site 1 corresponds to carboxylic acid functional groups (pK$_a$ = 3-5). The near-neutral site 2 was assigned to phosphates (pK_a = 6-7), and site 3 and 4 (pK$_a$ = 8-12) are basic sites, that correspond to either hydroxyl or amine groups (Cox et al., 1999). Generally, the apparent proton binding constants obtained in this study were almost similar at the different ionic strengths, except the pK_a values for site 2, which increased slightly with increasing ionic strength, in agreement with results by Borrok and Fein (2005). However, the apparent total site concentration showed a slight increase with increasing ionic strength; 8.33×10^{-3}, 9.17×10^{-3} and 9.54×10^{-3} mol/L for 0.01 M, 0.1 M and 0.5 M, respectively. Such observations have been reported by a number of researchers (Daughney and Fein, 1998; Cox et al., 1999; Martinez et al., 2002; Borrok and Fein, 2005). These observations suggest that the ionic strength effects on bacterial surface reactions are universal, despite the modeling approach adopted. Similar to earlier observations by Borrok and Fein (2005), insignificant differences were observed between the apparent proton binding constants and total site concentrations (about 12%) obtained over the ionic strength range of 0.01 to 0.5M.

Table 5.10 Compilation of SRB deprotonation constants, surface site densities and variance at 0.01 M, 0.1 M and 0.5 M $NaNO_3$ and 25°C as calculated by FITMOD.

Ionic	*pK_a values*				*Site concentrations ($\times10^{-3}$ mol/L)*				**V(*Y*)**
strength	1	2	3	4	C_1	C_2	C_3	C_4	
0.01 M	5.03				3.739				585.8
	4.55	7.31			2.362	2.985			73.0
	4.43	6.60	9.64		2.041	2.187	2.759		4.06
	4.40	6.39	8.22	10.27	1.966	1.893	1.002	3.473	1.17
0.1 M	5.20				4.597				601.3
	4.68	7.55			2.844	3.415			85.4
	4.55	6.81	9.73		2.451	2.525	2.982		14.7
	4.52	6.58	8.25	10.30	2.362	2.124	1.104	3.576	12.2
0.5 M	5.19				4.345				543.7
	4.84	8.18			2.928	3.970			71.2
	4.65	6.69	9.69		2.305	2.404	3.653		4.51
	4.62	6.43	8.35	10.24	2.201	2.016	1.362	3.964	1.77

[a] apparent pK$_a$ values corrected for ionic strength and temperature effects, [b] Overall variance computed by FITMOD

Such observations have been reported to demonstrate the insignificant effect of ionic strength on proton reactions on the bacterial surface are insignificant (Borrok and Fein, 2005). Results obtained in this study showed that the hydroxyl/amine sites were the most abundant binding sites (accounting for about 40% of the total concentration of binding sites), which is comparable to other studies reported in literature (Daughney et al., 1998; Haas et al., 2001; Ngwenya et al., 2003). Although the effects of ionic strength on the bacterial cell surface reactions are well documented, few studies report the effect of temperature on metal adsorption by bacteria (Ginn and Fein, 2009). With regards to varying temperature, the apparent proton binding constants of the consortium were assumed not to vary significantly from those obtained at 25°C. This assumption is based on results obtained a study by Wrightman and coworkers (2001), where it was concluded that a single set of pre-determined proton binding constants and site concentrations can be used to estimate proton adsorption over different experimental temperature ranges. Therefore, the apparent proton binding constants and site concentrations obtained for the bacterial consortium at 25°C and 0.1M $NaNO_3$ were used for determining the effect of temperature on proton and metal adsorption. A similar approach was followed by Borrok and Fein (2005) and Ginn and Fein (2009).

5.4.3 Determination of Apparent Stability Constants for Metal-bacteria Complexes

In this study, individual or combinations of the deprotonated form of the first three sites were considered for Sr^{2+}, Co^{2+} and Cs^{+} adsorption onto bacterial surfaces. The fourth site was not considered because metal adsorption at a higher pH (>8) was either insignificant, or resulted in significant chemical precipitation of the metal (as is the case with Co). Apparent stability constants for the formation of significant metal-bacteria complexes were estimated using the NEM model. Therefore, the constants reported are conditional on the ionic strength conditions in which the experiments were conducted. Sr^{2+}, Co^{2+} and Cs^{+} adsorption data obtained from experimental studies was used to provide constraints on the adsorption sites and apparent thermodynamic stabilities of the relevant metal–bacterial surface complexes.

Effect of Ionic Strength

The impact of ionic strength on the adsorption of metal cations onto bacterial surfaces has been studied Ledin et al., 1997; Daughney and Fein, 1998; Cox et al., 1999; Small et al., 2001; Yee et

al., 2004; Borrok and Fein, 2005; Beolchini et al., 2006). The adsorption behaviour of metal ions onto a sorbent under varying ionic strength conditions is assumed to be an indication of whether the metal is sorbed as an inner-sphere or outer sphere complex. Particularly, outer-sphere complexes are intrinsically more sensitive to variation in ionic strength than inner-sphere complexes, as the availability of free sorbent binding sites tends to decrease with increasing electrolyte concentrations (Stumm and Morgan, 1996). In this study, varying degrees of ionic strength dependence of Sr^{2+}, Co^{2+} and Cs^{+} adsorption onto the SRB biomass were observed in the present study. Figure 5.7 evidently shows that Sr^{2+} adsorption onto the SRB biomass was least affected under increasing ionic strength conditions, as minimal differences was observed even with a ten-fold (from 0.01 to 0.1M) increase in ionic strength. An almost similar observation was reported for the adsorption of U onto *Shewanella putrefaciens* by Haas and Dichristina (2001). However, increasing the ionic strength to 0.5M resulted in a slight decrease (about 10%) in Sr^{2+} adsorption by the SRB biomass. The observed slight sensitivity of Sr^{2+}, adsorption at higher ionic strengths is in agreement with earlier reports suggesting that adsorption occurs through an outer-sphere electrostatic complexation reactions, reported earlier (this study; Small et al., 2001; Yee et al., 2004; Borrok and Fein, 2005).

On the contrary, the adsorption of Co^{2+} and Cs^{+} onto the SRB biomass decreased with increasing ionic strength concentration. Since a non-electrostatic model was adopted for the present study, the contribution of the electrostatic effects on the bacterial cell surface cannot be confirmed to any degree of certainty. However, the observed reduction in adsorption capacity of these metal ions is a clear demonstration of the competition between the metal ions and the electrolyte cations for the adsorption sites on the bacterial cell surface. These results are in agreement with earlier observation in this study (Section 5.3.2), where a 76% reduction in Co^{2+} adsorption capacity was observed in the presence of a monovalent cation (Cs^{+}). Similarly, the decreased uptake of Cs^{+} ions by biosorbents in the presence of excess monovalent (electrolyte) cations has been reported before (Harjula and Lehto, 1986; Solecki, 2006). This phenomenon has been attributed to a number of factors, including; competition for deprotonated binding sites between the metal ion and the background electrolyte cation (Na^{+}), and changes in the activity of both the metal binding functional group sites and aqueous metal ions as a function of ionic strength (Borrok and Fein, 2005).

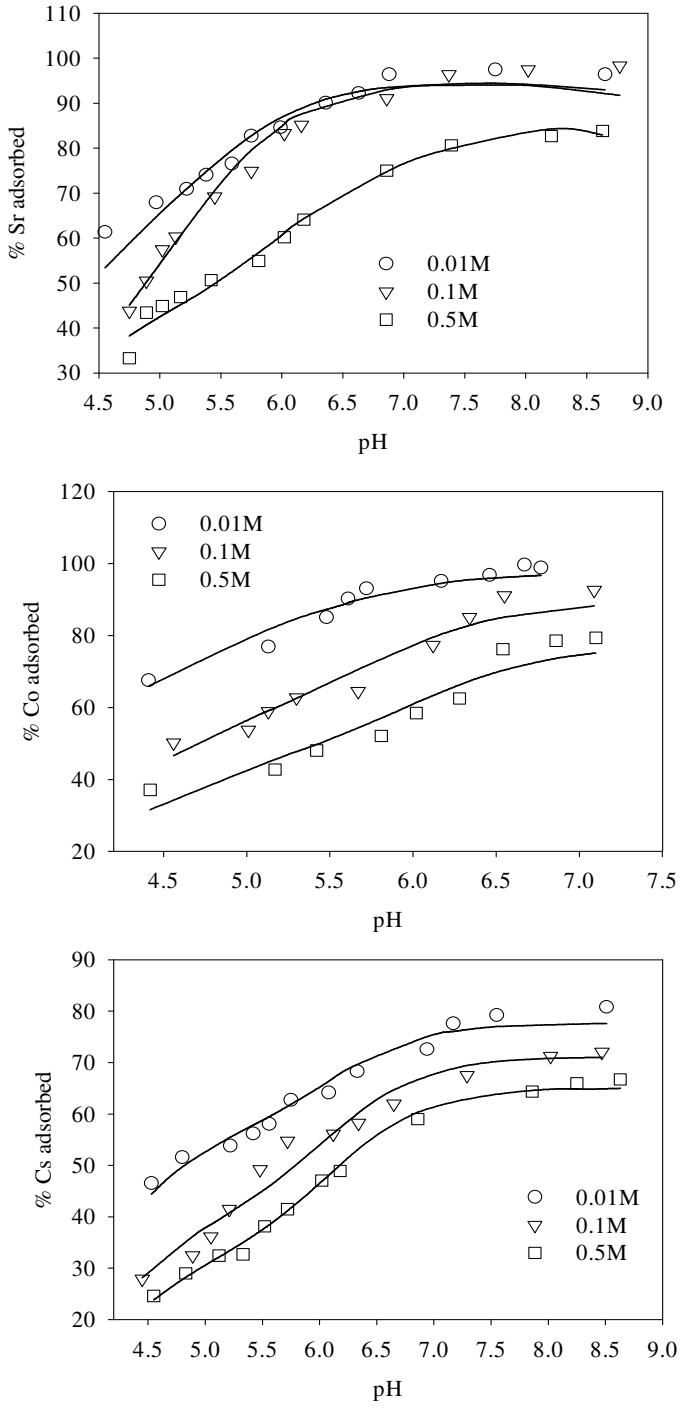

Figure 5.7: Ionic strength dependence on the adsorption behaviour of Sr^{2+}, Co^{2+} and Cs^{+} onto a viable SRB consortium at 25°C. Initial concentrations = 2.85×10^{-4}M, 8.85×10^{-5}M and 3.76×10^{-5}M for Sr^{2+}, Co^{2+} and Cs^{+} , respectively and bacterial biomass = 21.6 g/L (wet weight).

However, regardless of the ionic strength concentration, an adsorption capacity in the range 60-100% was observed for all the metal ions (Sr^{2+}, Co^{2+} and Cs^{+}) at pH ≥ 6.5, suggesting the presence of high affinity sites on the SRB cell surface that bind the metal ions as inner-sphere complexes. As mentioned before (Section 5.4.3), to exclude chemical precipitation reactions, only the first three sites were considered for Sr^{2+}, Co^{2+} and Cs^{+} adsorption. From Table 5.11, it is evident that a 2 site metal adsorption NEM, involving site 1 (carboxylic) and 2 (phosphates) yielded an excellent fit to the experimental Sr^{2+}, Co^{2+} and Cs^{+} adsorption data. All the apparent stability constants obtained were in the range 1-4, in agreement with results obtained by other researchers, which might suggest earlier reports that bacteria exhibit universal proton and metal adsorption behaviour (Borrok et al., 2004; Johnson et al., 2007). The apparent stability constants obtained in this study slightly increased with increasing ionic strength, further confirming the complexation of Sr^{2+}, Co^{2+} and Cs^{+} as outer-sphere complexes. However, further comparisons of the current results with earlier studies cannot be made with any certainty, as different bacteria species, were used, and the electrostatic effects on the bacterial cell surface were not considered.

Table 5.11 Compilation of Sr^{2+}, Co^{2+} and Cs^{+} apparent stability constants at different ionic strengths (0.01 M, 0.1 M and 0.5 M) and 25°C as calculated by FITMOD using the NEM.

Metal ion	Ionic strength (M)	Stability constants [a]			V(Y) [b]
		1	2	3	
Sr^{2+}	0.01	1.53	2.40	NA	2.70
	0.1	1.96	2.41	NA	4.66
	0.5	1.86	3.00	NA	21.5
Co^{2+}	0.01	1.42	2.29	NA	1.07
	0.1	2.04	3.21	NA	3.00
	0.5	2.47	3.93	NA	5.31
Cs^{+}	0.01	1.60	3.35	NA	0.29
	0.1	1.88	3.44	NA	0.71
	0.5	2.02	3.55	NA	0.11

[a] stability constants corrected for both ionic strength and temperature effects, [b] Overall variance computed by FITMOD, NA = not applicable

Effect of Temperature

Over the years very there have been limited studies on the effect of temperature on the adsorption of aqueous metal cations onto bacterial surfaces. Results from the few available

studies indicate that, bacteria demonstrate similar metal adsorption behaviors as a function of temperature. However, it has been hypothesized that under higher pH conditions, the effect of temperature on adsorption depends both on the metal and on the bacterial species of interest (Borrok and Fein, 2005; Ginn and Fein, 2009). In the present study, best-fit models for metal adsorption were generated using up to 3 sites for Sr^{2+} and Cs^{+}, while for Co^{2+} a combination of only site 1 and 2 yielded the best fit (Table 5.12). Generally, there were no marked differences in the apparent stability constants for Co^{2+} and Cs^{+} adsorption over the studied temperature range. As reported earlier (Section 5.2.2), Cs^{+} undergoes limited hydrolysis over the studied pH range, therefore, it is not surprising that the adsorption behaviour of these cations and apparent stability constants are not affected by varying temperature conditions.

Table 5.12 Compilation of Sr^{2+}, Co^{2+} and Cs^{+} apparent stability constants and variance at different temperatures and 0.1M as calculated by FITMOD using the nonelectrostatic model.

Metal ion	Temperature (°C)	Stability constants [a]			V(*Y*)[b]
		1	2	3	
Sr^{2+}	5	1.54	2.48	3.37	0.65
	50	1.69	2.20	3.34	1.33
	75	1.91	2.07	4.06	1.09
Co^{2+}	5	2.07	3.49	NA	5.89
	50	2.06	3.26	NA	2.91
	75	1.99	3.31	NA	5.31
Cs^{+}	5	1.58	3.44	4.78	0.19
	50	1.56	3.47	4.85	0.15
	75	1.58	3.43	5.03	0.08

[a] = apparent constants, [b]= calculated by FITMOD, and NA = not applicable

On the contrary, Co^{2+} readily undergoes hydrolysis with increasing pH, however, since our studies were constrained between a pH range of 2-7 (to exclude precipitation reaction), results obtained suggest that temperature has no effect on the availability of the Co^{2+} species critical for complexation. Similarly, no significant differences were observed for the adsorption of Cd onto the bacteria *Bacillus licheniforms* and *Pseudomonas mendocina* when the temperature was increased from 5 to 80°C (Zouboulis et al., 2004; Ginn and Fein, 2009). However, the observed misfit between the experimental and model Co^{2+} adsorption data at higher pH can be attributed to the contribution of precipitation reactions (hydroxides) at pH>6 (Figure 5.8).

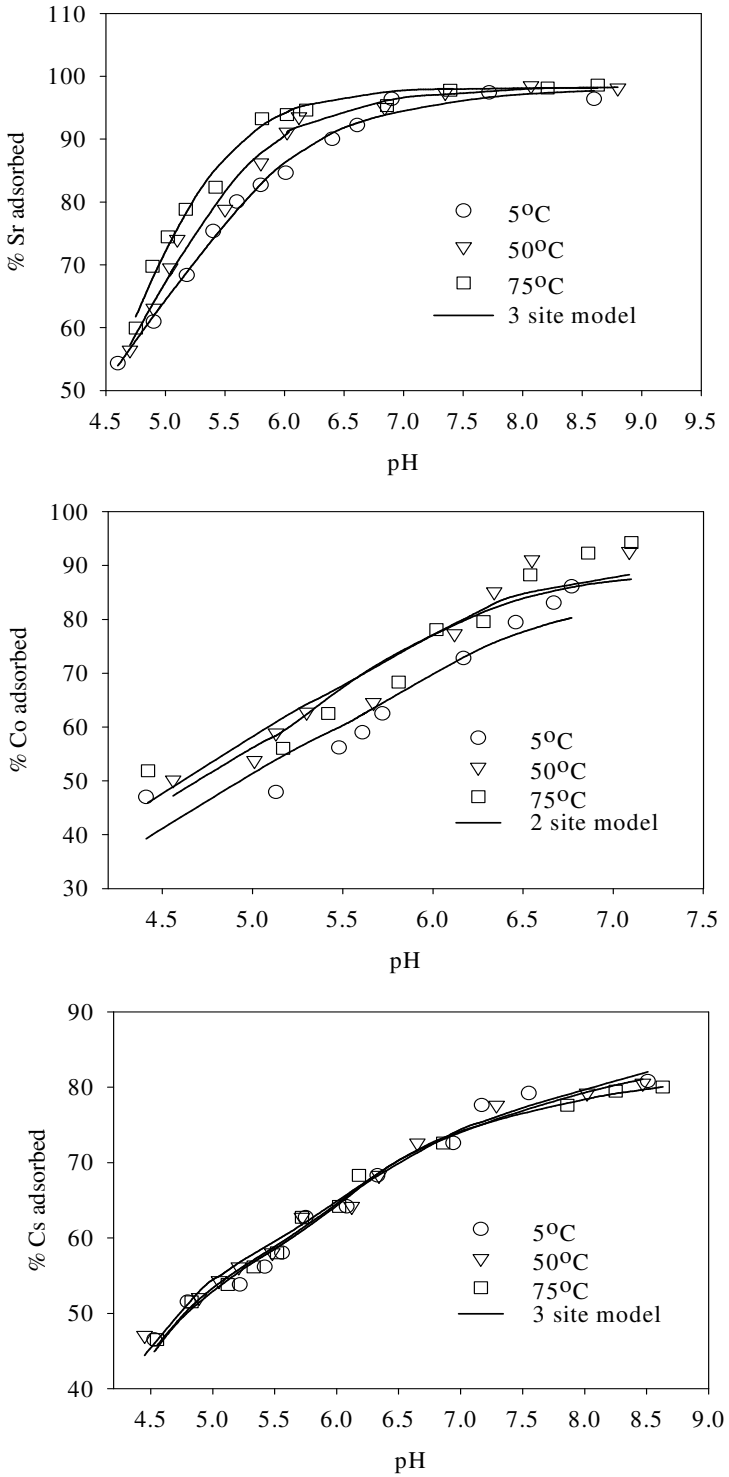

Figure 5.8: Temperature dependence on the adsorption behaviour of Sr^{2+}, Co^{2+} and Cs^{+} onto a viable SRB consortium at 0.1 M $NaNO_3$.

With regards to Sr^{2+} adsorption, an increase in temperature resulted in an increase in the apparent stability constants. It has been suggested that for some metal ions, increasing the temperature influences the speciation of the important metal-surface complexes, whereby the stability constants increase with increasing temperature (Ginn and Fein, 2009). Based on the results obtained in this study, it is apparent that the effect of temperature on metal ion adsorption onto bacterial surfaces varies with the metal ions involved and pH conditions. In summary, results obtained in this study showed that the formation of stable metal-ligand complexes involved the carboxylic sites, phosphates and a third basic site for Sr^{2+} and Cs^{+}, whereas for Co^{2+}, only the first two were involved.

5.5 SUMMARY

The results further suggest that metal binding by bacterial cells is a complex phenomenon, and cannot be fully explained by simple empirical models such as the Langmuir and Freundlich isotherms alone. The preliminary data on the kinetics of fission products removal by SRB in single metal systems and equilibrium binary component systems only serves as the basis for further research on the sorption behaviour of a range of metals onto bacterial sorbents. The preferential order of the SRB consortium for equilibrium metal ion uptake efficiency in single metal systems was observed in the order; Sr>Co>Cs, with maximum biosorption capacities of 405.5, 203.3 and 192.2 mg/g, respectively. In line with the high Sr^{2+} tolerance demonstrated by the present SRB consortium, a superior Sr^{2+} binding capacity was also observed. This value is higher that values reported for sorbents that have been used in other studies (Shaukat et al., 2005; Dabbagh et al., 2007, Chegrouche et al., 2009). Additionally, the SRB consortium also demonstrated a specialized Sr^{2+} binding, as its removal was least sensitive to the presence of other fission products. Initial metal concentration and solution pH are important factors in determining metal removal kinetics. Chemisorption is the main rate limiting step for the removal of Sr^{2+}, Co^{2+} and Cs^{+} from solution at different initial concentrations and pH values.

Results obtained from potentiometric titration studies of the bacterial consortium gave a qualitative measure of the acid-base properties of the bacterial cell surface. Results from this study indicate that the surfaces of the present SRB consortium can be adequately defined by a four-site nonelectrostatic model as the effect of ionic strength on the bacterial surface reactions

was insignificant. Site 1 corresponds to carboxylic acid functional groups (pK_a = 4-5). The near-neutral site 2 was assigned to phosphates (pK_a =6-7), site 3 and 4 are basic sites, and corresponds to phenolic sites (pK_a = 8-12). The most abundant apparent proton binding site belongs to the site 4 (hydroxyl/amine group) and accounts for about 40% of the total concentration of binding sites for the consortium. The apparent total site concentration (C_{tot}) slightly increased with increasing ionic strength, 8.33×10^{-3}, 9.17×10^{-3} and 9.54×10^{-3} mol/L for 0.01M, 0.1M and 0.5M, respectively. Previous studies on other selected bacteria as described by different models yielded lesser total site concentrations of reactive sites (in decreasing order); 3.31×10^{-3} mol/L, 2.24×10^{-3} mol/L, 1.42×10^{-3} mol/L, 1.46×10^{-3} mol/L, 1.27×10^{-3} mol/L, and 7.8×10^{-5} mol/L, for *Pseudomonas aeruginosa*, *Escherichia coli*, *Aquabacterium commune, Calothrix sp, Enterobacteriaceae sp*,and *Shewanella putrefaciens*, respectively (Yee and Fein, 2001; Haas et al., 2001; Ngwenya et al., 2003; Yee et al., 2004; Ojeda et al., 2008). Therefore, the high buffering capacity and metal ion adsorption capacity demonstrated by the mixed SRB culture can be directly attributed to the high total concentration of apparent reactive sites.

The effect of ionic strength on the adsorption of Co^{2+} and Cs^{+} was evident, where at higher ionic strengths decreased metal adsorption was observed. The observed decrease in adsorption capacity was attributed to the presence of excessive amounts of electrolyte cations, thereby competing with Co^{2+} and Cs^{+} for binding sites on the bacterial surface. However, Sr^{2+} adsorption was insensitive to changes in ionic strength in the range 0.01-0.1M. However, further increasing the ionic strength to 0.5M resulted in a slight decrease (about 10%) in Sr^{2+} adsorption by the SRB biomass. Co^{2+} and Cs^{+} adsorption was insensitive to changes in temperature, whereas changes in temperature, however, had a slight effect on the adsorption and immobilization of Sr^{2+} species. In summary, findings from this study strongly suggest that the biological adsorption and stability of the metal ions is influenced by; surface properties of the consortium (including the orientation of the surface functional groups), and metal speciation in the aqueous phase, due to changes in pH and ionic strength.

CHAPTER 6

CONCLUSIONS AND RECOMMENDATIONS

The main aim of the present study was to investigate the potential role of natural microbial processes, and their applicability in controlling metal and radionuclide pollution in the environment. A sulphidogenic bioreactor was used as a model for simulating conditions that closely mimic a groundwater system contaminated with variable metal concentrations, under oxygen-depleted (anoxic) and reducing conditions. Results from this study have demonstrated that the presence of specific metal-tolerant and binding bacterial cultures, lack of oxidizing of agents within the system, coupled with low metal solubility at variable pH and ionic strength conditions renders the immobilized metal complexes in the system stable. The stability of the immobilized metal complexes under variable environmental conditions is critical as it determines the overall applicability and long term performance of a microbial remediation system, particularly during *in situ* bioremediation (Satyawali et al., 2010). Through this project, the multifaceted interrelationships between microbial metal (Sr^{2+}, Co^{2+} and Cs^{+}) immobilization, and cell viability and activity were established. For the first time, our work has demonstrated the unique tolerance of individual SRB microorganisms, belonging to *Citrobacter, Paenibacillus* and *Stenotrophomonas* genera, towards Sr^{2+}, Co^{2+} and Cs^{+}, respectively.

Our work has demonstrated that lower initial Sr^{2+}, Co^{2+} and Cs^{+} concentrations (≤100 mg/L) have minimal effects on the growth and metabolism (biological sulphate reduction) of the present mixed SRB culture. These observations imply that at sufficiently low inhibitory concentrations, the growing SRB biomass can be effectively used for the *in situ* bioremediation of metals and radionuclides provided the energy and electron acceptor sources requirement is satisfied. The mixed SRB culture was less sensitive to the presence of Cs than Sr or Co, which eliminates one potential problem in the use of live cells for its removal. The results obtained indicate that Sr^{2+}, Co^{2+} and Cs^{+} removal from solution in the sulphidogenic bioreactor occurred through one or a combination of complex interaction mechanisms including; biosorption, chemical and biological precipitation, bioreduction, and bioaccumulation. Further analyses

revealed that cell viability is not a critical factor that determines the mechanism of microbial Sr^{2+} and Cs^{+} removal from solution, as removal occurred mainly through biosorption. On the other hand, Co^{2+} uptake from solution was dependent on cell viability, where under viable SRB conditions, metal removal through a combination of biosorption, bioprecipitation and bioaccumulation. Results from batch kinetic metal removal studies further confirmed that the removal efficiency of the metal ions (Sr^{2+}, Co^{2+} and Cs^{+}) was dependent on the initial metal concentration, solution pH and cell viability. Live bacterial cells consistently demonstrated a superior metal biosorption capacity, compared to heat-killed bacterial cells. The metal uptake efficiency of the SRB biomass increased up till the threshold limit of 405, 203 and 192 mg/g was reached for Sr^{2+}, Co^{2+} and Cs^{+}, respectively.

So far, the present study is the first to study the surface characteristics and proton and Sr^{2+}, Co^{2+} and Cs^{+} adsorption behaviour of an SRB consortium under anaerobic conditions. A combination of potentiometric titrations and FTIR spectroscopy eased the identification of the four discrete functional groups, carboxylic (pK_a = 3-5), phosphate (pK_a = 6-7), and 2 basic sites (pK_a = 8-12), belonging to either and hydroxyl or amine groups, which were unique to this culture. The high binding capacity of the bacterial consortium was attributed to the high concentration of reactive surface sites (C_{tot} = 9.17×10^{-3} mol/L). Whether, culture growth conditions, that is, aerobic or anaerobic and type of medium, have a direct influence on the observed results remains unclear, but can only be determined through further research. Results from this study suggest that a simple 2 site model (involving carboxylic and phosphoryl groups) is adequate to account for metal adsorption onto bacterial surfaces. The adsorption capacities of the metals decreased with increasing ionic strength, whereas variable temperature conditions had no effect on the sorptive properties of the bacterial cell surface. Consequently, taking into account the observed results, the following conclusions can be drawn;

- Exposure of the initial SRB consortium to Sr^{2+}, Co^{2+} and Cs^{+} resulted in the emergence of metal-specific and -tolerant novel SRB microorganisms, belonging *Citrobacter, Paenibacillus* and *Stenotrophomonas* genera, respectively.

- The toxic and inhibitory effects of the metal ions (Sr^{2+}, Co^{2+} and Cs^{+}) on the SRB culture were unique for each metal ion, due to the differences in their chemical and physical properties, thereby determining cell viability and activity. For example, in a heavily contaminated bioreactor system (≥300 mg/L metal), the growth of SRB and ability for sulphate reduction was retarded.
- The removal capacity of the metals in the bioreactors was dependent on biomass concentration, where high metal removal rates (up to 100%) were observed at less toxic and inhibitory metal concentrations.
- Metal removal by the biomass mainly occurred through non-specific electrostatic reactions by the formation of outer-sphere metal-bacteria complexes. The present SRB culture demonstrated superior Sr^{2+}, Co^{2+} and Cs^{+} binding capacities ($q_{max)}$ of 405, 203 and 192 mg/g for Sr^{2+}, Co^{2+} and Cs^{+}, respectively.
- The SRB surface is characterized by the presence of four discrete functional groups; carboxylic (pK_a = 3-5), phosphate (pK_a = 6-7), and 2 basic sites (pK_a = 8-12), belonging to either and hydroxyl or amine groups, which were unique to this culture. Compared to other bacteria, the high metal adsorption capacity demonstrated by this culture can be attributed to the high concentration of apparent reactive sites ($C_{tot} = 9.17\times10^{-3}$ mol/L).
- The adsorption of metal ions onto the bacterial surface was highly sensitive to changing ionic strength and pH conditions, and less sensitive to changes in temperature.

These findings suggest that indigenous anaerobic microorganisms, such as SRB, might hold a promise towards their use for *in situ* bioremediation processes due to their outstanding metal-tolerance and sequestering abilities. In particular, evaluation of the biomass population biology kinetic parameters forms an important aspect towards the development of effective radionuclide retardation strategies utilizing growing microorganisms. Taking all results together they contribute to a more realistic description of the influence of microbial actions on the migration behavior of radionuclide contaminants in the environment and are helpful for an improved risk assessment for instance for potential underground nuclear waste repositories. Further studies related to this subject should focus on two main directions. The first one should be concentrated on direct interactions of other high priority radionuclides with different microorgansisms,

including those isolated from potential nuclear waste repository areas. Prior to metal uptake studies, it is important that the phylogeny, radiotoxicity and metal tolerance of the cultures is established. Results obtained from this study suggested that the observed differences in metal tolerance and removal amongst the different microorganisms might be due to the inherent characteristics of the microorganisms as well as the metal itself. Therefore, future studies should focus on the application of rigorous screening procedures involving the use of autoradiography, which has great potential for isolation of microorganisms with particularly high affinities for different metal ions. Alternatively, manipulation of the physiological status of microorganisms can dramatically alter the transport and mobility of metal ions, particularly, monovalent cations, which are difficult to remove from solution. Particularly, osmotic shock procedures have so far proved to be the most successful treatments for stimulating Cs removal and recovery by microorganisms. Other manipulations, at both the cellular and molecular level, which are can influence metal uptake by bacterial biomass have yet to be characterized and investigated. Secondly, future research should also focus on the less studied indirect interaction between radionuclides and microbially produced bioligands. In addition, one important goal to be achieved in future studies will be the determination of the intrinsic stability constants and the structure of the formed metal-complexes species. These constants will be used directly in risk assessment programs.

BIBLIOGRAPHY

LIST OF REFERENCES

1. Ahmadpour, A., Zabihi, M., Tahmasbi, M. and Bastami, T.B. (2010) Effect of adsorbents and chemical treatments on the removal of strontium from aqueous solutions. *Journal of Hazardous Materials*, **182**(1-3): 552-556.
2. Ahuja, P., Gupta, R. and Saxena, R.K. (1999) Sorption and desorption of Cobalt by *Oscillatoria anguistissima. Current microbiology*. **39**: 49–52.
3. Akar, T. and Tunali, S. (2006) Biosorption characteristics of *Aspergillus flavus* biomass for removal of Pb(II) and Cu(II) ions from an aqueous solution. *Bioresource Technology*, **97**: 1780–1787.
4. Aksu, Z. (2001) Equilibrium and kinetic modelling of cadmium(II) biosorption by *C. vulgaris* in a batch system: effect of temperature. *Separation and Purification Technology,* **21**(3): 285-294.
5. Allison, J. D., Brown, D.S. and Novo-Gradac, K.J. (1991) MINTEQA2/ PRODEFA2, a geochemical assessment model for environmental systems (version 3.0) user's manual. Environmental Research Laboratory, Office of Research and Development, U.S. Environmental Protection Agency, Washington, D.C.
6. Amos, P.W. and Younger, P.L. (2003) Substrate characterisation for a subsurface reactive barrier to treat colliery spoil leachate. *Water research,* **37**(1): 108-120.
7. Anderson, S. and Appanna, V.D. (1994) Deposition of crystalline strontium carbonate by *Pseudomonas fluorescens*. *FEMS Microbiology Letters*, **116**: 43-48.
8. Ansaria, M.I. and Malik, A. (2007) Biosorption of nickel and cadmium by metal resistant bacterial isolates from agricultural soil irrigated with industrial wastewater. *Bioresource Technology*, **98**(16), 3149-3153.
9. APHA (1994) Standard methods for the Examination of Water and Wastewater. 18th edition. APHA, AWWA, WPCF Publishing, New York.
10. Avery, S.V. and Tobin, J.M. (1992) Mechanisms of strontium uptake by laboratory and brewing strains of Saccharomyces cerevisiae. *Applied and Environmental Microbiology,* **58**(12): 3883-3889.

11. Avery, S.V., Codd, G.A. and Gadd, G.M. (1993) Transport kinetics, cation inhibition and intracellular location of accumulated cesium in the green microalga *Chlorella salina*. *Journal of General Microbiology,* **139**: 827-834.
12. Avery, S.V. (1995) Cesium accumulation by microorganisms: uptake mechanisms, cation competition, compartmentalisation and toxicity. *Journal of Industrial Microbiology*, **14**(2): 76-84.
13. Baes C.F. and Mesmer R.E. (1976) The Hydrolysis of Cations. Wiley, New York.
14. Banaszak, J., Rittmann, B. and Reed, D. (1999) Subsurface interactions of actinide species and microorganisms: Implications for the bioremediation of actinide-organic mixtures. *Journal of Radioanalytical and Nuclear Chemistry,* **241**(2): 385-435.
15. Banerjee, M. and Yesmin, L. (2002) Sulphur-oxidizing plant growth promoting rhizobacteria for enhanced canola performance. US Patent 07491535 (2002).
16. Barkay, T. and Schaefer, J. (2001) Metal and radionuclide bioremediation: issues, considerations and potentials. *Current opinion in microbiology,* **4**(3): 318-323.
17. Barton, L.L. (1992) Sulphur metabolism. Encyclopedia of Microbiology, pp. 135– 150.
18. Beech, I.B. & Cheung, C.W.S. (1995) Interactions of exopolymers produced by sulphate-reducing bacteria with metal ions. *International Biodeterioration and Biodegradation,* **35**(1-3): 59-72.
19. Bellot, J.C. and Condoret, J.S. (1993) Modeling of liquid chromatography equilibrium. *Process Biochemistry*, **28**: 365–376.
20. Benner, S.G., Blowes, D.W., Gould, W.D., Herbert, R.B. and Ptacek, C.J. (1999) Geochemistry of a permeable reactive barrier for metals and acid mine drainage. *Environmental Science and Technology,* **33**(16): 2793-2799.
21. Bennett, D.G. and Gens, R. (2008) Overview of European concepts for high-level waste and spent fuel disposal with special reference waste container corrosion. *Journal of Nuclear Materials,* **379**(1-3): 1-8.
22. Beolchini F, Pagnanelli F, Toro L, Vegliò F. (2006) Ionic strength effect on copper biosorption by *Sphaerotilus natans*: equilibrium study and dynamic modelling in membrane reactor. *Water Research*, **40**: 144–52.
23. Beveridge, T.J., and Murray, R.G.E. (1980) Sites of metal deposition in the cell wall of *Bacillus subtilis*. *Journal of Bacteriology,* **141**: 876–887.
24. Beveridge, T.J. (1981) Ultrastructure, chemistry, and function of the bacterial wall. *International Reviews of Cytology*, **72**: 229–317.

25. Beveridge, T.J. (1989) Role of cellular design in bacterial metal accumulation and mineralization. *Annual Review of Microbiology,* **43**: 147-171.

26. Blowes, D.W., Ptacek, C.J., Benner, S.G., McRae, C.W.T., Bennett, T.A., Puls, R.W., 2000. Treatment of inorganic contaminants using permeable reactive barriers. *Journal of Contamination Hydrology*, **45**: 123–137.

27. Borrok, D., Fein, J.B. and Kulpa, C.F. (2004) Proton and Cd adsorption onto natural bacterial consortia: testing universal adsorption behavior. *Geochimica et Cosmochimica Acta*, **68**: 3231–3238.

28. Borrok, D.M. and Fein, J.B. (2005) The impact of ionic strength on the adsorption of protons, Pb, Cd, and Sr onto the surfaces of Gram negative bacteria: testing non-electrostatic, diffuse, and triple-layer models. *Journal of Colloid and Interface Science,* **286**(1): 110-126.

29. Borrok, D.M., Fein, J.B. and Turner, B.F. (2005) A universal surface complexation framework for modeling proton binding onto bacterial surfaces in geologic settings, *American Journal of Science,* **305**, 826–853.

30. Botes, E., Van Heerden, E. and Litthauer, D. (2007) Hyper-resistance to arsenic in bacteria isolated from an antimony mine in South Africa. *South African Journal of Science,* **103**, 279-283.

31. Brainard, J.R., Strietelmeier, B.A., Smith, P.H., Langston-Unkefer, P.J., Barr, M.E. and Ryan, R.R. (1992) Actinide Binding and Solublization by Microbial Siderophores. *Radiochimica Acta,* **58/59**: 357-363.

32. Braissant, O., Decho, A.W., Dupraz, C., Glunk, C., Przekop, K.M. and Visscher, P.T. (2007) exopolymeric substances of sulphate-reducing bacteria: Interactions with calcium at alkaline pH and implication for formation of carbonate minerals. *Geobiology,* **1**: 1-11.

33. Brodie, E.L., Desantis, T.Z., Joyner, D.C., Baek, S.M., Larsen, J.T., Andersen, G.L., Hazen, T.C., Richardson, P.M., Herman, D.J., Tokunaga, T.K., Wan, J.M. and Firestone, M.K. (2006) Application of a high-density oligonucleotide microarray approach to study bacterial population dynamics during uranium reduction and reoxidation. *Applied and Environmental Microbiology,* **72**(9): 6288-6298.

34. Brown, S.D., Thompson, M.R. and Verberkmoes, N.C. (2006). Molecular dynamics of the *Shewanella oneidensis* response to chromate stress. *Molecular Cell Proteomics,* **5**: 1054–1071.

35. Bruhn, D.F., Breckenridge, C.R., Tsang, M.N., Watkins, C.S., Windes, W.E., Roberto, F.F., Wright, R.N., Pinhero, P.J. and Brey, R.F. (1999) Irradiation of Microbes from Spent Nuclear Fuel Storage Pool Environments. Global '99 Report. USA.

36. Bruhn, D.F., Frank, S.M., Roberto, F.F., Pinhero, P.J. and Johnson, S.G. (2009) Microbial biofilm growth on irradiated, spent nuclear fuel cladding. *Journal of Nuclear Materials,* **384**(2): 140-145.

37. Brunauer, S., Emmett, P.H. and Teller, E. (1938) Adsorption of gases in multimolecular layers. *Journal of American Chemical Society* (USA), **60**: 309–319.

38. Bruno, J. and Ewing, R.C. (2006) Spent Nuclear Fuel. *Elements,* **2**: 343-349.

39. Buck, E.C., Hanson, B.D. and McNamara, B.K. (2004) The geochemical behaviour of Tc, Np and Pu in spent nuclear Fuel in an oxidizing environment. In: Gieré R, Stille P (eds) Energy, Waste, and the Environment: a Geochemical Perspective. *The Geological Society of London Special Publication,* **236**: 65-88.

40. Bueno, B.Y.M., Torem, M.L., Molina, F. and de Mesquita, L.M.S. (2008) Biosorption of lead(II), chromium(III) and copper(II) by *R. opacus*: equilibrium and kinetic studies. *Minerals Engineering* **21**: 65–75.

41. Bunn, M., Fetter, S., Holdren, J.P. and van der Zwan, B. (2003) The Economics of Reprocessing vs. Direct Disposal of Spent Nuclear Fuel. Final Report. Cambridge, Mass. Project on Managing the Atom, Harvard University. USA.

42. Burnett, P.G., Daughney, C.J. and Peak, D. (2006) Cd adsorption onto *Anoxybacillus flavithermus*: surface complexation modelling and spectroscopic investigations. *Geochimica et Cosmochimica Acta,* **70**: 5253-5269.

43. Butlin, K.R., Adams, M.E. and Thomas, M. (1949) The isolation and cultivation of sulphate-reducing bacteria. *Journal of General Microbiology,* **3**(1): 46-59.

44. Calfa, B.A. and Torem,M.L. (2008) On the fundamentals of Cr (III) removal from liquid streams by a bacterial strain. *Minerals Engineering* **21:** 48–54.

45. Carlsson, E., Thunberg, J., Ohlander, B. and Holmstrom, H. (2002) Sequential Extraction of Sulfide-Rich Tailings Remediated by the Application of Till Cover, Kristineberg Mine, Northern Sweden, *The Science of The Total Environment,* **299**(1-3): 207-226.

46. Caron, F. and Mankarios, G. (2004) Pre-assessment of the speciation of 60Co, 125Sb, 137Cs and 241Am in a contaminated aquifer. *Journal of Environmental Radioactivity,* **77**(1): 29-46.

47. Chaalal, O. and Islam, M.R. (2001) Integrated management of radioactive strontium contamination in aqueous stream systems. *Journal of Environmental Management,* **61**(1): 51-59.

48. Chandrasekhar, K., Subramanian, S., Modak, J.M. and Natarajan, K.A. (1998) Removal of metal ions using an industrial biomass with reference to environmental control. *International Journal of Mineral Processing*, **53**: 107-120.

49. Chegrouche, S., Mellah, A. and Barkat, M. (2009) Removal of strontium from aqueous solutions by adsorption onto activated carbon: kinetic and thermodynamic studies. *Desalination,* **235**(1-3): 306-318.

50. Chen, B.Y., Utgikara, V.P., Harmona, S.M., Tabak, H.H., Bishopa, D.F. and Govind, R. (2000) Studies on biosorption of zinc(II) and copper(II) on *Desulfovibrio desulfuricans*. *International Biodeterioration and Biodegradation*, **46**(1): 11-18.

51. Chen, W.L., Luan, Y.C., Shieh, M.C., Chen, S.T., Kung, H.T., Soong, K.L., Yeh, Y.C., Chou, T.S., Mong, S.H., Wu, J.T., Sun, C.P., Deng, W.P., Wu, M.F. and Shen, M.L. (2007) Effects of Cobalt-60 Exposure on Health of Taiwan Residents Suggest New Approach Needed in Radiation Protection. *Dose Response,* **5**(1): 63-75.

52. Chen, Z., Ma, W. and Han, M. (2008) Biosorption of nickel and copper onto treated alga (*Undaria pinnatifida*): Application of isotherm and kinetic models. *Journal of Hazardous Materials* **155** (1-2): 327-333.

53. Chicote, E., Moreno, D.A., Garcia, A.M., Sarro, I.M., Lorenzo, P.I. and Montero, F. (2004) Biofouling on the walls of a spent nuclear fuel pool with radioactive ultrapure water. *Biofouling: The Journal of Bioadhesion and Biofilm Research,* **20**(1): 35.

54. Chien, C-C. and Han, C-T. (2009) Tellurite resistance and reduction by a *Paenibacillus* sp. isolated from heavy metal–contaminated sediment. *Environmental Toxicology and Chemistry*, **28**(8): 1627–1632.

55. Chirwa, E.M.N. (2010) Developments in bioremediation for separation and recovery. In Advanced Separation Techniques for Nuclear Fuel.

56. Choi, S.B. and Yun, Y.S. (2004) Lead biosorption by waste biomass of *Corynebacterium glutamicum* generated from lysine fermentation process. *Biotechnology Letters* **26**: 331–336.

57. Choi, J., Leea, J.Y. and Yanga, J.S. (2009) Biosorption of heavy metals and uranium by starfish and *Pseudomonas putida*. *Journal of Hazardous Materials*, **161**(1): 157-162.

58. Choudhary, S. and Sar, P. (2009) Characterization of a metal resistant *Pseudomonas* sp. isolated from uranium mine for its potential in heavy metal (Ni^{2+}, Co^{2+}, Cu^{2+}, and Cd^{2+}) sequestration. *Bioresource technology,* **100**(9): 2482-2492.

59. Churchill, S.A., Walters, J.V. and Churchill, P.F. (1995). Sorption of heavy metals by prepared bacterial cell surfaces. *Journal of Environmental Engineering*, **121**, 706-711.

60. Costa, M., Martins, M., Jesus, C. and Duarte, J. (2008) Treatment of acid mine drainage by sulphate-reducing bacteria using low cost matrices. *Water, Air, & Soil Pollution,* **189**(1): 149-162.

61. Cox, S., Smith, D.S., Warren, L.A. and Ferris, F.G. (1999) Characterising heterogeneous bacterial surface functional groups using discrete affinity spectra for proton binding. *Environmental Science and Technology*, **33**: 4514–4521.

62. Creamer, N. J., Baxter-Plant, V. S., Henderson, J., Potter, M. and Macaskie, L.E. (2006). Palladium and gold removal and recovery from precious metal solutions and electronic scrap leachates by Desulfovibrio desulfuricans. *Biotechnology Letters*, **28**(18): 1475-1484.

63. Crowley K.D. (1997) Nuclear waste disposal: the technical challenges. *Physics Today*, **50**(6): 32-39. American Institute of Physics, S-0031-9228-9706-030-4.

64. Dabbagh, R., Ghafourian, H., Baghvand, A., Nabi, G., Riahi, H. and Ahmadi Faghih, M. (2007) Bioaccumulation and biosorption of stable strontium and 90Sr by Oscillatoria homogenea cyanobacterium. *Journal of Radioanalytical and Nuclear Chemistry,* **272**(1): 53-59.

65. Dahl, O., Nurmesniemi, H. and Poykio, R. (2008) Sequential extraction partitioning of metals, sulfur, and phosphorus in bottom ash from a coal-fired power plant. *International Journal of Environmental Analytical Chemistry,* **88**(1): 61–73.

66. Darnall, D.W., Green, B., Hosea, M., Mcpherson, R.A., Henzl, M. and Alexander, M.D. (1986) Recovery of heavy metal ions by immobilized alga. In *Trace Metal Removal from Aqueous Solution, ed. R. Thompson*. Royal Society of Chemistry, Special Publication No.61, London.

67. Daughney, C.J. and Fein, J.B. (1998) The effect of ionic strength on the adsorption of H^+, Cd^{2+}, Pb^{2+} and Cu^{2+} by *Bacillus subtilis* and *Bacillus licheniformis*: a surface complexation model. *Journal of Colloid Interface Science*, **198**: 53–77.

68. Daughney, C.J., Fein, J.B. and Yee, N., (1998) A comparison of the thermodynamics of metal adsorption onto two common bacteria. *Chemical Geology,* **144**: 161–176.

69. Daughney, C.J., Fowle, D.A. and Fortin, D. (2001) The effect of growth phase on proton and metal adsorption by *Bacillus subtilis*. *Geochimica et Cosmochimica Acta,* **65**: 1025-1035.

70. Daughney, C.J., Siciliano, S.D., Rencz, A.N., Lean, D.R.S. and Fortin, D. (2002) Hg(II) adsorption by bacteria: a surface complexation model and its application to shallow acidic lakes and wetlands in Kejimkujik National Park, Nova Scotia, Canada. *Environmental Science and Technology*, **36**: 1546–1553.

71. Daughney, C.J., Chatellier, X., Chan, A., Kenward, P., Fortin, D., Suttle, C.A. and Fowle, D.A. (2004) Adsorption and precipitation of iron from seawater on a marine bacteriophage (PWH3A-P1). *Marine Chemistry,* **91**: 101-115.

72. Davis, J.A. and Kent, D.B. (1990) Surface complexation modeling in aqueous geochemistry. In: Hochella Jr, M.F. and White, A.F., Editors, 1990. Mineral-Water Interface Geochemistry 23, Reviews in Mineralogy, pp. 177–260 Mineralogical Society of America.

73. Deplanche, K. and Macaskie, L.E. (2008) Biorecovery of gold by *Escherichia coli* and *Desulfovibrio desulfuricans. Biotechnology and Bioengineering*, **99**(5), 1055–1064.

74. De Rome, L. and Gadd, G.M. (1987). Copper adsorption by to *Rhizopus arrhizus*, *Cladosporium resinae* and *Penicillium italicum*. *Applied Microbiology and Biotechnology*, **26**: 84-90.

75. Dewiere, L., Bugai, D., Grenier, C., Kashparov, V. and Ahamdach, N. (2004) 90Sr migration to the geo-sphere from a waste burial in the Chernobyl exclusion zone. *Journal of Environmental Radioactivity,* **74**(1-3): 139-150.

76. Dzombak, D.A. and Morel, F.M.M. (1990) Surface Complexation Modeling: Hydrous Ferris Oxide, John Wiley, New York.

77. Ebner, A.D., Ritter, J.A. and Navratil, J.D. (2001) Adsorption of cesium, strontium, and cobalt Ions on magnetite and a magnetiteâ silica composite. *Industrial & Engineering Chemistry Research,* **40**(7): 1615-1623.

78. Eccles, H. (1995) Removal of heavy metals from effluent streams — why select a biological process? *International Biodeterioration and Biodegradation,* **35**(1-3): 5-16.

79. Ekstrom, E.B. and Morel, F.M.M. (2008) Cobalt limitation of growth and mercury methylation in sulphate reducing bacteria. *Environmental Science and Technology,* **42**(1): 93-99.

80. Esposito, A. Pagnanelli, F., Lodi, A., Solisio, C. and Veglio, F. (2001) Biosorption of heavy metals by *Sphaerotilus natans*: an equilibrium study at different pH and biomass concentrations. *Hydrometallurgy,* **60**: 129–41.

81. Fan, T., Liu, Y., Feng, B., Zeng, G., Yang, C., Zhou, M., Zhou, H., Tan, Z. and Wang, X. (2008) Biosorption of cadmium(II), zinc(II) and lead(II) by *Penicillium simplicissimum*: isotherms, kinetics and thermodynamics. *Journal of Hazardous Materials*, **160**: 655–661.

82. Fein, J.B., Daughney, C.J., Yee, N. and Davis, T.A. (1997) A chemical equilibrium model for metal adsorption onto bacterial surfaces. *Geochimica et Cosmochimica Acta,* **61**(16): 3319-3328.

83. Fein, J.B. (2000) Quantifying the effects of bacteria on adsorption reactions in water–rock systems. *Chemical Geology,* **169**(3-4): 265-280.

84. Fein, J.B., Boily, J-F., Yee, N., Gorman-Lewis, D. and Turner, B.F. (2005) Potentiometric titrations of *Bacillus subtilis* cells to low pH and a comparison of modelling approaches. *Geochimica et Cosmochimica Acta,* **69**(5): 1123-1132.

85. Fourest, E. and Roux, J.C. (1992) Heavy metal biosorption by fungal mycelia by-products: mechanism and influence of pH. *Applied Microbiology and Biotechnology,* **37**, 399–403.

86. Fowle, D.A. and Fein, J.B. (1999) Competitive adsorption of metal cations onto two gram positive bacteria: Testing the chemical equilibrium model. *Geochimica et Cosmochimica Acta*, **19/20**: 3059–3067.

87. Francis, A.J. (1998) Biotransformation of uranium and other actinides in radioactive wastes. *Journal of Alloys and Compounds,* **271-273**: 78-84.

88. Freundlich, H.M.F. (1906) Over the adsorption in solution. *Journal of Physical Chemistry* **57,** 385–470.

89. Friis, N. and Myers-Keith, P. (1986) Biosorption of uranium and lead by *Streptomyces longwoodensis*. *Biotechnology and Bioengineering*, **28**: 21–28.

90. Gadd, G.M. (1986) The uptake of heavy metals by fungi and yeasts : the chemistry and physiology of the process and applications for biotechnology, in *Immobilisation of Ions by Bio-sorption*, ed. By Eccles H and Hunt S. Ellis Horwood Ltd, Chichester, pp. 135–147.

91. Gadd, G.M. (1988) Accumulation of Metals by Microorganisms and Algae. In: Biotechnology- A comprehensive Treatise. Rehm, H.J. (ed.). Fifth edition. VCH Verlagsgesellschaft, Weinheim.

92. Gadd, G.M., White, C. and De Rome, L. (1988) Heavy metal and radionuclide uptake by fungi and yeasts. In: Norris, P.R. and Kelly, D.P. (eds.) Biohydrometallurgy. A. Rowe, Chappenham, Wilts., UK.
93. Gadd, G.M. (1989) Green means clean: biomass and metal accumulation. *Trends in Biotechnology*, **7**(12): 325-326.
94. Gadd, G.M. (2000) Bioremedial potential of microbial mechanisms of metal mobilization and immobilization. *Current Opinion in Biotechnology*, **11**(3): 271-279.
95. Gadd, G.M. (2004) Microbial influence on metal mobility and application for bioremediation. *Geoderma,* **122**(2-4): 109-119.
96. Gadd, G.M. (2009) Biosorption: critical review of scientific rationale, environmental importance and significance for pollution treatment. *Journal of Chemical Technology and Biotechnology,* **84**(1): 13-28.
97. Gao, W., Gentry, T.J., Mehlhorn, T.L., Carroll, S.L., Jardine, P.M. and Zhou, J. (2010) Characterization of Co(III) EDTA-reducing bacteria in metal-and radionuclide-contaminated groundwater. *Geomicrobiology Journal*, **27**: 93–100.
98. Garcia, D.O., Timenetsky, J., Martinez, M.B., Francisco, W., Sinto, S.I., Yanaguita, R.M. (2002) Protease (Caseinase and Elastase), hemolysins, adhesion and susceptibility to antimicrobials of *Stenotrophomonas maltophilia* isolates obtained from clinical specimens. *Brazilian Journal of Microbiology*, **33**: 157-162.
99. Gavaskar, A.R. (1999) Design and construction techniques for permeable reactive barriers. *Journal of Hazardous Materials,* **68**(1-2): 41-71.
100. Gibert, O., de Pablo, J., Cortina, J.L., Ayora, C. (2002) Treatment of acid mine drainage by sulphate-reducing bacteria using permeable reactive barriers: a review from laboratory to full-scale experiments. *Environmental Science and Bio/Technology*, **1**: 327–333.
101. Ginn, B. and Fein, J.B. (2009) Temperature dependence of Cd and Pb binding onto bacterial cells. *Chemical Geology*, **259**: 99–106.
102. Goncalves, M.M.M., Da Costa, A.C.A., Leite, S.G.F., and Sant'Anna, G.L. (2007) Heavy metal removal from synthetic wastewaters in an anaerobic bioreactor using stillage from ethanol distilleries as a carbon source. *Chemosphere*, **69**: 1815.
103. Gorby, Y.A., Caccavo Jr., F. and Bolton Jr., H. (1998) *Environmental Science and Technology,* **32**(2): 244-250.

104. Greve, K., Nielsen, E. and Ladefoged, O. (2007) Evaluation of health hazards by exposure to strontium in drinking water. *Toxicology letters,* **172** (Supplement 1): S210-S210.

105. Haas, J. R., Dichristina, T. J. and Wade, R. (2001) Thermodynamics of U(VI) sorption onto *Shewanella putrefaciens*. *Chemical Geology,* **180**: 33-54.

106. Haas, J.R. (2004) Effects of cultivation conditions on acid–base titration properties of Shewanella putrefaciens. *Chemical Geology,* **209**(1-2), 67-81.

107. Haveman, S.A. and Pedersen, K. (2002) Microbially mediated redox processes in natural analogues for radioactive waste. *Journal of Contaminant Hydrology,* **55**: 161– 174.

108. HaiLei, W., MianPing, Z. and XiaoXing, H. (2007) Cesium accumulation by bacterium *Thermus* sp. TibetanG7: hints for biomineralisation of cesium-bearing geyserite in hot springs n Tibet, China. *Chinese Science Bulletin*, **52**(19): 2680-2686.

109. Harjula, R. and Lehto, J. (1986) Effect of sodium and potassium ions on cesium absorption from nuclear power plant waste solutions on synthetic zeolites. *Nuclear and Chemical Waste Management*, **6**(2): 133-137.

110. Hedin, R.S., Narin, R.W., Kleinmann, L.P. (1994) Passive Treatment of Coal Mine Drainage. US Bureau of Mines LC9389. US Department of the Interior, Washington, DC 35pp.

111. Heinrich, H.T.M., Bremer, P.J., McQuillan, A.J. and Daughney, C.J. (2008) Modelling of the acid-base properties of two thermophilic bacteria at different growth times. *Geochimica et Cosmochimica Acta*, **72**: 4185-4200.

112. Hetzer, A., Daughney, C.J. and Morgan, H.W. (2006) Cadmium ion biosorption by the thermophilic bacteria *Geobacillus stearothermophilus* and *G. thermocatenulatus*, Applied Environmetal Microbiology, **72**(6), 4020–4027.

113. Ho, Y.S. and McKay, G. (1998) Sorption of dye from aqueous solution by peat. *Chemical Engineering Journal,* **70**(2): 115-124.

114. Ho, Y.S. and McKay, G. (2000) The kinetics of sorption of divalent metal ions onto sphagnum moss peat. *Water Research,* **34**(3): 735-742.

115. Holt, J. G., Krieg, N. R., Sneath, P. H. A., Staley, J. T., and Williams, S. T. (1994) Group 7: Dissimilatory sulfate- or sulfur- reducing bacteria. *In* Bergey's Manual of Determinative Bacteriology, 9th ed., Williams and Wilkins, Baltimore, Maryland, pp. 335–339.

116. IAEA (2009) Nuclear Technology Review. International Atomic Energy Agency Scientific and Technical Publication Series, Vienna.

117. Istok, J.D., Senko, J.M., Krumholz, L.R., Watson, D., Bogle, M.A., Peacock, A., Chang, Y.-J. and White, D.C. (2004) In situ bioreduction of Technetium and Uranium in a nitrate-contaminated Aquifer. *Environmental Science and Technology,* **38**(2): 468–475.

118. Jalali-Rad, R., Ghafourian, H., Asef, Y., Dalir, S.T., Sahafipour, M.H. and Gharanjik, B.M. (2004) Biosorption of cesium by native and chemically modified biomass of marine algae: introduce the new biosorbents for biotechnology applications. *Journal of Hazardous Materials*, **B116**: 125–134.

119. Jamil, K., Ali, S. Iqbal, M., Qureshi, A.A. and Khan, H.A. (1998) Measurements of radionuclides in coal samples from two provinces of Pakistan and computation of external γ-ray dose rate in coal mines. *Journal of Environmental Radioactivity,* **41**(2): 207-216.

120. Jasinska, M., Mietelski, J.W. and Pociask-Karteczka, J. (1998) Radionuclide content in the upper Vistula river sediments in a coal mining region in Poland (East Central Europe). *Earth and Environmental Science,* **102**(3-4): 355-360.

121. Jeong, B.C., Hawes, C., Bonthrone, K.M. and Macaskie, L.E. (1997) Localization of enzymatically enhanced heavy metal accumulation by *Citrobacter* sp. and metal accumulation *in vitro* by liposomes containing entrapped enzyme. *Microbiology* **143**: 2497-2507.

122. Jin, S., Drever, J.I. and Colberg, P.J.S. (2007) Effects of copper on sulphate reduction in bacterial consortia enriched from metal-contaminated and uncontaminated sediments. *Environmental Toxicology and Chemistry*, **26**(2): 225-230.

123. Johnson, K.J., Szymanowski, J.E.S., Borrok, D., Huynh, T.Q. and Fein, J.B. (2007) Proton and metal adsorption onto bacterial consortia: Stability constants for metal–bacterial surface complexes. *Chemical Geology,* **239**(1-2): 13-26.

124. Johnson, L. and King, F. (2008) The effect of the evolution of environmental conditions on the corrosion evolutionary path in a repository for spent fuel and high-level waste in Opalinus Clay. *Journal of Nuclear Materials,* **379**(1-3): 9-15.

125. Jonsson, M., Nielsen, F., Roth, O., Ekeroth, E., Nilsson, S. and Hossain, M.M. (2007) Radiation induced spent nuclear fuel dissolution under deep repository conditions. *Environmental Science and Technology,* **41**(20): 7087-7093.

126. Jukes, T.H. and Cantor, C.R. (1969) Evolution of protein molecules. In Munro, H.N., ed. Mammalian Protein Metabolism, pp. 21-132, Academic Press, New York.

127. Kalyuzhnyi, S., Fedorovich, V., Lens, P., Pol, L.H. and Lettinga, G. (1998) Mathematical modelling as a tool to study population dynamics between sulphate reducing bacteria and methanogenc bacteria. *Biodegradation,* **9**(3-4): 187-199.

128. Kapoor, A. and Viraraghavan, T. (1995) Fungal Biosorption- an alternative treatment option for heavy metal bearing wastewaters: a review. *Bioresource Technology*, **53**: 195–206.

129. King, F. and Stroes-Gascoyne, S. (1995) Microbially Influenced Corrosion of Nuclear Fuel Waste Disposal Containers. In: Proceedings of the 1995 International Conference on Microbially Influenced Corrosion (P. Angel et al., Eds.). NACE International.

130. Kleykamp, H. (1985) The chemical state of the fission products in oxide fuels. *Journal of Nuclear Materials,* **131**(2-3): 221-246.

131. Kosareva, I., Savushkina, M., Kabakchi, S., Korotkevich, S. and Kudryavtsev, V. (2006) Safety assessment of liquid radioactive wastes buried for a long time in deep repositories. *Atomic Energy,* **100**(2): 83-89.

132. Kosseva, M. and Hansford, G.S. (2001) Modelling of competition between sulphate reduction and methane production in continuous bioreactor. *Journal of Environmental Protection and Ecology*, **2**(2): 502-509.

133. Kossman, S.E. and Weiss, M.A. (2000) Acute myelogenous leukemia after exposure to strontium-89 for the treatment of adenocarcinoma of the prostate. *Cancer,* **88**(3), 620-624.

134. Kovacova, S., Lesyn, J. and Sturdik, E. (2002) Recent Trends in Nuclear Waste Disposal. HEJ Manuscript. Slovakia.

135. Kovarova-Kovar, K. and Egli, T. (1998) Growth kinetics of suspended microbial cells: from single-substrate-controlled growth to mixed-substrate kinetics. *Microbiology and Molecular Biology Reviews,* **62**(3): 646–666.

136. Kratochvil, D. and Volesky, B. (1998) Advances in the biosorption of heavy metals. *Trends in Biotechnology,* **16**(7): 291-300.

137. Krumholz, L.R., Elias, D.A. and Suflita, J.M. (2003) Immobilization of Co by sulphate reducing bacteria in subsurface sediments. *Geomicrobiology Journal,* **20**: 61-72.

138. Kumar, R., Singh, S. and Singh, O.V. (2007) Bioremediation of radionuclides: emerging technologies. *Omics : A Journal of Integrative Biology,* **11**(3): 295-304.

139. Kuyucak, N. and Volesky, B. (1988) Biosorbents for recovery of metals from industrial solutions. *Biotechnology Letters*, **10**(2): 137-142.

140. Lagergren, S., (1898) About the theory of so-called adsorption of soluble substances. *Kungliga Svenka Vetenskapsakademiens, Handlingar*, **24** (4): 1–39.

141. Lagus, T.P. (2005) Reprocessing of spent nuclear fuel: a policy analysis. *Journal of Engineering and Public Policy,* **9**: 1-20.

142. Langmuir, I. (1918) The adsorption of gases on plane surfaces of glass, mica and platinum. *Journal of American Chemical Society*, 1361–1403.

143. Lazaridis, N.K. and D. D. Asouhidou, D.D. (2003) Kinetics of sorptive removal of chromium(VI) from aqueous solutions by calcined Mg–Al–CO3 hydrotalcite. *Water Research*, **37**(12): 2875-2882.

144. Ledin, M., Pederson, K. and Allard, B. (1997) Effects of pH and ionic strength on the adsorption of Cs, Sr, Eu, Zn, Cd and Hg by Pseudomonas putida. *Water Air Soil Pollution*, **93**: 367–381.

145. Lior, N. (2008) Energy resources and use: The present situation and possible paths to the future. *Energy,* **33**(6): 842-857.

146. Liu, H.L., Chen, B.Y., Lan, Y.W. and Cheng, Y.C. (2004) Biosorption of Zn(II) and Cu(II) by the indigenous *Thiobacillus thiooxidans*. *Chemical Engineering Journal*, **97**: 195–201.

147. Little, B., Wagner, P. and Mansfeld, F. (1991) Microbiologically influenced corrosion of metals and alloys. *International Materials Review,* **36**: 253-272.

148. Lloyd, J.R., Yong, P., Macaskie, L.E. (1998) Enzymatic recovery of elemental palladium by using sulfate-reducing bacteria. *Applied and Environmental Microbiology*, **64**: 4607–4609.

149. Lloyd, J.R., Ridley, J., Khizniak, T., Lyalikova, N.N. and Macaskie, L.E. (1999) Reduction of technetium by *Desulfovibrio desulfuricans:* biocatalyst characterization and use in a flowthrough bioreactor. *Applied Envirnmental Microbiology,* **65**: 2691-2696.

150. Lloyd, J.R. and Macaskie, L.E. (2000) Bioremediation of Radionuclide-Containing Waste

Waters. in: D.R. Lovley (Ed.), Environmental Microbe-Metal Interactions, American Society for Microbiology Press, Washington, DC, pg 277.

151. Lloyd, J.R. and Lovley, D.R. (2001) Microbial detoxification of metals and radionuclides. *Current Opinion in Biotechnology,* **12**(3): 248-253.

152. Lloyd, J.R., Mabbett, A., Williams, D.R., Macaskie, L.E. (2001) Metal reduction by sulfate-reducing bacteria: physiological diversity and metal specificity. *Hydrometallurgy*, **59**: 327–337.

153. Lloyd, J.R., Chesnes, J., Glasauer, S., Bunker, D.J., Livens, F.R. and Lovley, D.R. (2002) Reduction of actinides and fission products by Fe(III)-Reducing bacteria. *Geomicrobiology Journal,* **19**(1): 103-120.

154. Lloyd, J.R. (2003) Microbial reduction of metals and radionuclide. *FEMS Microbiology Reviews*, **27**(2-3): 411–425.

155. Lloyd, J.R., Lovley, D.R. and Macaskie, L.E. (2003) Biotechnological application of metal-reducing bacteria. *Advances in Applied Microbiology,* **53**: 85–128.

156. Lloyd, J.R. and Renshaw, J.C. (2005) Bioremediation of radioactive waste: radionuclide–microbe interactions in laboratory and field-scale studies. *Current Opinion in Biotechnology,* **16**(3): 254-260.

157. Long, J.C.S. and Ewing, R.C. (2004) Yucca Mountain: Earth Science Issues at a Geologic Repository for High-Level Nuclear Waste. *Annual Review of Earth and Planetary Science,* **32**: 363-401.

158. Lovley, D.R. and Phillips, E.J. (1992) Reduction of uranium by *Desulfovibrio desulfuricans. Applied and Environmental Microbiology,* **58**: 850-856.

159. Lu, W.-B., Shi, J.-J., Wang, C.-H. and Chang, J.-S. (2006) Biosorption of lead, copper and cadmium by an indigenous isolate *Enterobacter* sp. J1 possessing high heavy-metal resistance, *Journal of Hazardous Materials,* **134**: 80–86.

160. Lujaniene, G., Sapolaite, J., Amulevicius, A., Mazeika, K. and Motiejunas, S. (2006) Retention of cesium, plutonium and americium by engineered and natural barriers. *Czechoslovak Journal of Physics,* **56**(1): D103-D110.

161. Macaskie, L.E. and Dean, A.C.R. (1982) Cadmium accumulaton by microorganisms. *Environmental Technology Letters*, **3**: 49-56.

162. Macaskie, L.E., Watesm, J.M. and Dean, A.C.R. (1987) Cadmium accumulation by a *Citrobacter sp*. immobilized on gel and solid supports: applicability to the treatment of liquid wastes containing heavy metal cations. *Biotechnology and Bioengineering*, **30**: 66–73.

163. Macaskie, L.E., Empson, R.M., Cheetham, A.K., Grey, C.P. and Skarnulis, A.J. (1992) Uranium accumulation by a *Citrobacter* sp. As a result of enzyme mediated growth of polysrystalline HUO2PO4. *Science*, **257**: 782-784.

164. Macaskie, L.E., Bonthrone, K.M., Yong, P. and Goddard, D.T. (2000) Enzymatically mediated bioprecipitation of uranium by a *Citrobacter* sp.: a concerted role exocellular lipopolysaccharide and associated phosphatase in biomineral formation. *Microbiology,* **146**: 1855-1867.

165. Marinsky, J.A. and Ephraim, J. (1986) A unified physicochemical description of the protonation and metal ion complexation equilibria of natural organic acids (humic and fulvic acids). 1. Analysis of the influence of polyelectrolyte properties on protonation equilibria in ionic media: fundamental concepts. *Environmental Science and Technology*, **20**(4): 349–354.

166. Martinez, R.E., Smith, D.S., Kulczycki, E. and Ferris, F.G. (2002) Determination of intrinsic bacterial surface acidity constants using a donnan shell model and a continuous pKa distribution method. *Journal of Colloid and Interface Science*, **253**: 130–139.

167. Mattuschka, B. and Straube, G. (1993) Biosorption of metals by a waste biomass. *Journal of Chemical Technology and Biotechnology*, **58**: 57-63.

168. Mazidji CN, Koopman B, Bitton G, Neita D. (1992) Distinction between heavy metal and organic toxicity using EDTA chelation and microbial assays. *Environmental Toxicology and Water Quality: An International Journal*, **7**: 339–353.

169. McKay, G. and Ho, Y.-S., Biosorption of copper from waste waters: a review. S*eparations and Purification Methods*, 1999, **28**: 87–125.

170. Means, J.L., Crerar, D.A. and Duguid, J.O. (1978) Migration of radioactive wastes: radionuclide mobilization by complexing agents. *Science,* **200**(4349): 1477–1481.

171. Monod, J. (1949) The growth of bacterial cultures. *Annual Reviews of Microbiology,* **3**: 371 394.

172. Morrison, S.J., Metzler, D.R. and Dwyer, B.P. (2002) Removal of As, Mn, Mo, Se, U, V and Zn from groundwater by zero-valent iron in a passive treatment cell: reaction progress modeling. *Journal of Contaminant Hydrology,* **56**(1-2): 99-116.

173. Motamedi, M. and Pedersen, K. (1998) *Desulfovibrio aespoensis* sp., a mesophilic sulfate reducing bacterium from deep groundwater at aspo hard rock laboratory, Sweden. *International Systemic Bacteriology,* **48**: 311-315.

174. Mourogov, V., Fukuda, K. and Kagramanian, V. (2002) The need for innovative nuclear reactor and fuel cycle systems: Strategy for development and future prospects. *Progress in Nuclear Energy,* **40**(3-4): 285-299.

175. Mullen, M.D., Wolf, D.C., Ferris, F.G., Beveridge, T.J., Flemming, C.A. and Bailey, G.W. (1989) Bacterial sorption of heavy metals. *Applied and Environmental Microbiology,* **55**(12): 3143-3149.

176. Mulligan, C.N., Yong, R.N. and Gibbs, B.F. (2001) An evaluation of technologies for the heavy metal remediation of dredged sediments. *Journal of Hazardous Materials*, **85**(1-2): 145-163.

177. Musango, J.K., Brent, A.C. and Bassi, A.(2009) South African Energy Model: a systems dynamics approach. Conference Proceedings of the 27th International Conference of the System Dynamics Society, July 26-30, 2009, New Mexico, USA.

178. Nada, T., Baba, H., Kawamura, K., Ohkura, T., Torii, K. and Ohta, M. 2004. A small outbreak of third generation cephem resistant *Citrobacter freundii* : infection on a surgical ward. *Japanese Journal of Infection,* **57**: 181-182.

179. National Research Council (1996) Nuclear Wastes: technologies for separation and transmutation. Washington DC: National Academy Press.

180. Neculita, C.M., Zagury, G.J. and Bussiere, B. (2007) Passive treatment of acid mine drainage in bioreactors using sulfate-reducing bacteria: critical review and research needs. *Journal of Environmental Quality,* **36**(1): 1-16.

181. Neria-Gonzalez, I., Wang, E. T., Ramirez, F., Romero, J.M. and Hernandez-Rodriquez, C. (2006) Characterization of bacterial community associated to biofilms of corroded oil pipelines from the southeast of Mexico. *Anaerobe,* **32**: 213-228.

182. Ngwenya, B.T., Sutherland, I. and Kennedy, L. (2003) Comparison of the acid-base behaviour and metal adsorption characteristics of a gram-negative bacterium with other strains. *Applied Geochemistry,* **18**: 527-538.

183. Ngwenya, N. and Whiteley, C.G. (2006) Recovery of rhodium (III) from solutions and industrial wastewaters by a sulphate-reducing bacteria consortium. *Biotechnology Progress*, **22**(6): 1604-1611.

184. Ngwenya, B.T., Mosselmansb, J.F.W., Magennisa, M., Atkinsonb, K.D., Tourneya, J., Olivec, V. and Ellamc, R.M. (2009) Macroscopic and spectroscopic analysis of lanthanide adsorption to bacterial cells. *Geochimica et Cosmochimica Acta*, **73**(11), 3134-3147.

185. Ngwenya, N. And Chirwa, E.M.N. (2010) Single and binary component sorption of the fission products Sr^{2+}, Cs^{+} and Co^{2+} from aqueous solutions onto sulphate reducing bacteria. *Minerals Engineering*, **23**(6): 463-470.

186. Noshchenko, A.G., Moysich, K.B., Bondar, A., Zamostyan, P.V., Drosdova, V.D. and Michalek, A.M. (2001) Patterns of acute leukaemia occurrence among children in the Chernobyl region. *International Journal of Epidemiology JID - 7802871.*

187. North, D.W. (1998) Nuclear waste management: shifting the paradigm. *Reliability Engineering and System Safety,* **59**: 123-128.

188. North, D.W. (1999) A perspective on nuclear waste. *Risk Analysis*, **19**(4): 751-758.

189. Nyamagara, J. (1998) Use of sequential Extraction To Evaluate Zinc And Copper in a Soil Amended With Sewage Sludge and Inorganic Metal Salts, *Agriculture Ecosystems and Environment,* **69**(2): 135-141.

190. Odom, J.M. and Singleton, R. (1992) The sulphate-reducing bacteria: Contemporary perspectives. New York: Springer-Verlag.

191. Ojeda, J.J., Romero-Gonzalez, M.E., Bachmann, R.T., Edyvean, R.G.J. and Banwart, S.A. (2008) Characterization of the cell surface and cell wall chemistry of drinking water bacteria by combining XPS, FTIR spectroscopy, modelling, and potentiometric titrations. *Langmuir,* **24**: 4032-4040.

192. Ortiz-Bernad, I., Anderson, R.T., Vrionis, H.A. and Lovley, D.R. (2004) Resistance of solid-phase U(VI) to microbial reduction during in situ bioremediation of uranium-contaminated groundwater. *Applied and Environmental Microbiology,* **70**(12): 7558-7560.

193. Ohshima, H. and Kondo, T. (1990) Relationship among the surface potential, Donnan potential, surface free energy and charge density of ion-penetrable membranes. *Biophysical Chemistry*, **38**: 117–122.

194. Özdemir, S., Kilinc, E., Poli, A., Nicolaus, B., and Güven, K. (2009) Biosorption of Cd, Cu, Ni, n and Zn from aqueous solutions by thermophilic bacteria, *Geobacillus toebii sub.sp. decanicus* and *Geobacillus thermoleovorans sub.sp. stromboliensis*: Equilibrium, kinetic and thermodynamic studies. *Chemical Engineering Journal*, **152**: 195-206.

195. Pagnanelli, F. Esposito, A. and Veglio, F. (2002) Multi-metallic modeling for biosorption of binary systems. *Water Research*, **36**: 4095–4105.

196. Pagnanelli, F., Bornoroni, L., Moscardini, E. and Toro, L. (2006) Non-electrostatic surface complexation models for protons and lead(II) sorption onto single minerals and their mixture. *Chemosphere,* **63**(7): 1063-1073.

197. Pagnanelli, F., Cruz Viggi, C. and Toro, L. (2010) Isolation and quantification of cadmium removal mechanisms in batch reactors inoculated by sulphate reducing

bacteria: Biosorption versus bioprecipitation. *Bioresource Technology,* **101**(9): 2981-2987.

198. Pan, X., Meng, X., Zhang, D. and wang, J. (2009) Biosorption of strontium by immobilised *Aspergillus niger*. *International Journal of Environment and Pollution*, **37**(2-3): 276-288.

199. Pardo, R., Herguedas, M., Barrado, E. and Vega, M. (2003) Biosorption of cadmium, copper, lead and zinc by inactive biomass of *Pseudomonas putida*. *Annals of Bioanalytical Chemistry*, **376**: 26–32.

200. Parmar, N., Warren, L.A., Roden, E.E. and Ferris, F.G. (2000) Solid phase capture of strontium by the iron reducing bacteria *Shewanella alga* strain BrY. *Chemical Geology,* **169**(3-4): 281-288.

201. Paterson-Beedle, M., Macaskie, L.E., Lee, C.H., Hriljac, J.A., Jee, K.Y. and Kim, W.H. (2006) Utilisation of a hydrogen uranyl phosphate-based ion exchanger supported on a biofilm for the removal of cobalt, strontium and caesium from aqueous solutions. *Hydrometallurgy,* **83**(1-4): 141-145.

202. Pederson, K, Motamedi, M., Karnland, O. and Sanden, T. (2000) Cultivability of microorganisms introduced into a compacted bentonite clay buffer under high-level radioactive waste repository conditions. *Engineering Geology,* **58**(2): 149-161.

203. Phillips, E.J.P., Landa, E.R. and Lovley, D.R. (1995) Remediation of uranium contaminated soils with bicarbonate extraction and microbial U(VI) reduction. *Journal of Industrial Microbiology*, **14**: 203-207.

204. Philip, L. and Venkobachr, C. (2001) An insight into mechanism of biosorption of Cu by *B. polymyxa*. *Indian Journal of Environmental Pollution*, **15**: 448-460.

205. Plette, A.C.C., Benedetti, M.F. and Van Reimsdijk, W.H. (1996) Competitive binding of protons, calcium, cadmium, and zinc to isolated cell walls of a gram-positive soil bacterium. *Environmental Science and Technology,* **30**: 1902–1910.

206. Postgate, J.R. (1984) The sulphate reducing bacteria. Cambridge University Press, Cambridge-New York, USA.

207. Puranik, P.R., Chabukswar, N.S. and Paknikar, K.M. (1995) Cadmium biosorption by *Streptomyces pimprina* waste biomass. *Applied Microbiology and Biotechnology*, **43**: 1118–1121.

208. Puranik, P.R. and Paknikar, K.M. (1997) Biosorption of lead and zinc from solutions using *Streptoverticillium cinnamoneum* waste biomass. *Journal of Biotechnology*, **55**: 113–124.

209. Puranik, P.R. and Paknikar, K.M. (1999) Influence of co-cations on biosorption of lead and zinc: a comparative evaluation in binary and multimetal systems. *Bioresource Technology*, **70**: 269–276.

210. Qui, R., Zhao, B., Liu, J., Huang, X., Li, Q., Brewer, E., Wang, S. and Shi, N. (2010) Sulfate reduction and copper precipitation by a *Citrobacter* sp. isolated from a mining area. *Journal of Hazardous Materials*, **164**(2-3): 1310-1315.

211. Quintelas C., Rocha Z., Silva B., Fonseca B., Figueiredo H. and Tavares T. (2009) Removal of Cd(II), Cr(VI), Fe(III) and Ni(II) from aqueous solutions by an *E. coli* biofilm supported on kaolin, *Chemical Engineering Journal*, **149**: 319-324.

212. Radke, C.J. and Prausnitz, J.M. (1972) Thermodynamics of multi-solute adsorption from dilute liquid solutions, AIChE *Journal*, **18**: 761–768.

213. Raj, K., Prasad, K.K. and Bansal, N.K. (2006) Radioactive waste practices in India. *Nuclear Engineering and Design,* **236**(7-8): 914-930. India's Reactors: Past, Present, Future.

214. Rashamuse, J.R. (2003) The bioaccumulation of platinum(IV) from aqueous solution using sulphate reducing bacteria: role of a hydrogenase enzyme. MSc Thesis. Rhodes University, South Africa.

215. Reichert, P. (1998) AQUASIM 2.0 – Tutorial, Computer Program for the Identification and Simulation of Aquatic Systems. Dübendorf, Switzerland: EAWAG.

216. Redlich, O. and Peterson, D.L. (1959) A useful adsorption isotherm. *Journal of Physical Chemistry*, **63**: 1024.

217. Ristow, N.E. and Hansford, G.S. (2001) Modelling of a falling sludge bed reactor using AQUASIM. *Water SA*, **27**(4): 445-454.

218. Robinson, J.A. and Tiedje, J.M. (1983) Nonlinear estimation of monod growth kinetic parameters from a single substrate depletion curve. *Applied and Environmental Microbiology,* **45**:1453–1458.

219. Romanovskaia, V.A., Rokikto, P.V., Mikheev, A.N., Gushcha, N.I., Malashenko, I.R. and Chernaia, N.A. (2002) The effect of gamma radiation and desiccation on the viability of the soil bacteria isolated from the alienated zone around the Chernobyl Nuclear Power Plant. *Mikrobiologia,* **71**: 705–712.

220. Ryan, P.R., Monchy, S., Cardinale, M., Taghavi, S., Crossman, L., Avison, M.B., Berg, G., van der Lelie, D. and Dow, J.M. (2009) The versatility and adaptation of bacteria from the genus *Stenotrophomonas. Nature,* **7**: 514-525.

221. Sag, Y. and, Kutsal, T. (1995) Biosorption of heavy metals by Zoogloea ramigera: use of adsorption isotherms and a comparison of biosorption characteristics. *The Chemical Engineering Journal and the Biochemical Engineering Journal*, **60**(1-3): 181-188.

222. Sahrani, F.K., Ibrahim, Z., Yahya, A. and Aziz, M. (2008) Isolation and identification of marine sulphate-reducing bacteria, *Desulfovibrio* sp. And *Citrobacter freundii* from Pasir Gudang, Malaysia. *Sains Malaysiana,* **37**(4): 365–371.

223. Sarkar, M., Acharya, P.K. and Battacharya, B. (2003) Modeling the adsorption kinetics of some priority organic pollutants in water from diffusion and activation energy parameters. *Journal of Colloids and Interface Science*, **266**(1): 28–32.

224. Sarro, M.I., Garcia, A.M. and Moreno, D.A. (2005) Biofilm formation in spent nuclear fuel pools and bioremediation of radioactive water. *International Microbiology: the official journal of the Spanish Society for Microbiology,* **8**(3): 223-230.

225. Scott, J.A. and Palmer, S.J. (1990) Sites of cadmium uptake in bacteria used for biosorption. *Applied Microbiology and Biotechnology*, **33**: 221-225.

226. Selatnia, A., Bakhti, M.Z., Madani, A., Kertous, L. and Mansouri, Y. (2004) Biosorption of Cd^{2+} from aqueous solution by a NAOH-treated bacterial dead *Streptomyces rimosus* biomass. *Hydrometallurgy*, **75**: 11–24.

227. Senn, H., Lendenmann, U., Snozzi, M., Hamer, G. and Egli, T. (1994) The growth of *Escherichia coli* in glucose-limited chemostat cultures: a re-examination of the kinetics. *Biochimica et Biophysica Acta (BBA) - General Subjects*, **1201**: 424-436.

228. Sharma, J. and Fulekar, M.H. (2009) Potential of *Citrobacter freundii* for bioaccumulation of heavy metal – copper. *Biology and Medicine,* **1**(3): 7-14.

229. Shaukat, M.S., Sarwar, M.I. and Qadeer, R. (2005) Adsorption of strontium ions from aqueous solution on Pakistani coal. *Journal of Radioanalytical and Nuclear Chemistry,* **265**(1): 73-79.

230. Shimeld, L.A. and Rodgers, A.T. (1999) Essentials of Diagnostic Microbiology. Cengage Learning, pp 405-406.

231. Shoesmith, D.W. (2000) Fuel corrosion processes under waste disposal conditions. *Journal of Nuclear Materials,* **282**(1): 1-31.

232. Simonoff, M., Sergeant, C., Poulain, S. and Pravikoff, M.S. (2007) Microorganisms and migration of radionuclides in environment. *Comptes Rendus Chimie,* **10**(10-11): 1092-1107.

233. Sips, R. (1948) On the structure of a catalyst surface. *Journal of Chemistry and Physics*, **16**: 490–495.

234. Skeen, R.S., Luttrell, S.P., Brouns, T.M., Hooker, B.S. and Petersen, J.N. (1993) In-situ bioremediation of hanford groundwater. *Remediation Journal,* **3**(3): 353-367.

235. Small, T.D., Warren, L.A., Roden, E.E. and Ferris, F.G. (1999) Sorption of Strontium by Bacteria, Fe(III) Oxide, and Bacteriaâˆ'Fe(III) Oxide Composites. *Environmental Science and Technology,* **33**(24): 4465-4470.

236. Smellie, J.A.T. and Karlsson, F. (1999) The use of natural analogues to assess radionuclide transport. *Engineering Geology,* **52**(3-4): 193-220.

237. Smičiklas, I., Dimović, S., Plećaš, I. and Mitrić, M. (2006) Removal of Co^{2+} from aqueous solutions by hydroxyapatite. *Water Research,* **40**(12): 2267-2274.

238. Smith, W.L. and Gadd, G.M. (2000) Reduction and precipitation of chromate by mixed culture sulphate reducing bacterial biofilms. *Journal of Applied Microbiology,* **88**: 983–991.

239. Solecki, J. (2006) Investigation of 85Sr adsorption in the presence of Na^+, K^+ and Cs^+ on selected soils from different horizons. *Journal of Radioanalytical and Nuclear Chemistry,* **268**(2): 357-364.

240. Srinath, T., Garg, S.K. and Ramteke, P.W. (2003) Biosorption and ellusion of Cr from immobilized *Bacillus coagulens* biomass. *Indian Journal of Experimental Biology*, **41**: 986-990.

241. Stumm, W. and Morgan, J.J. (1996) Aquatic Chemistry, Chemical Equilibria and Rates in Natural Waters, 3rd ed. John Wiley and Sons, nc., New York.

242. Suhasini, I.P., Sriram, G., Abolekar, S.R. and Sureshkumar, G.K. (1999) Biosorptive removal and recovery of cobalt from aqueous systems. *Process Biochemistry*, **34**: 239–247.

243. Suzuki, Y., Kelly, S.D., Kemner, K.M. and Banfield, J.F. (2003) Microbial populations stimulated for hexavalent uranium reduction in uranium mine sediment. *Applied and Environmental Microbiology,* **69**(3): 1337-1346.

244. Tajer, M.G.P., Ghorbanzadeh, M.S. and Ghafourian, H. (2007) Bio sorption of strontium from aqueous solution by New Strain Bacillus sp. GTG-83. Proceedings WM'07: Waste Management Symposium, Tucson, AZ (United States), 25 Feb - 1 Mar 2007.

245. Tebo, B.M., Obraztsova, A.Y. (1998) Sulfate-reducing bacterium grows with Cr(VI), U(VI), Mn(IV), and Fe(III) as electron acceptors. *FEMS Microbiology Letters*, **162**: 193–198.

246. Tessier, A., Campbell, P.G.C. and Bisson, M. (1979) Sequential Extraction Procedure for the Speciation of Particulate Trace Metals", *Analytical Chemistry,* **51**(7): 844-851.

247. Thomas, R.A., Beswick, A.J., Basnakova, G., Moller, R. and Macaskie, L.E. (2000) Growth of naturally occurring microbial isolates in metal-citrate medium and bioremediation of metal-citrate wastes. *Journal of Chemical Technology and Biotechnology,* **75**(3): 187-195.

248. Tourney, J., Ngwenya, B.T., Mosselmans, J.W.F., Tetley, L. and Cowie, G. L. (2008) The effect of extracellular polymers (EPS) on the proton adsorption characteristics of the thermophile *Bacillus licheniformis* S-86. *Chemical Geology*, **247**: 1-15.

249. Tsezos, M. and Volesky, B. (1982) The mechanism of thorium biosorption by *Rhizopus arrhizus. Biotechnology and Bioengineering,* **24**(1): 955–969.

250. Tucker, M.D., Barton, L.L. and Thompson, B.M. (1998) Removal of U and Mo from water by immobilized *Desulfovibrio desulfuricans* in column reactors. *Biotechnology and Bioengineering,* **60**: 90-96.

251. Turner, J.S. and Robinson, N.J. (1995) Cyanobacterial metallothioneins: Biochemistry and molecular genetics. *Journal of Industrial Microbiology and Biotechnology,* **14**(2): 119-125.

252. Urrutia, M.M. (1997) General Bacterial Sorption Processes. In: J. Wase and C. Forster, Editors, Biosorbents for metal ions, CRC Press, London, UK, pp. 39–66.

253. van der Wal, A., Minor, M., Norde, W., Zehnder, A.J.B. and Lyklema, J. (1997) Electrokinetic potential of bacterial cells. *Langmuir*, **13**: 165–171.

254. van Hullebusch, E. D., Zandvoort, M. H. and Lens, P. N. (2004) Nickel and cobalt sorption on anaerobic granular sludges: kinetic and equilibrium studies. *Journal of Chemical Technology and Biotechnology*, **79**(11): 1219–1227.

255. Valls, M. and de Lorenzo, V. (2002) Exploiting the genetic and biochemical capacities of bacteria for the remediation of heavy metal pollution. *FEMS Microbiology Reviews,* **26**(4): 327–338.

256. Vasquez, T.G.P., Botero, A.E.C., de Mesquita, L.M.S. and Torem, M.L. (2007) Biosorptive removal of Cd and Zn from liquid streams with a *Rhodococcus opacus* strain. *Minerals Engineering* **20:** 939–944.

257. Veglio, F. and Beolchini, F. (1997) Removal of metals by biosorption: a review. *Hydrometallurgy*, **44**(3): 301-316.

258. Veglio, F., Esposito, A. and Reverberi, A.P. (2003) Standardisation of heavy metal biosorption tests: equilibrium and modeling study. *Process Biochemistry*, **38**: 953–961.

259. Vijayaraghavan, K and Yun, Y.-S. (2008) Bacterial biosorbents and biosorption. *Biotechnology Advances,* **26**: 266–291.

260. Volesky, B. (1990) Removal and recovery of heavy metals by biosorption. In: B. Volesky, Editor, Biosorption of heavy metals, CRC press, Florida, pp. 8–43.

261. Volesky, B. and Holan, Z.R. (1995) Biosorption of heavy metals. *Biotechnology Progress*, **11**(3): 235-250.

262. Volesky, B. (2003) Biosorption process simulation tools. *Hydrometallurgy*, **71**: 179–190.

263. Volesky, B (2007) Biosorption and me. *Water Research*, **41**: 4017–4029.

264. Vullo, D.L., Cerettia, H.M., Daniela, M.A., Ramíreza, S.A.M. and Zaltsa, A. (2008) Cadmium, zinc and copper biosorption mediated by *Pseudomonas veronii* 2E. *Bioresource Technology*, 99(13): 5574-5581.

265. Wang, J. and Chen, C. (2006) Biosorption of heavy metal by *Saccharomyces cerevisiae*: a review. *Biotechnolgy Advances*, **24**: 427–451.

266. Wang, J. and Chen, C. (2009) Biosorbents for heavy metals removal and their future. *Biotechnology Advances*, **27**(2): 195-226.

267. Wasserman, E. and Felmy, A.R. (1998) Computation of the electrical double layer properties of semi-permeable membranes in multi-component electrolytes. *Applied and Environmental Microbiology*, **64**: 2295–2300.

268. Watson, J.S., Scott, C.D. and Faison, B.D. (1989) Adsorption of Sr by Immobilized Microorganisms. *Applied Biochemical Biotechnology,* **20/21**: 699-709.

269. Weber, W.J. and Morris, J.C. (1963) Kinetics of adsorption on carbon solution. *Journal of Sanitary Engineering*, **89**: 31–59.

270. Weijma, J., Pol, L.W.H., Stams, A.J.M. and Lettinga, G. (2000) Performance of a thermophilic sulphate and sulphite reducing high rate anaerobic reactor fed with methanol. *Biodegradation,* **11**: 429-439.

271. Weon, B. Cindy, H., Wu, J.K., Ashok, M. and Wilfred, C. (2003) Enhanced Hg Biosorption by bacterial cells with surface-displayed MerR. *Applied Environmental Microbiology*, **69**: 3176-3180.

272. Westall, J. C. (1982) FITEQL, a computer program for determination of chemical equilibrium constants from experimental data. Department of Chemistry, University of Oregon Report 82-02.

273. West, J.M. and McKinley, I.G. (2001) Progress in the Geomicrobiology of Radioactive Waste Disposal. Materials Research Society Symposium Proceedings, Volume 663. Materials Research Society.

274. White, C. and Gadd, G.M. (1996) Mixed sulphate reducing bacterial cultures for bioprecipitation of toxic metals: a factorial and response-surface analysis of the effects of dilution rate, sulphate and substrate concentration. *Microbiology,* **142**: 2197-2205.

275. White, C., Sayer, J.A. and Gadd, G.M. (1997) Microbial Solubilization and Immobilization of Toxic Metals: key biological processes for treatment of contamination. *FEMS Microbiology Reviews,* **20**: 503-516.

276. Wightman, P.J., Fein, J.B., Wesolowski, D.J., Phelps, T.J., Benezeth, P. and Palmer, D.A. (2001) Measurement of bacterial surface protonation constants for two species at elevated temperatures. *Geochimica et Cosmochimica Acta*, **65**: 3657–3669.

277. Xie, X.Q., Li, X.M., Yang, Q., Liao, D.X. and Zeng, G.M. (2008) Biosorption of lead and copper ions by *Penicillium simplicissimum* immobilized on a loofa sponge immobilized biomass (in Chinese), *Acta Science Circumstance*, **28**: 95–100.

278. Yee, N. and Fein, J.B. (2001) Cd adsorption onto bacterial surfaces: A universal adsorption edge? *Geochimica et Cosmochimica Acta,* **65**(13): 2037-2042.

279. Yee, N., Benning, L. G., Phoenix, V. R. and Ferris, F. G. (2004) Characterization of metal-cyanobacteria sorption reactions: A combined macroscopic and infrared spectroscopic investigation. *Environmental Science and Technology,* **38:** 775-782.

280. Yilmaz, M., Tay, T., Kivanc, M. and Turk, H. (2010) Removal of copper(II) ions from aqueous solution by a lactic acid bacterium. *Brazilian Journal of Chemical Engineering*, **27**(2): 309-314.

281. Yong, P. and Macaskie, L.E. (1997) Removal of lanthanum, uranium and thorium from the citrate complexes by immobilized cells of *Citrobacter* sp. In a ßow-through reactor: implications for the decontamination of solutions containing plutonium. *Biotechnology Letters,* **19**(3): 251–255.

282. Younger, P.L., Banwart, S.A., Hedin, R.S. (2002) Minewater: Hydrology Pollution and Remediation, 1st Edition. Kluwer Academic Publishers, Dordrecht.

283. Ziagova, M., Dimitriadis, G., Aslanidou, D., Papaioannou, X., Tzannetaki, E.L. and Liakopoulou-Kyriakides, M. (2007) Comparative study of Cd(II) and Cr(VI) biosorption on *Staphylococcus xylosus* and *Pseudomonas sp*. in single and binary mixtures. *Bioresource Technology*, **98**: 2859–2865.

284. Zouboulis, A.I., Loukidou, M.X. and Matis, K.A. (2004) Biosorption of toxic metals from aqueous solutions by bacteria strains isolated from metal polluted soils. *Process Biochemistry*, **39**: 909–916.

APPENDICES

1. TOC ANALYSIS

Table 1 Instrument specifications and operating conditions for TOC analysis.

Function	Specification
Measurement principle	Wet chemical oxidation with NDIR
Measuring range	0-3500 mg/L
Detection limits	0.5 µg/L
Sample injection volume	2500 µL
Pre-treatment for IC	Automatic acid addition and sparging
Carrier gas	UHP nitrogen gas
Carrier gas flow rate	200 mL/min

2. SRB CHARACTERIZATION

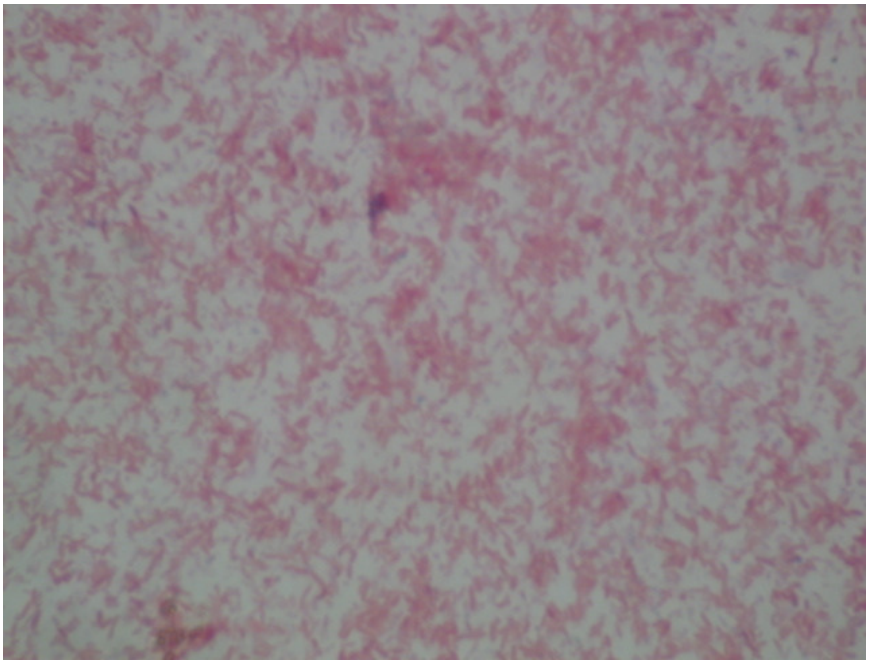

Figure 1: Gram staining image of a sulphate reducing bacteria consortium (magnification = X100).

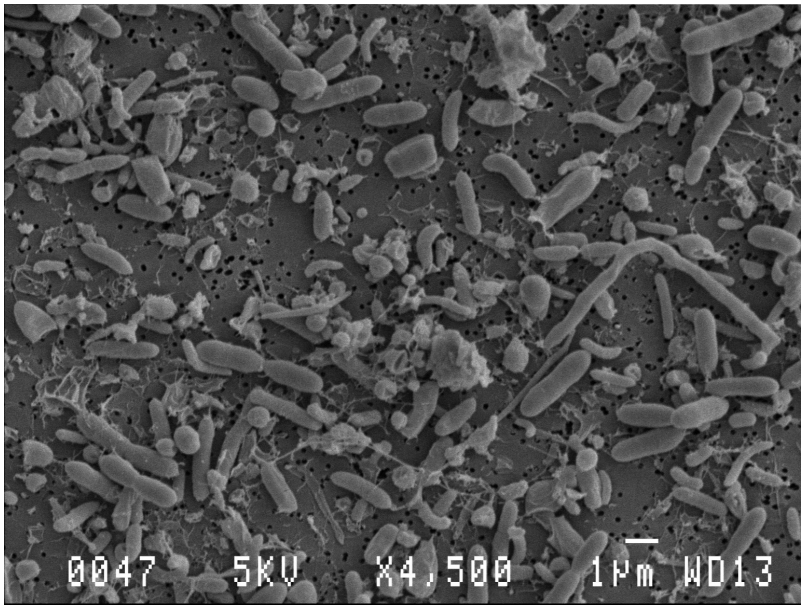

Figure 2: Scanning electron microscope image of sulphate reducing bacteria.

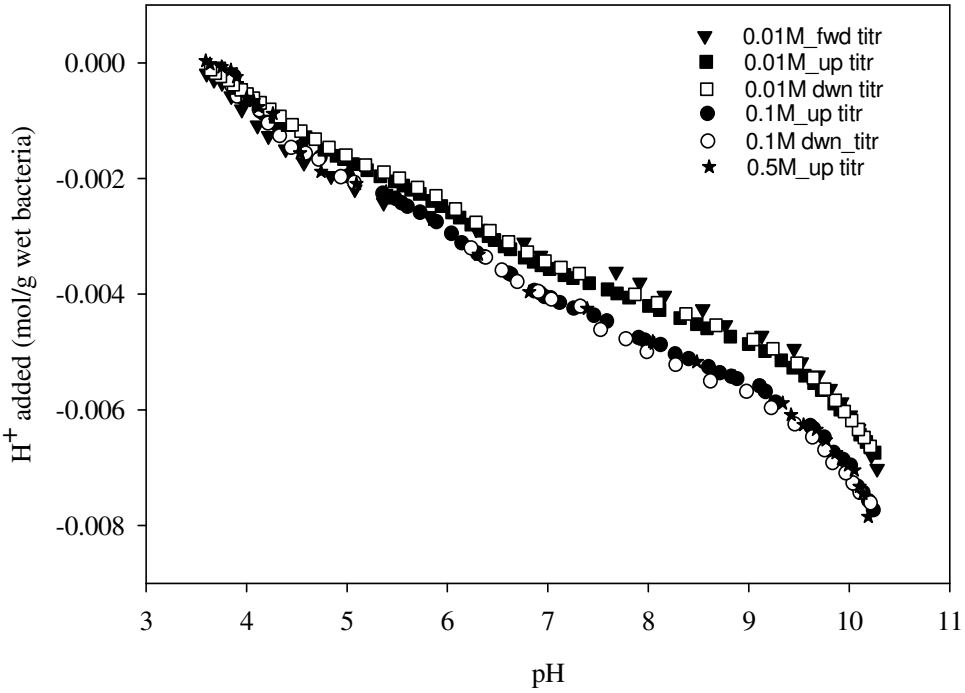

Figure 3: Experimental potentiometric titration data of variable masses of a viable SRB consortium in 0.01M, 0.1M and 0.5M $NaNO_3$ and 25°C.

Table 2 Absorption bands of SRB and functional groups assignment

Wavenumber (cm^{-1})	*Functional group/assignment*
~3414	Broad stretches of hydroxy group, H-bonded OH
~2925	Stretching vibrations of CH3 and CH2 due to fatty acid components of membranes
~1657	Primary amine, NH bend
~1545	Secondary amine, NH bend
~1453	Bending vibrations of CH, CH2 and CH3 due to a carboxylate (carboxylic acid salt)
~1400	Stretching vibrations of hetero-oxy compounds due to organic sulfates
~1240	Stretching vibrations of aromatic phosphates in polysaccharides and nucleic acids
~1081	stretching vibrations of phosphodiester, phosphorylated proteins, or polyphosphate products

3. AQUASIM SIMULATIONS

a. Description of parameters and input values

Table 2 Definition of variables used for SRB bioreactor processes model calibration.

Variable	*Variable Type*	*Description*	*Units*	*Initial value*	*Range*	*Std dev*	*Optimised value*
μ_{max}	Constant	Maximum specific growth rate coefficient	1/hr	0.4	0-20	1	0.985
$Y_{x/s}$	Constant	Bacterial yield coefficient	mg/mg	0.074	0-10	1	0.0735
K_s	Constant	Half velocity concentration	mg/L	150	0-1000	1	187
C	State	Metal concentration at time t	mg/L	N/A	N/A	1	N/A
C_{ini}	Constant	Initial concentration of metal	mg/L	75	0-100	1	0.976
C_{meas}	Real list	Experimental metal concentration	mg/L	N/A	N/A	1	N/A
S	State	Concentration of sulphate at time t	mg/L	N/A	N/A	1	N/A
S_0	Constant	Initial concentration of sulphate	mg/L	3000	2000-4000	1	3021
S_{meas}	Real list	Experimental sulphate concentration	mg/L	N/A	N/A	1	N/A
X	State	Concentration of bacteria at time t	mg/L	N/A	N/A	1	N/A
X_0	Constant	Initial concentration of biomass	mg/L	48	45-55	1	48.6
X_{meas}	Real list	Experimental bacterial concentration	mg/L	N/A	N/A	1	N/A
K_i	Constant	Inhibition coefficient	mg/L	0.1	0-10	1	0.616
k_C	Constant	Pseudo second-order rate coefficient	L/mg/h	0.0001	0-1	1	0.0004
t	Programme	Time	hr	N/A	N/A	1	N/A

b. Definition of Dynamic processes

Process	Description	Rate	Stoichiometry
Cell Growth	Bacterial growth rate	$(\mu_{max}*S*X/Ks+S)*I$	X: 1
Sulphate Reducti	Sulphate reduction rate	$(1/Y_{x/s})(\mu_{max}*S*X/Ks+S)*I$	S: -1
Metal Removal	Metal removal rate	k_C*C*X	C: -1

4. MODELLING METAL UPTAKE ONTO BACTERIAL SURFACES

a. Fitmod Input File (NEM) for Modelling the Acid Base Properties of SRB

```
1
       0
       1
       1
       1
      90
       3       1       0       0       0
00001  0.0    1.44E-4   H1
00002  0.0    3.86E-4   H2
00003  0.0    2.70E-4   H3
00050  0.0    0.00E00    H

00050  0.0    050 01
00051  -13.90 050 -1
00001  0.0    001 01
00101  -4.2   001 01 050 -1
00002  0.0    002 01
00201  -6.5   002 01 050 -1
00003  0.0    003 01
00301  -8.2   003 01 050 -1


      03       3
     101
     201
     301
      01
      02
      03
```

```
      75        1        1        1
      50
-0.000141907
-0.000235023
-0.000374698
-0.000514372
-0.000654047
-0.000700605
-0.000747163
-0.000886837
-0.001026512
-0.001212744
-0.00130586
-0.001445535
-0.001538651
-0.001585209
-0.001631767
-0.001678326
-0.001818
-0.001911116
-0.002004233
-0.002097349
-0.002190465
-0.002237023
-0.002283581
-0.00233014
-0.002376698
-0.002423256
-0.002469814
-0.002516372
-0.00256293
-0.002609488
-0.002609488
-0.002656047
-0.002702605
-0.002749163
-0.002842279
-0.002888837
-0.002888837
-0.002981953
-0.003028512
-0.003121628
-0.003168186
-0.003261302
-0.003447535
-0.003587209
```

-0.003633767
-0.003726884
-0.003773442
-0.00382
-0.003866558
-0.003913116
-0.003959674
-0.004006233
-0.004052791
-0.004099349
-0.004145907
-0.004239023
-0.004285581
-0.004378698
-0.004425256
-0.004518372
-0.00456493
-0.004658047
-0.004751163
-0.004797721
-0.004937395
-0.005030512
-0.005123628
-0.005216744
-0.005496093
-0.005775442
-0.006008233
-0.006287581
-0.006427256
-0.006660047
-0.006939395
50
-3.678005713
-3.757638709
-3.849389769
-3.953258894
-3.984419631
-4.03289189
-4.109062581
-4.219856314
-4.309876223
-4.389509218
-4.472604518
-4.571280187
-4.607634381
-4.652644335

-4.737470787
-4.782480741
-4.843071064
-4.920972907
-4.976369774
-5.078507747
-5.109668484
-5.135635766
-5.244698347
-5.365878992
-5.469748117
-5.542456505
-5.635938717
-5.776162036
-5.897342682
-5.994287198
-6.072189042
-6.15355319
-6.219336969
-6.319743789
-6.470354021
-6.638275773
-6.762918722
-6.929109322
-6.998355406
-7.169739462
-7.296113564
-7.389595776
-7.528087943
-7.678698174
-7.818921492
-7.914134857
-7.97472518
-8.06647624
-8.159958452
-8.248247209
-8.314030988
-8.410975504
-8.54081191
-8.6567991
-8.769323985
-8.861075045
-8.944170345
-9.041114862
-9.129403618
-9.203843158

-9.290400762
-9.344066476
-9.408119103
-9.449666753
-9.525837445
-9.58815892
-9.633168874
-9.688565741
-9.811477538
-9.924002424
-10.01229118
-10.09538648
-10.17501948
-10.22176058
-10.27715745
0.998
0.998
0.997
0.997
0.997
0.997
0.997
0.997
0.996
0.996
0.996
0.996
0.995
0.995
0.995
0.995
0.995
0.995
0.995
0.995
0.994
0.994
0.994
0.994
0.994
0.994
0.994
0.994
0.994
0.994
0.994

0.994
0.993
0.993
0.993
0.993
0.993
0.993
0.993
0.993
0.993
0.993
0.992
0.992
0.992
0.992
0.992
0.992
0.992
0.991
0.991
0.991
0.991
0.991
0.991
0.991
0.991
0.991
0.991
0.990
0.990
0.990
0.990
0.990
0.990
0.990
0.989
0.989
0.989
0.988
0.988
0.987
0.987
0.987
0.986
00 00

where:
Line 1-6: Program control input
Line 7-11: Matrix A components (Group of components, where Group I = components for which only T is known, Group II = components for which both X and T are known, and Group III = components for which only X is known).
Line 12: Blank card
Line 13-20 Matrix B components (Definition of species and reactions to form species)
Line 21: Blank card
Line 22: Blank card
Line 23: Definition of parameters for optimization (number of Log Ks and Ts)
Line 24-26: ID of 1st, 2nd and 3rd Log K values to be adjusted
Line 27-29: ID of 1st, 2nd and 3rd T values to be adjusted
Line 30: Serial data definition (number of data points, T serial data for 1 component, X serial data for 1 component, dilution factor serial data for 1 component).
Line 31: Total concentration of component (ID number)
Line 32-107: $[H^+]$ added concentration serial data points
Line 108: Log $[H^+]$
Line 109-184: Serial data points
Line 185-260: Dilution coefficient data
Line 261: Termination (00 00)

b. Extrapolation of Equilibrium Constants to Zero Ionic Strength

The deprotonation of a bacterial reactive surface site, e.g., a carboxyl site can be described by the following generic acid-base equilibrium:

$$\text{Carboxyl:} \qquad R-COOH^0 \Leftrightarrow R-COO^- + H^+ \qquad [1]$$

where: R = cell wall and –S-H = the protonated reactive surface site. The corresponding mass action equation for these deprotonation reactions can be expressed as:

$$K_1 = \frac{\left[R-COO^-\right]a_{H^+}}{\left[R-COOH^0\right]} \qquad [2]$$

where: K_1 = deprotonation constants for the reaction, a_i = activity of species *i* in the solution and the [ ] represents molal concentration of the surface species. The deprotonation constant were corrected to zero ionic strength using the Davies equation as follows:

$$\log \gamma_i = -Z_i^2 \left(\frac{A\sqrt{I}}{1+\sqrt{I}} - bI \right) \qquad [3]$$

where: γ = the activity (deprotonation) constant, A= Debye-Hückel constant, which incorporates temperature effects, and is equal to 0.5091 at 25°C (Fernandez et al., 1997), b = 0.1, and z_i = the ion charge. The ionic strength is defined as:

$$I = \frac{1}{2}\sum_k m_k Z_k^2 \qquad [4]$$

where: m_k = the molality (mol kg^{-1}) of ion k. At different temperatures, A can be expressed as:

$$A = 1.8252\times10^6\left(\frac{\rho_w}{\epsilon^3 T^3}\right) \qquad [5]$$

where: ρ_w = the density of water (g cm^{-3}), ϵ = the dielectric constant of water and T = the temperature in Kelvin. The latter is expressed as a function of temperature as follows:

$$\epsilon = \frac{5321}{T} + 233.76 - 0.929T + 1.417\times10^{-3}T^2 - 8.292\times10^{-7}T^3 \qquad [6]$$

c. Fitmod input file for modelling metal adsorption onto SRB cell surfaces

```
      1
      0
      1
      1
      1
     90
      6       1       1       0
00100  0.0    2.36E-3   H1
00200  0.0    2.12E-3   H2
00300  0.0    1.10E-3   H3
00400  0.0    3.58E-3   H4
00001  0.0    0.00E00   Sr2
00002  0.0    0.00E00   NO3-
00020  0.0    0.00E00   Srads
00050  0.0    0.00E00   H

00002  0.0    002 01
00050  0.0    050 01
00051  -13.91 050 -1
00100  0.0    100 01
00101  -4.32  100 01 050 -1
00200  0.0    200 01
00201  -6.38  200 01 050 -1
```

```
00300  0.0    300 01
00301  -8.05  300 01 050 -1
00400  0.0    400 01
00401  -10.18 400 01 050 -1
01000  0.0    001 01
01001  -13.29 001 01 050 -1
01002  -28.51 001 01 050 -2
01005  -4.47  001 02 050 -1
01022  -0.07  001 01 002 02
01111  -9.0   100 01 050 -1 001 01 020 01
01112  -9.0   200 01 050 -1 001 01 020 01
01113  -9.0   300 01 050 -1 001 01 020 01


      03        0
    1111
    1112
    1113
      12        3        1        1
       1
2.85E-04
2.85E-04
2.85E-04
2.85E-04
2.85E-04
2.85E-04
2.85E-04
2.85E-04
2.85E-04
2.85E-04
2.85E-04
2.85E-04
2.85E-04
      20
9.50E-05
1.24E-04
1.28E-04
1.34E-04
1.45E-04
1.57E-04
1.72E-04
1.83E-04
2.14E-04
2.30E-04
2.36E-04
2.39E-04
       2
```

```
1.00E-01
1.00E-01
1.00E-01
1.00E-01
1.00E-01
1.00E-01
1.00E-01
1.00E-01
1.00E-01
1.00E-01
1.00E-01
1.00E-01
      50
-4.75
-4.89
-5.02
-5.17
-5.42
-5.81
-6.02
-6.18
-6.86
-7.39
-8.21
-8.63
0.999
0.999
0.998
0.998
0.997
0.997
0.996
0.995
0.994
0.993
0.992
0.992
      00      00
```

where:

Line 1-6: Program control input

Line 7-15: Matrix A components (Group of components, where Group I = components for which only T is known, Group II = components for which both X and T are known, and Group III = components for which only X is known).

Line 16: Blank card

Line 17-35: Matrix B components (Definition of species and reactions to form species)

Line 36: Blank card
Line 37: Blank card
Line 38: Definition of parameters for optimization (number of Log Ks and Ts)
Line 39-40: ID of 1st and 2nd Log K values to be adjusted
Line 41: Serial data definition (number of data points, T serial data for 1 component, X serial data for 1 component, dilution factor serial data for 1 component).
Line 42: Total concentration of metal (ID = 1)
Line 43-54: [Metal ion] concentration serial data points
Line 55: Concentration of adsorbed metal
Line 56-67: Serial data points for adsorbed metal
Line 68: Nitrate concentration
Line 69-80: Nitrate concentration serial data points
Line 81: Log $[H^+]$
Line 82-93: Serial data for Log $[H^+]$
Line 94-105: Dilution coefficient data
Line 106: Termination (00 00)